ROLE OF MSX HOMEOBOX GENES IN UTERUS DURING EMBRYO IMPLANTATION

BY

SHANMUGASUNDARAM NALLASAMY

DISSERTATION

Submitted in partial fulfillment of the requirements
for the degree of Doctor of Philosophy in VMS – Comparative Biosciences
in the Graduate College of the
University of Illinois at Urbana–Champaign, 2012

Urbana, Illinois

Doctoral Committee:

       Professor Indrani C. Bagchi, Chair
       Professor Milan K. Bagchi
       Professor Jodi A. Flaws
       Assistant Professor Suzanne E. Miller

ABSTRACT

Implantation of the embryo into the wall of the uterus is a crucial event in mammalian embryogenesis. This complex event involves a series of interactions between the developing embryo and the receptive endometrium ultimately leading to successful establishment of pregnancy. The sequential events of implantation include apposition of the blastocyst to the uterine luminal epithelium followed by adhesion to the epithelium and then penetration through the epithelium and basal lamina into the uterine stroma. Uterine sensitivity with respect to implantation has been classified as prereceptive, receptive, and nonreceptive phases. In the mouse, day 1–3 of pregnancy constitutes the prereceptive phase and day 4 is considered receptive. The window of uterine receptivity is transient and lasts for a limited time. On day 5 of pregnancy, the uterus is nonreceptive or refractory. Studies over the past decade have identified a variety of molecules including growth factors, cytokines, transcription factors, and extracellular matrix proteins as potential regulators of this complex process. This dissertation work investigates the critical role of *Msx* homeobox genes in the uterus during embryo implantation.

The mammalian *Msx* homeobox genes, *Msx1* and *Msx2,* encode transcription factors that control organogenesis and tissue interactions during embryonic development. Uterine specific deletion of *Msx1* and *Msx2* resulted in female infertility due to a failure in implantation. Further analysis indicated that mice lacking uterine *Msx1* and *Msx2* ($Msx1^{d/d}Msx2^{d/d}$) exhibited a failure in uterine receptivity due to enhanced estrogen signaling in the luminal epithelium, failure of microvilli remodeling, sustained epithelial cell polarity and persistent proliferative activity of luminal and glandular epithelium. More recent studies revealed that canonical Wnt/ β-catenin signaling were

upregulated in the *Msx1Msx2*-null uteri, which in turn stimulated the production of a subset of fibroblast growth factors (FGFs) in the stromal cells. The FGFs subsequently activate FGFR-ERK-MAP kinase signaling pathway in the luminal epithelium resulting in sustained epithelial cellular proliferation. These results uncovered a unique signaling network, involving Msx1/2, Wnts, and FGFs, which regulate stromal-epithelial cross talk in the mouse uterus at the time of receptivity.

The last chapter addresses the role of *Msx* homeobox genes during uterine stromal cell decidualization. As the embryo attaches to the uterine wall and invades into the stromal bed, the stromal cells surrounding the implanting blastocyst differentiate into decidual cells in a process known as decidualization. This process is critical for embryo survival, angiogenesis and successful establishment of pregnancy. We previously reported that Bone morphogenetic protein 2 (BMP2) regulates uterine stromal cell differentiation in the mouse and the human. Subsequent studies revealed that the expressions of *Msx1* and *Msx2* were markedly altered in response to exogenous BMP2. Functional studies performed using $Msx1^{d/d}Msx2^{d/d}$ mice revealed that mouse uteri lacking *Msx1* and *Msx2* fail to elicit a decidual response, indicating a critical role of these homeobox genes in stromal cell differentiation. Further studies revealed that the addition of BMP2 stimulated *MSX1* and *MSX2* expression in human endometrial stromal cell cultures and enhanced the differentiation process. Silencing of *MSX1* or *MSX2* expression by siRNAs severely impaired human stromal differentiation indicating that MSX1 and MSX2 are key regulators of BMP2-mediated decidualization in the mouse and the human.

To my parents and wife Prema

TABLE OF CONTENTS

CHAPTER I

INTRODUCTION AND REVIEW OF LITERATURE

1.1 INTRODUCTION

The endometrium is a specialized dynamic tissue that undergoes sequential events of proliferation, differentiation, regression and regeneration during the reproductive cycle in response to ovarian steroids, estrogen and progesterone [1-5]. In each cycle, the endometrium becomes competent for implantation for a short period of time termed as the "window of uterine receptivity" during which the blastocyst will be allowed to attach to the uterine wall [6-9]. In rodents, it occurs on day 4 of pregnancy (the day of vaginal plug is day 1 of pregnancy) and lasts only for 24h [3,4,8,10,11]. In humans, the uterus enters the receptive phase during the mid-secretory phase, between cycle days 20 to 24 (6 to 10 days after ovulation) and lasts for about 5 days [12-14].

The acquisition of uterine receptivity is a critical step during embryo implantation and any perturbation in this step causes infertility [6]. Assisted reproductive technologies including in vitro fertilization (IVF) are the most commonly sought medical procedures to treat infertility [15]. However, the average implantation rate in IVF is only ~25% [16]. The recurrent implantation failure (RIF) is a major attributed factor for this reduced success rate [17-19]. Failure to achieve a pregnancy following 2–6 IVF cycles, in which more than 10 high-grade embryos were transferred to the uterus, was defined by various clinicians as RIF [20]. It is believed that two-thirds of implantation failures in RIF are due to an altered uterine receptive

1

status of the endometrium [21], while the embryo itself is responsible for one-third of these failures [12,22].

The diminished uterine receptivity is also observed during controlled ovarian stimulation used in IVF [23]. In addition, the common gynecologic disorders, including thin endometrium [24], endometriosis [25,26], polycystic ovarian syndrome [27], hydrosalpinges [28,29] and luteal phase defect, appear to exhibit impaired uterine receptivity [30]. Any alteration in uterine status is generally evaluated by histological techniques, biochemical changes in the endometrial fluid and altered expression of critical endometrial factors [31,32].

The histological evaluation of the endometrium has been the gold standard for clinical diagnosis for the past five decades [31]. However, its accuracy and the functional relevance of this system as predictor of receptivity have been questioned in recent randomized studies due to a high degree of variability in results [12]. Hence, it is necessary to identify new markers of endometrial receptivity.

To invent new technique to manipulate uterine receptivity during clinical interventions, it is imperative to understand the basic molecular mechanism of this intriguing process. As of now, it is impossible to study uterine receptivity by using in vitro human cell culture system. Hence, it is necessary to find a suitable animal model [1,33]. The availability of genetically engineered mouse models, the existence of evolutionarily conserved pathways in rodents and humans and similarities in the implantation process such as uterine stromal cell decidualization make the mouse an attractive animal model to study uterine receptivity [2].

1.2 UTERINE RECEPTIVITY

1.2.1 Physiological events during uterine receptivity

The fertilized oocyte or zygote undergoes a series of cleavage divisions to become blastocyst. In mice, the blastocyst enters the uterine cavity on day 4 of pregnancy. At the same time, the uterus prepares itself to become competent to receive the blastocyst. In mice, the uterus is considered pre-receptive on days 1–3 of pregnancy, receptive on day 4 and is non-receptive after day 5 [3]. During the receptive phase, the blastocyst interacts with the uterine epithelium through three sequential steps: apposition, adhesion, and invasion [1,34,35]. During apposition, the trophectoderm cells will be closely apposed to the uterine luminal epithelium. In mice, the blastocysts are oriented with their inner cell mass (ICM) directed towards the mesometrial side of the uterus, whereas in humans the ICM is directed towards the antimesometrial side. During adhesion, the intimacy and adherence between the trophectoderm and the luminal epithelium will be further strengthened. The generalized edema occurring in the uterine stroma and subsequent closure of the uterine lumen will aid these processes significantly. The edema is due to localized increase in stromal vascular permeability which can be visualized as distinct blue bands upon intra venous injection of a Chicago blue dye [36]. During the third stage, the trophectoderm penetrates the luminal epithelium and invades the uterine stromal compartment [4].

1.2.2 Ultra-structural changes of uterine epithelium during receptivity

The uterine epithelium undergoes a remarkable ultrastructural change during the receptive phase. On day 1 of pregnancy, the epithelium is of ciliated columnar type, which will transform into a

cuboidal type on day 4 of gestation. In addition, the epithelium will display flattening of microvilli and the loss of epithelial cell polarity [37].

Microvilli flattening of uterine epithelial cells

The microvilli on the apical surface of the cells undergo characteristic changes during receptivity. In the pre-receptive period, the apical plasma membrane will be layered with long thin microvilli and covered with carbohydrate containing coat or glycocalyx which acts as a physical barrier [37]. During the receptive phase, the apical plasma membrane of uterine epithelial cells gradually loses regular microvilli and becomes flat on d 4 of pregnancy [38,39]. This microvilli flattening and subsequent reduction in the level of glycocalyx is an important process to facilitate the embryo attachment.

Loss of epithelial cell polarity

The polarity of the uterine luminal epithelial cells is believed to be maintained by various cell-cell junctional complexes (adherens junctions, tight junctions and desmosomes) located at the basolateral membrane [40]. Similar to apical plasma membrane, the baso-lateral membrane will also undergo changes during uterine receptivity. The adherens junction as well as its associated terminal web will be lost completely from the lateral plasma membrane [37]. The family of calcium dependent cell–cell adhesion molecules such as E-cadherin, is highly expressed at the adherens junctions during the prereceptive period; however, its level is downregulated during uterine receptivity [41,42]. The desmosome proteins are also reported to be down regulated during the receptive period [37].

1.2.3 Molecules regulating uterine receptivity

Research over the past decade has identified a variety of molecules involved in the regulation of uterine receptivity. Through studies using mutant mouse models, global as well as conditional knockouts, report the critical factors that are involved in this process [3,43]. The mutant mouse models exhibiting lack of uterine receptivity are listed in the following table.

Table 1 Mutant mouse models exhibiting infertility phenotype due to lack of uterine receptivity

Genes	Protein	Spatial expression	Temporal expression (Days of pregnancy) 4	5	References
Lif	Cytokine	GE	+	-	[44]
Esr1	TF	LE	+	-	[45,46]
		GE	+	+	
		S	+	+	
Pgr	TF	LE	+	-	[47,48,49]
		GE	+	+	
		S	+	+	
C/EBPβ	TF	E, S	N/A	N/A	[50]
Fkbp52	Chaperone	LE, GE	++	+	[51]
		S	+	+++	
Ihh	Ligand	LE,GE	+	-	[52]
COUP-TFII	TF	S	+	+	[53]
Hand2	TF	S	+	+	[54]

(TF – Transcription factor; GE – Glandular Epithelium; LE – Luminal Epithelium; S – Stroma; N/A – Not Available)

Leukemia Inhibitory Factor

Leukemia Inhibitory Factor (LIF), a member of the interleukin (IL)-6 family, is a highly glycosylated 40–50 kDa glycoprotein with multiple biological functions [55]. In mice, it is transiently expressed in the luminal epithelium on day 1 of pregnancy and is expressed in glandular epithelium on the morning of day 4 of pregnancy [56]. In ovariectomized mice, uterine LIF mRNA is induced within 1 h of estrogen injection and is not affected by progesterone, suggesting that it might be regulated by estrogen [56]. An elegant study conducted using the LIF null mouse model unequivocally established the role of LIF in mouse uterus during uterine receptivity. In the absence of LIF, embryos developed normally but they fail to attach to the uterine epithelium [44].

Estrogen receptor

Estrogens are indispensable for female reproductive functions. The physiological effects of estrogens are mediated by the estrogen receptor, a member of the nuclear receptor superfamily of transcription factors. Two estrogen receptors have been identified: estrogen receptor alpha (ERα) and estrogen receptor beta (ERβ) [57]. The ERα is predominant form expressed in the uterus. It is localized primarily in the luminal and glandular epithelia on days 1 and 2 of pregnancy. On days 3 and 4, it is localized in both stroma and epithelium [58,59]. Three different estrogen receptor knockout (ERKO) mouse models carrying a null mutation in the ERα gene (αERKO), the ERβ gene (βERKO) or both genes (αβERKO) have been generated. Both αERKO and αβERKO female mice are infertile and exhibit impaired uterine receptivity [45,46]. However, βERKO female mice do not exhibit obvious uterine defects [46,60].

Progesterone receptor

The steroid hormone progesterone is considered a pregnancy hormone. The progesterone receptor, a member of the nuclear receptor superfamily of transcription factors, mediates physiological effects of progesterone [49,61-67]. On day 1 and 2 of pregnancy, the expression level of PR is low. On day 3, a marked increase in the level of PR is observed in the epithelium. On day 4, while the PR level is reduced in the epithelium the expression goes up in the stroma [58,62]. The PRKO mouse, in which both PRA and PRB isoforms are deleted, is infertile due to multiple reproductive defects including lack of uterine receptivity [47]. Knockout mouse models specific for the PR isoforms have been generated. The female PRA isoform knockout (PRAKO) mouse is infertile and displays defects similar to PRKO mice [63]. In contrast, the PRB isoform knockout (PRBKO) mouse is fertile [68].

C/EBPβ

C/EBPβ, a transcription factor belongs to C/EBP family of basic leucine-zipper proteins, is a critical regulator of proliferation and/or differentiation in multiple tissues. It is expressed in both the uterine epithelium and stroma in response to estrogen and progesterone. The female C/EBPβ-null mice are infertile due to a defect in uterine receptivity [50,69,70].

Indian Hedgehog

Indian hedgehog, a member of the hedgehog family of proteins, was identified as a PR target gene in mouse uterus. It is maximally expressed in uterine epithelium on day 3 of pregnancy. Conditional deletion of this gene in mouse uterus resulted in loss of uterine receptivity and infertility [52,71,72].

COUP-TFII

COUP-TFII (Chicken ovalbumin upstream promoter transcription factor II, also known as NR2F2), a member of the nuclear receptor superfamily, is highly expressed in the uterine stroma. It is expressed in mouse uterus during early pregnancy in response to progesterone–Indian hedgehog signaling. Similar to PR and Ihh mutant mouse models, the conditional deletion of COUP-TFII rendered the mice infertile due to lack of uterine receptivity [53,73].

Hand2

*Hand2 (*Heart and neural crest derivatives expressed protein 2) is a basic helix-loop-helix transcription factor. Its expression is restricted to uterine stromal cells and is controlled by the progesterone receptor during early pregnancy. Conditional ablation of *Hand2* in mouse uterus resulted in normal ovarian function and proper embryo development; however, the embryos failed to attach to the uterine epithelium due to lack of uterine receptivity [54].

FKBP52

FKBP52/FKBP4 is a member of FK506 binding family of immunophilins and functions as a cochaperone to PR. The overlapping expression pattern of FKBP52 and PR was observed on day 4 and 5 of pregnancy in mouse uterus. The female null mice were infertile due to lack of uterine receptivity [51].

1.2.4 Endometrial glands and uterine receptivity

Endometrial glands are an integral part of mammalian uteri and their secretions are critical regulators of peri-implantation embryo survival and establishment of uterine receptivity [74-79].

However, the composition of endometrial secretions has not been fully characterized. The critical factors like LIF [56], Foxa2 [80], and Spink3 [81] are exclusively expressed in the uterine glands at the time of receptivity. The indispensable role of endometrial glands in uterine function has gained much attention when mice lacking uterine glands or LIF were generated [44]. The endometrial glands failed to develop in sheep [82,83] and mice [84] when treated with progesterone during their neonatal life and in Wnt5a [85], Wnt7a [86-88] and β-catenin [89] knockout mouse models. The uteri of these animals failed to achieve receptive phase during their adult life.

1.2.5 Stromal-epithelial cross talk during uterine receptivity

It is well known that the interactions between uterine stromal cells and epithelial cells play a critical role in the regulation of uterine receptivity [90-93]. Conventional tissue recombination studies provided insight into this process [94]. Recently, the development of compartment specific conditional knockout mouse models further confirmed the stromal-epithelial cross-talk during uterine receptivity and is contributing tremendously to reveal the underlying molecular mechanism [48,95].

1.2.5.1 Uterine epithelial cell proliferation and differentiation during uterine receptivity

In mice, the concerted action of estrogen and progesterone regulate proliferation and/or differentiation of uterine epithelial cells during the window of implantation [96-99]. On the first day of pregnancy in mice, the preovulatory estrogen secretion induces epithelial cells to proliferate and the increasing levels of progesterone secreted from freshly formed corpora lutea induce epithelial cell differentiation [1,4,64,97,100]. The sequential events of epithelial cell

proliferation and differentiation are achieved by interactions between the molecules expressed in the uterine stroma and epithelium [67,90].

E through stromal ER induces epithelial cell proliferation

By using tissue recombination technique, it was demonstrated that the stromal ER is necessary to induce epithelial cell proliferation [94]. This was further confirmed in studies involving epithelial specific ERα mutant mouse models. In this model it was clearly observed that the E2-induced uterine epithelial proliferation is dependent on stromal ER and epithelial ERα is dispensable in this process [95].

Growth factors mediate epithelial cell proliferation

Administration of estrogen to ovariectomized mice mediates epithelial cell proliferation by inducing growth factors such as EGF [101,102], IGF1 [103] and TGFα [104]. While these growth factors are mostly expressed in the uterine stroma, the receptors corresponding to those growth factors are shown to be expressed mostly in the neighboring epithelial cells [105].

P through stromal PR/Hand2 inhibits E induced epithelial cell proliferation

Tissue recombination studies revealed that P mediates its inhibitory effects on E induced epithelial proliferation through stromal PR [106]. In an elegant study from our laboratory, it was reported that the conditional ablation of Hand2, a PR target gene in mouse uterus, caused upregulation of FGF family members Fgf2, Fgf9, and Fgf18 in uterine stroma. This resulted in the activation of FGFR/ERK1/2 signaling in the uterine epithelium which ultimately prevented the uterine epithelium from undergoing differentiation to achieve the receptive phase [54].

1.2.5.2 PR/IHH-PTCH1/COUP TF II regulates uterine receptivity

P through PR and its downstream signaling pathways regulate uterine receptivity. It has been identified that Ihh is the major mediator of progesterone signaling in the uterus at the time of receptivity [52]. It is expressed exclusively in the uterine luminal and glandular epithelium during pre-receptive and receptive phases of the uterus. However, its receptor, Ptch1 and the downstream targets, Gli1 and 2 are expressed in the uterine stroma [71,107]. COUP TFII, reported be a downstream mediator of Ihh signaling, is expressed exclusively in the uterine stroma[53]. These studies clearly demonstrate that PR/IHH-PTCH1/COUP TF II pathways regulate uterine receptivity through stromal-epithelial cross talk [67].

1.2.6 Markers of uterine receptivity

The identification of the receptive stage of the uterus is the critical determining factor for the success of assisted reproductive technologies including IVF [12,108]. The reliable marker is expected to be exclusively expressed in the endometrium at the time of receptivity and to be easily identified with a simple procedure even in the routine clinical settings. There are various markers that have been identified but used with little success. Hence, the search to identify the definitive marker of uterine receptivity continues [109]. At present, the following are considered to be potential markers of uterine receptivity.

Pinopods

Scanning electron microscopy of endometrial samples demonstrated that pinopods are a good marker of uterine receptivity. Pinopods are smooth mushroom like projections that arise from the apical surface of the luminal epithelium of the endometrium, measuring several micrometers in

diameter [108,110]. These structures have been identified in a variety of animals, however, with notable morphological differences in shape, size and content. The duration of their presence in species also varies between hours to weeks. In the rat, their presence is reported to be mostly around the time of implantation. But in mice and human, there are conflicting reports on the duration of pinopods and their use as a marker of uterine receptivity [109,110].

MUC1

The apical surface of uterine epithelial cells is protected by a thick glycocalyx composed mostly of mucins. Among all mucins, Mucin-1 (MUC1) is found to be the major subtype in the mice and human endometrium [111-113]. It is expressed on day 1 of pregnancy and is down-regulated before implantation in the receptive mouse endometrium to facilitate embryo attachment [114,115]. Hence, its disappearance is essential for the achievement of endometrial receptivity and is considered a marker of receptive uterus [108,109].

Other markers

The other potential endometrial biomarkers include αvβ3 integrin, LIF, E-cadherin, trophinin, L-selectin ligand, prostaglandins, IL6 and heparin-binding epidermal growth factor. These factors are still being investigated to assess their usefulness as a marker of endometrial receptivity [108,109,116].

1.3 UTERINE STROMAL CELL DECIDUALIZATION

Differentiation of endometrial stromal cells to decidual cells in a process termed as decidualization is a critical event during early pregnancy. In mice, decidualization is initiated when the embryo attaches to the receptive epithelium on day 4 of pregnancy [117,118]. After the attachment, the embryo penetrates the luminal epithelium and invades into the uterine stroma. In response to embryo attachment and invasion, the stromal cells surrounding the implanted embryo will undergo extensive proliferation and differentiation to become functionally and morphologically distinct decidual cells [4]. In the human, the stromal cell differentiation occurs during the secretory phase of every menstrual cycle even in the absence of embryo. This initial process of predecidualization, however, will become more pronounced in the presence of embryo. The decidual cells are involved in the secretion of variety of factors which regulate embryonic growth and trophoblast invasion during early pregnancy [118]. The precise mechanism of decidualization is not clearly understood, though there are a number of factors that have been implicated in the formation and function of decidua [118]. Some of these factors are listed below.

1.3.1 BMP2 and WNT4

Bmp2 is a member of the BMP family of morphogens and is a downstream target of PR in the mouse uterus [119]. It is expressed in the uterine stromal cells at the site of attachment and persists through the early phases of decidualization. Mutant mice lacking uterine BMP2 fail to elicit decidual response clearly indicating an essential role of this factor in decidualization [120]. Further studies showed that a conserved pathway involving BMP2 also plays a critical role in

human endometrial stromal cell differentiation. [121]. the wingless-related MMTV integration site 4 or *Wnt4* is expressed downstream of BMP2 signaling during endometrial stromal cell differentiation [121]. In *Wnt4* null uteri, decidualization is impaired [122]. These mice failed to undergo the decidual response in response to deciduogenic stimuli. Its importance in regulating human stromal cell differentiation was studied by using primary endometrial stromal cell culture [121].

1.3.2 Connexin 43

Connexin 43 (Cx43), a major gap junction protein, is expressed in uterine stromal cells surrounding the implanted embryo during decidualization. The mice uteri lacking *Cx43* gene in their stromal cells exhibited disrupted gap junctions and impaired decidualization. This causes defective neovascularization within the uterine decidua resulting in the embryo resorption and early pregnancy loss [123].

1.4 HOMEOBOX GENES

The evolutionarily conserved homeobox genes are first identified in Drosophila [124,125]. Soon after, the homologous genes were found in various animal species [126,127]. They are characterized by a conserved 180-bp DNA sequence (Homeobox) coding for a 60-aminoacid DNA-binding domain called the 'homeodomain' [128]. They function as transcription factors recognizing specific DNA sequences and regulate target genes [127]. Homeodomain containing proteins are considered as master regulators of embryonic development and play crucial roles in axial patterning, specifying cell identity and proliferation during embryonic development [125].

Mutations in these genes can cause dramatic developmental defects including loss of specific structures as well as changes in the identity of a body part or segment, which are known as 'homeotic transformations' [128].

More than 200 vertebrate homeobox genes have been identified in a variety of species [129]. Based on sequence homology among their respective homeodomains, homeobox genes are categorized into two large groups. Class I genes, called Hox genes, share a high degree of identity (>80%), with the first discovered homeobox gene of Drosophila, called Antennapedia, in their homeodomain [129]. In mammals, there are 39 Hox genes and are organized in four clusters, labeled as A, B, C and D. Each cluster is divided into 13 paralogous families on the basis of sequence similarity and chromosomal position within each linkage group. There is a correlation between the position of Hox genes in the cluster and their expression pattern along the anterior-posterior axis of the body, with genes located most 5' in the cluster expressed most posteriorly while the more 3' located genes are expressed in more anterior regions[125]. The class II, or diverged homeobox genes, exhibit less than 50% identity with the Antp gene. Class II homeobox genes are grouped into many subfamilies, such as *MSX*, PAX, POU, EMX, and OTX, based on the presence of additional conserved sequences [129,130].

1.4.1 Homeobox genes and reproductive system

The homeobox genes regulate the development of reproductive system during embrogenesis and postnatal life [125,131]. The *Hoxa9, Hoxa10, Hoxa11* and *Hoxa13* genes regulate the differentiation of the Müllerian ducts into adult genital structures. The expression of *Hoxa9* is limited to the fallopian tube; *Hoxa10* is expressed in the uterine epithelium, stroma and muscle;

Hoxa11 is expressed in the uterine stroma, cervical glands and epithelium; and *Hoxa13* is expressed in the vaginal epithelium [132,133]. In addition to playing a major role in the development of reproductive organs, they also critically regulate their function during adult life [133]. For example homeobox genes are known to regulate uterine function during pregnancy [134-136]. Hoxa-10 mutant mice exhibit oviductal transformation of the proximal one third of the uterus. Further, blastocyst implantation and decidualization were impaired in adult *Hoxa10* null mice [137]. The reduced proliferation of uterine stromal cells in response to progesterone was identified as the main cause of decidualization defect in these mice [138]. The uterine stromal cell proliferation was also severely impaired in *Hoxa11*-deficient mice [139]. Additionally, these mice exhibit hypoplastic uteri and lack of uterine glands.

1.5 *MSX* HOMEOBOX GENES

The *Msx* is a sub-family of class II homeobox gene superfamily [140]. They were initially cloned from mice and were identified as homologous to the Drosophila muscle segment homeobox gene (msh) [141,142]. Later, *Msx* genes have been identified from a variety of organisms, including ascidians, sea urchin, zebrafish, frogs, birds, and humans[143]. The mammalian *Msx* gene family consists of 3 members, namely *Msx1 (Hox 7.1), Msx2 (Hox 8),* and *Msx3* and are chromosomally unlinked residing on chromosomes 5, 13 and 7 respectively [144]. *Msx1* and *Msx2* are widely expressed in many organs during embryogenesis [141,145-148]. However, *Msx3* is only expressed in the dorsal neural tube [149,150].

1.5.1 Role of *Msx* during gene transcription

The *Msx* proteins are important modulators of craniofacial, tooth, limb, skin, mammary gland and nervous system development [143,144,151]. They function as transcriptional repressors in vitro and in vivo by interacting directly with the TATA binding protein (TBP) [152,153]. They also interact with other homeodomain proteins such as Dlx2, Dlx5, Lhx2 and Pax3 to regulate transcription [154,155,156].

1.5.2 *Msx* and human diseases

Mutation in human *MSX*1 and *MSX*2 genes causes diseases. Loss of function mutations in *MSX*1 causes Witkop syndrome [157,158] and Wolf-Hirschhorn syndrome [159]. A gain of function mutation in *MSX*2 causes Boston type craniosynostosis [160] and loss of function mutation causes Familial Parietal Foramina [161].

1.5.3 Functional redundancy of *Msx*1 and *Msx*2

Biochemical studies revealed that *MSX*1 and *MSX*2 have common DNA-binding and transcriptional properties and they both recognize the same DNA consensus site [162]. Their role during development and their functional redundancy are clearly demonstrated after the generation and analysis of knockout mouse models. *Msx*1 null mice are neonatally lethal due to defects in the development of teeth and cleft palate [163]. *Msx*2 null mice are viable and fertile, but exhibit defects in the development of the skin, teeth, jaws, skull vault and mammary gland [164]. However, *Msx*1/2 null mice with mutations of both Msx1 and 2 die at E16 − E18 and display more severe phenotype than the loss of any one during cranial and cardiac neural crest, CNS, craniofacial complex, ventral body wall, tooth, ear, limb, hair follicle, limb and mammary gland development[164-166].

1.5.4 *Msx* expression in the uterus

Msx genes are expressed in many tissues during embryogenesis; but their levels decline significantly soon after birth except in a few tissues like the uterus, mammary gland and skin [167-169]. The expression of *Msx*1 is detected in the Müllerian ductal epithelium on E19 and it is expressed in the presumptive uterus, cervix and vagina. *Msx*1is detected in uterus during postnatal period including adulthood. However, the level of *Msx*1 is greatly reduced in the vagina on postnatal day 4-5 and disappears from the cervix at 2 weeks. Thus, *Msx*1 expression is restricted to the presumptive uterus during postnatal development. In the uterus, it is predominantly expressed in the luminal and glandular epithelial cells. In pregnant uteri, the level of *Msx*1 is markedly reduced at 4.5 days p.c. coincident with embryonic implantation and is not expressed during decidualization [168]. Unlike *Msx1, Msx2* is expressed in the uterine stroma during decidualization. [170].

1.5.5 *Msx* and signaling pathways

imported *Msx* and *Wnt*

Msx genes are reported to interact with *Wnt* signaling in many different tissues. *Wnt1* expression is induced by *Msx1* in the neural tube of the chick embryo and its expression is abolished in double *Msx1/2* mutants [171]. Immunoprecipitation studies revealed the presence of multiple DNA biding sites for *Msx*1 on Wnt5a gene [172]. *Wnt7a* expression is greatly up-regulated in *Msx2 null* uterine epithelium compared to wild-type controls [173]. *Msx*2 induces *Wnt3a* and *Wnt7a* during vascular calcification [174] and it also promotes osteogenic differentiation by enhancing the expression of *Wnt7* genes and by downregulating Dkk1 expression [175]. *Msx*1

and *Pax3* cooperate to mediate *Fgf8* and *Wnt* signals during Xenopus neural crest development [176]. Previous studies also indicated that *Msx*1 and *Msx*2 are downstream targets of the Wnt/beta-catenin signaling pathway during lip formation and fusion [177].

Msx, Bmp and *Fgf*

Msx genes interact with many growth factor signaling pathways including BMP, FGF, endothelin, dhand and SHH during organogenesis [178-181]. It has been reported that *BMP2, BMP4, FGF2, FGF4, FGF8,* and *FGF9* from the oral and/or the dental epithelia are capable of inducing *Msx*1 expression in the subjacent mesenchyme of the mandible and maxilla [141,182,183]. In particular, the expression of *BMPs* and *MSXs* are often co-localized during morphogenesis [167,184,185]. The expression of *MSX*1/2 is induced in response to BMP2/4 addition in tooth mesenchyme explant [186] and in facial primordia [187]. Interestingly, it has also been reported that BMP signaling induces *Msx*1 which in turn inhibits FGF-ERK signaling to cause cardiomyocyte differentiation [188].

Wnt and *Fgf*

The interaction between WNTs and FGFs is well known during different developmental systems, including tracheal development in Drosophila, mesoderm induction and neural patterning in Xenopus, and early embryogenesis, body-axis formation, limb-bud formation, and neurogenesis tooth, and kidney development in other vertebrates [189-192]. During limb development, Wnt2b, Wnt-3a and Wnt 8c signal through β-catenin to regulate Fgf 8/10 expression that in turn direct limb initiation and apical ectodermal ridge induction [193]. The cross-talk between Wnt and Fgf

signaling pathways has also been reported in human colorectal carcinogenesis, mouse mammary tumor virus (MMTV)-induced carcinogenesis, and E2A-Pbx-induced leukemogenesis [194,195].

Msx and *dHAND*

*Msx*1, *Msx*2 and the bHLH transcription factor *dHAND* are expressed in a similar pattern in the distal mesenchyme of the branchial arches. In *dHAND*-null embryos, *Msx*1 is not expressed and the branchial arches become hypoplastic. However, *Msx*2 expression is unaltered suggesting that *Msx*1 is downstream of *dHAND* in the mesenchyme of the branchial arches [181]. In contrast, it was reported that the expression of both *Hand1* and *Hand2* is reduced in the *Msx1/2* null mutant myocardium. Hence, it was suggested that *Hand1* and *Hand2* are candidate target genes regulated by *Msx1* and *Msx2* during atrio-ventricular valve formation [196].

1.5.6 *Msx* and epithelial-mesenchymal interactions

Epithelial–mesenchymal interactions play a pivotal role during organogenesis in many tissues. Interestingly, *Msx* genes are reported to play critical role in this process during tooth, heart, mammary gland and placenta formation [170,184,196-198]. During tooth development, the expression of *Msx*1 in mesenchyme requires an epithelial signal, whereas *Msx*2 expression in either epithelium or mesenchyme requires reciprocal interactions between specialized dental cell populations [198]. In the mammary gland, *Msx*2 expression in stroma requires the presence of contiguous epithelium [197]. In tissue recombination experiments conducted using neonatal mouse uterine and vaginal tissues, the expression of *Msx*1 in the uterine epithelium was only observed when it was combined with uterine mesenchyme; and not when it was combined with vaginal mesenchyme [168].

20

1.5.7 *Msx* and Endocrine disruptors

The neonatal mice exposed to diethylstilbestrol (DES) will encounter a variety of uterine and vaginal malformations which have severe impact on their fertility during their adult life [199]. The malformations are reported to be caused by changes in the expression of many developmental genes including *Msx*2 [173]. It has been reported that *Msx*2 is consistently down regulated in the uterus of DES exposed animals. Studies have also shown that upon DES exposure, *Msx2* null uteri exhibit enlarged lumen with a reduction in the amount of stromal tissue [173], a complete failure of Müllerian vaginal epithelial stratification and a severely dilated vaginal lumen [200]. These reports suggest that *Msx*2 counteracts the deleterious effects of DES during female reproductive tract development.

CHAPTER II

MSX HOMEOBOX GENES CRITICALLY REGULATE UTERINE RECEPTIVITY DURING EMBRYO IMPLANTATION

2.1 ABSTRACT

The mammalian *Msx* homeobox genes, *Msx1* and *Msx2,* encode transcription factors that control organogenesis and tissue interactions during embryonic development. We observed overlapping expression of these factors in uterine epithelial and stromal compartments of pregnant mice prior to embryo implantation. Conditional ablation of both *Msx1* and *Msx2* (*Msx1/2*) in the uterus resulted in female infertility; however, the deletion of either one resulted in subfertility. Mice deficient of uterine *Msx*1 and *Msx*2 (termed as $Msx1^{d/d}Msx2^{d/d}$) exhibited normal ovarian function and pre-implantation embryo development. $Msx1^{d/d}Msx2^{d/d}$ uteri however failed to exhibit implantation sites as indicated by blue bands in response to administration of Chicago blue dye indicating failure in implantation. In these mutant mice, the uterine epithelium failed to attach to the embryos. Further analysis indicated that estrogen signaling was elevated in the uterine epithelium of $Msx1^{d/d}Msx2^{d/d}$ mice. Transmission electron microscopy of uterine epithelium from $Msx1^{d/d}Msx2^{d/d}$ mice revealed failure of microvilli remodeling on day 4 of pregnancy. In addition, expression of MUC-1 protein, a major component of the microvilli glycocalyx during early pregnancy, was greatly enhanced in $Msx1^{d/d}Msx2^{d/d}$ mice. The level of E-cadherin, a component of adherens junction, was elevated in $Msx1^{d/d}Msx2^{d/d}$ uteri indicative of sustained epithelial cell polarity. In conclusion, the loss of *Msx1/2* prevents the uterine epithelium to achieve functional receptive status. Collectively, these findings demonstrate that *Msx1/2* critically regulate uterine receptivity during embryo implantation.

2.2 INTRODUCTION

The heterogeneous cellular compartments of the uterus, (luminal and glandular) epithelium and stroma, contribute in distinct ways to the proper functioning of the endometrium and its interaction with the blastocyst during implantation process [1,3,4]. During each cycle, the endometrium becomes competent for a short period of time, termed as the window of uterine receptivity, during which the blastocyst will attach and implant to the uterine wall [6,8,201]. In rodents, it occurs on day 4 of pregnancy (the day of vaginal plug is day 1 of pregnancy) and lasts for 24h [1,2,11]. The receptive phase is comprised of distinct phases including apposition, adhesion, and invasion. During apposition, the trophectoderm cells will be closely apposed to the uterine luminal epithelium. This interaction between the two cellular components will become more intimate and will be strengthened at the adhesive phase. The generalized edema occurring in the uterine stroma and subsequent closure of the uterine lumen will aid these processes significantly [4]. The edema is due to localized increase in stromal vascular permeability which can be visualized as distinct blue bands upon intra venous injection of a Chicago blue dye [36].

Extensive research over the past decade using genetically altered mutant mouse models, has identified several factors that critically regulate uterine function during embryo implantation [50-54,120,123,202-207]. However, there is only limited insight into the molecular mechanisms and signaling pathways that interconnect the various cellular compartments of the uterus to render it receptive to embryo implantation. In the present study, we investigated the role of *Msx* homeobox genes in regulating uterine receptivity.

The *Msx* transcription factors belong to the superfamily of homeobox genes. They were initially identified as homologous to the Drosophila muscle segment homeobox gene (msh). The mammalian *Msx* gene family consists of 3 members, such as *Msx1* (Hox 7.1), *Msx2* (Hox 8), and *Msx3* [141,143,144]. *Msx1* and *Msx2* are widely expressed in many organs during embryogenesis [147,208]. However, *Msx3* is expressed only in the dorsal neural tube [150]. It was previously reported that *Msx*1 and *Msx*2 are expressed in the neonatal as well as in adult mouse uterus [168,173,209]. We observed that MSX1 and MSX2 are expressed in an overlapping pattern in the epithelial and stromal compartments of the preimplantation uterus during days 1-4 of pregnancy. Expressions of MSX1 and MSX2 were markedly reduced in both compartments following embryo attachment. These findings raised the possibility that the pathways regulated by MSX1 or MSX2 or both regulate the receptive state of the preimplantation uterus.

Msx1 null mice are neonatally lethal due to defects in the development of teeth and cleft palate [163]. *Msx2* null mice are viable and fertile, but exhibit defects in the development of skin, teeth, jaws, skull vault and mammary gland [164]. The double *Msx1/2* null mice die at E17 − E18 [165,166]. Hence, it is necessary to conditionally delete these genes in the uterus to study their functions during implantation. We generated mutant mice in which *Msx1/2* are ablated in uterine cells by using cre-lox technology. We observed that ablation of uterine *Msx1/2* leads to infertility in mice. The results of superovulation experiment and analysis of hormonal profiles indicate normal functioning of hypothalamus-pituitary-ovarian axis in animals lacking *Msx1/2*. Absence of implantation sites in mice lacking *Msx1/2* following administration of Chicago blue dye indicates implantation failure. Histological analyses of uterine sections show that in absence of

Msx1/2, the embryos fail to attach to the epithelium indicating a defect in uterine receptivity. Further analysis revealed an enhanced estrogen signaling, failure of microvilli flattening and sustained epithelial cell polarity in epithelium of *Msx1/2* deleted uteri. These alterations culminate in severe impairment of epithelial cell function and lack of uterine receptivity.

2.3 MATERIALS AND METHODS

Animals

Mice were maintained in the designated animal care facility at the College of Veterinary Medicine of the University of Illinois, Urbana-Champaign, according to the institutional guidelines for the care and use of laboratory animals. To generate the conditional *Msx1Msx2*-null mice (*Msx1$^{d/d}$Msx2$^{d/d}$*), *Msx1Msx2*-floxed (*Msx1$^{f/f}$Msx2$^{f/f}$*) [210] mice were mated with PR-Cre knock-in mice [211]. For breeding studies, cycling *Msx1$^{d/d}$Msx2$^{d/d}$* and *Msx1$^{f/f}$Msx2$^{f/f}$* female mice were housed with wild-type C57BL/6 male mice (Charles Rivers) for 6 months. The presence of a vaginal plug after mating was designated as day 1 of pregnancy. The number of litters and pups born were recorded at birth to assess the fertility status.

To induce superovulation, 3-week old female mice were administered intraperitoneally with 5 IU of pregnant mare serum gonadotrophin (PMSG, Sigma St. Louis, MO) followed by 5 IU of human chorionic gonadotropin (hCG, Sigma St. Louis, MO) 48 hours later. The mice were killed 16–18 hours post-hCG administration to flush the oviducts and the oocytes were recovered and counted. To collect blastocysts, 8-week old female mice were mated with wild-type males. To assess the pre- implantation development of embryos, blastocysts were flushed from day 4 pregnant uteri and examined under a stereo-zoom microscope.

Transmission electron microscopy

Uterine tissues isolated from *Msx1$^{f/f}$Msx2$^{f/f}$* and *Msx1$^{d/d}$Msx2$^{d/d}$* female mice on day 4 of pregnancy were fixed in 2.0 % paraformaldehyde and 2.5% glutaraldehyde in buffer containing

0.1 M sodium cacodylate. Tissues were then washed and fixed with 1.0% aqueous osmium tetroxide in 0.1 M sodium cacodylate buffer. Following dehydration with ethanol and propylene oxide, the tissues were embedded in 100% Polybed 812 mixture. Sections (80 nm) were cut with an Ultramicrotome, stained and examined under a Philips CM 200 Transmission Electron Microscope.

Quantitative real time PCR analysis (qPCR)

Uterine tissue was homogenized and total RNA was extracted by using TRIZOL reagent, according to the manufacturer's protocol. cDNA was prepared by standard protocols. The cDNA was amplified by quantitative PCR using gene-specific primers and SYBR Green (Applied Biosystems, Warringtom, UK). The expression level of *36B4* or cytokeratin 18 (*Ck18*) was used as the internal control. For each treatment, the mean Ct and standard deviation were calculated from individual Ct values obtained from three replicates of a sample. The normalized ΔCt in each sample was calculated as mean Ct of target gene subtracted by the mean Ct of internal control gene. $\Delta\Delta$Ct was then calculated as the difference between the ΔCt values of the control and treatment sample. The fold change of gene expression in each sample relative to a control was computed as $2^{-\Delta\Delta Ct}$. The mean fold induction and standard errors were calculated from three or more independent experiments.

Immunohistochemistry

Uterine tissues were processed and subjected to immunohistochemistry as described previously [212]. Briefly, paraffin-embedded tissues were sectioned at 5 μm and mounted on microscopic slides. Sections were deparaffinized in xylene, rehydrated through a series of ethanol washes,

and rinsed in water. Antigen retrieval was performed by immersing the slides in 0.1M citrate buffer solution, pH 6.0, followed by heating in the microwave for 25 min. The slides were allowed to cool and endogenous peroxidase activity was blocked by incubating sections in 0.3% hydrogen peroxide in methanol for 15 min at room temperature. After washing with PBS for 15 min and the slides were incubated in a blocking solution for 1 h before incubating them in primary antibody overnight at 4°C with antibodies specific for MSX1 (Abcam, ab73883), MSX2 (Santa Cruz, sc-15396), MUC1 (Novus biological, NB120-15481), ESR1 (Santa Cruz, sc-7207), p-ESR1 (Santa Cruz, sc-12915), PGR (Neomarkers MS-194-PO) and E-Cadherin (Santa Cruz, sc-7870). The slides were incubated with the biotinylated secondary antibodies at room temperature for 1h, followed by incubation with horseradish peroxidase-conjugated streptavidin (Invitrogen Corp., MD 21704). The sections were stained in 3-amino-9-ethylcarbazole chromogen (AEC) solution until optimal signal was developed. Sections were counterstained with Mayer's Hematoxylin and examined by bright field microscopy.

Measurement of serum E and P levels

The levels of E and P in the serum were measured by radioimmunoassay (RIA) performed at the Ligand Core facility of the University of Virginia at Charlottesville.

Statistical Analysis

Statistical analysis was performed by t-test or ANOVA. The values were expressed as mean $\pm$ SEM and considered significant if $p < 0.05$.

2.4 RESULTS

*Msx*1 and *Msx*2 are expressed in the pre-implantation uterus

The spatio-temporal profiles of mRNAs and proteins corresponding to *Msx1* and *Msx2* were examined in the mouse uterus during the pre-implantation phase by real-time PCR and immunohistochemistry (IHC), respectively. The expression of both *Msx*1 and *Msx*2 mRNAs followed a similar pattern: a marked increase on days 2-3 of pregnancy followed by a sharp decline on day 4 at the time of embryo implantation (Fig.1A, left panel; Fig.1B, left panel). Both MSX1 and MSX2 proteins were abundantly expressed in uterine epithelium on day 1 of pregnancy (Fig.1A, panel a; Fig.1B, panel a). The expression of these proteins increased further on days 2 and 3 of pregnancy and was localized to both glandular epithelium and stroma (Fig.1A, panels b and c; Fig.1B, panels b and c). The expression of MSX1 and MSX2 proteins then declined on day 4 at the time of embryo implantation and was undetectable on day 5 (Fig.1A, panels d & e; Fig.1B, panels d & e). Therefore, overlapping expression of *Msx*1 and *Msx*2 was observed in the uterine epithelial and stromal compartments in the pre-implantation phase (Fig. 1C and Table 2).

Hormonal regulation of *Msx1* and *Msx2* in mouse uterus

The regulation of *Msx1* and *Msx2* by ovarian steroids estrogen and progesterone appears to be complex. The levels of *Msx1* or *Msx2* were not induced in the uteri of ovariectomized mice in response to estrogen and/or progesterone. On the other hand their levels were reduced in response to hormones when compared to oil-treated control uteri. Further, *Msx1* level was markedly reduced in response to estrogen and *Msx2* level was significantly reduced in response

to progesterone (Fig. 2A, upper panel; 2B, upper panel). Consistent with the RNA profile, immunohistochemical analysis revealed prominent expression of *Msx1* and *Msx2* in both luminal and glandular epithelium of ovariectomized oil-treated uteri. The expression of these proteins declined in response to hormones (Fig. 2A, lower panel; 2B, lower panel) indicating that the uterine expression of *Msx* homeobox genes is negatively regulated by ovarian steroids. The factors involved in upregulation of Msx genes remain currently unknown.

Ablation of *Msx1* and *Msx2* in the uterus leads to infertility

To investigate the function of *Msx*1 and *Msx*2 in the uterus, we employed the Cre-LoxP strategy to create conditional single knockout of *Msx1* or *Msx2* or double knockout of *Msx1* and *Msx2* in the uteri of adult mice. Transgenic mice expressing Cre under the control of progesterone receptor (PR) promoter were previously used to ablate "floxed" genes selectively in cells expressing PR, including uterine cells [52,53,54,120,123]. We, therefore, crossed the PR-Cre mice with mice harboring the "floxed" *Msx1* or *Msx2* or both to create $Msx1^{d/d}$, $Msx2^{d/d}$ or $Msx1^{d/d}Msx2^{d/d}$ mice. We confirmed the deletion of *Msx1* or *Msx2* in the uteri of these mutant mice by real-time PCR and IHC. As shown in Fig.3, neither *Msx1/Msx2* mRNA nor MSX1/MSX2 protein was detected in uteri of $Msx1^{d/d}Msx2^{d/d}$ mice on day 3 of pregnancy, confirming successful abrogation of both *Msx* genes in uteri of $Msx1^{d/d}Msx2^{d/d}$ mice. A six-month breeding study demonstrated that the single mutant females, $Msx1^{d/d}$ and $Msx2^{d/d}$, are sub-fertile but the double mutant females, $Msx1^{d/d}Msx2^{d/d}$, are completely infertile (Table 3). While $Msx1^{f/f}Msx2^{f/f}$ mice exhibited normal litter size and pregnancy rates, the $Msx1^{d/d}Msx2^{d/d}$ females failed to become pregnant when mated with wild-type males. However, copulatory plugs were observed upon mating, indicating normal mating behavior.

Ovarian functions and pre-implantation events remain unaffected in $Msx1^{d/d}Msx2^{d/d}$ mice

To investigate the cause of infertility in $Msx1^{d/d}Msx2^{d/d}$ females, we examined their ovarian functions by inducing superovulation. Pre-pubertal $Msx1^{f/f}Msx2^{f/f}$ and $Msx1^{d/d}Msx2^{d/d}$ mice were treated with a regimen of gonadotropin hormones as described in materials and methods. We observed that, upon gonadotropin stimulation, the number of eggs produced by $Msx1^{d/d}Msx2^{d/d}$ was comparable to that produced by the $Msx1^{f/f}Msx2^{f/f}$ females (Fig.4A), indicating that ovulation is not affected in the absence of $Msx1$ and $Msx2$. To further examine the ovulation and fertilization in these mice under normal physiological conditions, blastocysts were recovered from uteri of $Msx1^{f/f}Msx2^{f/f}$ and $Msx1^{d/d}Msx2^{d/d}$ mice on day 4 of pregnancy prior to implantation. Once again, no significant difference was found in either the number or the morphology of the embryos recovered from $Msx1^{f/f}Msx2^{f/f}$ and $Msx1^{d/d}Msx2^{d/d}$ uteri (Figs.4B and 3C). In further support of normal ovarian activity, the serum levels of estrogen and progesterone were comparable in $Msx1^{f/f}Msx2^{f/f}$ and $Msx1^{d/d}Msx2^{d/d}$ females on day 4 of pregnancy (Figs.4D and E). Collectively, these results suggested that the infertility of $Msx1^{d/d}Msx2^{d/d}$ females is not due to impairment in the hypothalamic-pituitary-ovarian axis or lack of fertilization, but is likely due to defective implantation or pregnancy failure following implantation.

Ablation of $Msx1$ and $Msx2$ in the uterus affects embryo attachment to the luminal epithelium

In mice, the attachment of the embryos to the uterine wall initiates the process of implantation. This is accompanied by increased vascular permeability at the implantation sites, which can be scored visually as distinct blue bands following an intravenous injection of Chicago blue dye [212]. As shown in Fig.5A, $Msx1^{f/f}Msx2^{f/f}$ mice displayed distinct implantation sites on day 5 of

pregnancy. In contrast, the $Msx1^{d/d}Msx2^{d/d}$ females did not show any sign of implantation. Implanted embryos were also assessed on days 6 and 7 of pregnancy by visual inspection. Our results indicated that implantation sites are absent in $Msx1^{d/d}Msx2^{d/d}$ uteri (Fig.5A).

Histological analysis of $Msx1^{f/f}Msx2^{f/f}$ females on day 5 of pregnancy showed, as expected, a close contact of embryonic trophectoderm with uterine luminal epithelium (Fig.5B, panel a). In contrast, in $Msx1^{d/d}Msx2^{d/d}$ uteri, embryos did not attach to luminal epithelium. Instead, blastocysts remained free-floating in the lumen and were readily recovered by uterine flushing of the $Msx1^{d/d}Msx2^{d/d}$ females (Fig.5B, panel b). Taken together, these results indicated that the loss of *Msx1* and *Msx2* expression in the uterus resulted in the inability of the luminal epithelium to acquire competency for embryo implantation.

Estrogen receptor activity is elevated in uterine epithelium of $Msx1^{d/d}Msx2^{d/d}$ mice at the time of implantation

In mice, the window of uterine receptivity is critically regulated by the steroid hormones 17α-estradiol (E) and progesterone (P), acting through their cognate nuclear receptors. We therefore examined the expression levels of progesterone receptor (PGR), estrogen receptor alpha (ESR1), and their downstream genes in the uteri of $Msx1^{d/d}Msx2^{d/d}$ mice by immunohistochemistry and real-time PCR analyses. As shown in Fig.6A, the expression levels of PGR (top panel) and ESR1 (middle panel) proteins in the luminal epithelium or stromal compartment of $Msx1^{d/d}Msx2^{d/d}$ uteri were comparable to those of $Msx1^{f/f}Msx2^{f/f}$ controls. However, we noted that the expression of the transcriptionally active form of ESR1, phosphorylated at serine 118 [213], was markedly up-regulated in the luminal epithelial cells of $Msx1^{d/d}Msx2^{d/d}$ uteri, indicating that ER activity is

elevated in the uterine epithelia of these mice (lower panel). This observation indicated that the pathways directed by *Msx1/Msx2* play an important role in controlling the ESR1 activity, which is normally suppressed in uterine epithelium during the receptive phase [61,214,215]. Consistent with this up-regulation of transcriptional activity of ESR1, expression of mRNAs corresponding to well-known E-regulated genes, such as lactotransferrin (*Ltf*) [216], chloride channel, calcium activated, family member 3 (*Clca3*) [217], lipocalin 2 [218] and mucin 1 (*Muc-1*) [114], was significantly elevated in uterine epithelium of $Msx1^{d/d}Msx2^{d/d}$ uteri on day 4 of pregnancy (Fig.6B).

Progesterone signaling is not altered in $Msx1^{d/d}Msx2^{d/d}$ mice uteri

The expression of *Ihh,* a P-responsive gene in uterine epithelium [52] remained unaltered in $Msx1^{d/d}Msx2^{d/d}$ uteri. Additionally, the mRNA levels of *Hand2* [54] and *Hoxa10* [118] , well-known P-regulated genes in uterine stroma, and that of chicken ovalbumin upstream promoter-transcription factor II (*COUP-TF II*), a downstream target of IHH in the uterine stroma [53], were unaffected in the uteri of $Msx1^{d/d}Msx2^{d/d}$ mice (Fig.7). These results indicated that the loss of *Msx1* and *Msx2* did not have any impact on the transcriptional activity of PGR.

Lack of uterine receptivity in $Msx1^{d/d}Msx2^{d/d}$ mice

The membrane transformation of uterine epithelium at the time of implantation is an important parameter of receptive uterus. The presence of long microvilli, containing a thick layer of glycoprotein known as the glycocalyx, on the uterine epithelium is indicative of the non-receptive stage. A marked flattening of these microvilli occurs in the receptive phase prior to implantation [37]. Transmission electron microscopy (TEM) revealed that, in contrast to the

control epithelium, the epithelia of $Msx1^{d/d}Msx2^{d/d}$ uteri fail to undergo appropriate remodeling to promote microvilli flattening, indicating impaired uterine receptivity in these mice (Fig.8A).

The impaired functional state of uterine epithelium in $Msx1^{d/d}Msx2^{d/d}$ mice was also confirmed when we analyzed the expression of MUC-1 protein, a major component of the endometrial glycocalyx, during early pregnancy. The expression status of MUC-1 is considered an important indicator of uterine receptivity [114]. As the luminal epithelium differentiates and the uterus achieves receptivity, MUC-1 expression is down regulated in this tissue. Persistent MUC-1 expression is indicative of a non-receptive uterus, which is not conducive to embryo implantation. As shown in Fig.8B, prominent expression of MUC-1 was detected in the uterine epithelia of control $Msx1^{f/f}Msx2^{f/f}$ mice on day 1 of pregnancy (panel a). As the pregnancy advanced to days 4 (panel b) and 5 (panel c), Muc-1 was progressively down regulated in uterine epithelia of these mice, consistent with the attainment of receptive status. In contrast, an intense expression of MUC-1 was observed in uteri of $Msx1^{d/d}Msx2^{d/d}$ mice on days 4 and 5 (panels d–f). This elevated epithelial ESR1 signaling is likely involved in the persistent expression of MUC-1 in luminal epithelium. This in turn disrupted uterine receptivity resulting in implantation failure in $Msx1^{d/d}Msx2^{d/d}$ mice.

Sustained epithelial cell polarity in $Msx1^{d/d}Msx2^{d/d}$ mice

The uterine epithelium will lose its polarity when it transforms from pre-receptive to receptive status. The polarity of the uterine luminal epithelial cells is believed to be maintained by various cell-cell junctional complexes including adherens junctions. The family of calcium dependent cell–cell adhesion molecule, E-cadherin, is expressed at the adherence junctions during pre-receptive period; however, its level is dramatically down regulated during uterine receptivity

[41,42]. The expression of E-cadherin was elevated in the uterine epithelia of $Msx1^{d/d}Msx2^{d/d}$ mice when compared to control $Msx1^{f/f}Msx2^{f/f}$ mice on day 4 of pregnancy indicating sustained epithelial cell polarity (Fig.9).

Functional redundancy of *Msx1* and *Msx2* during uterine receptivity

The functional redundancy of *Msx1* and *Msx2* is well known during embryonic development. This is not unexpected because of their overlapping expression pattern [162,164,167]. Similarly, in the adult uterus *Msx1* and *Msx2* are expressed in the same cellular compartments during the reproductive cycle and early pregnancy. Thus deletion of either *Msx1* or *Msx2* compensates for the loss of the other member and renders mice sub-fertile, while deletion of both *Msx1* and *Msx2* leads to infertility. Interestingly we observed that the expression of *Msx2* is markedly elevated in *Msx1*-null uterus in the receptive phase (Fig.10A). In contrast the expression of *Msx1* is not elevated in *Msx2*-null uterus in the receptive phase (Fig.10B). This indicates that *Msx1* might be the dominant contributor of uterine receptivity during early pregnancy.

2.5 DISCUSSION

The uterine receptivity is a critical step during embryo implantation process and alterations to this step causes infertility [6]. Assisted reproductive technologies including in vitro fertilization (IVF) are the most commonly sought medical procedures to treat infertility [15]. However, the average implantation rate in IVF is only ~25% [16]. The recurrent implantation failure (RIF) is a major attributed factor for this reduced success rate [17,18,19]. The RIF could be due to altered receptive status of the endometrium which is responsible for approximately two-thirds of implantation failures [21], whereas the embryo itself is responsible for only one-third of these failures [12,22]. Hence to increase the success rate of IVF, it is important to understand the molecular basis of uterine receptivity. The present study demonstrates the expression of *Msx*1 and *Msx2* in adult uterus and addresses, for the first time, their roles in uterine receptivity.

Using mutant mouse models harboring conditional deletions of *Msx1* and/or *Msx2* in the uterus, we established that these factors play critical roles in regulating uterine function during implantation. The deletion of both *Msx1/2* renders the mice completely infertile. The ovarian functions and preimplantation embryo development are not affected upon deletion of *Msx1/2*. This indicates that the infertility phenotype is intrinsic to uterus. The lack of implantation sites in mice lacking *Msx1/2* following administration of Chicago blue dye indicates implantation failure. Histological analyses of uterine sections show that in the absence of *Msx1/2*, the embryos fail to attach to the epithelium indicating a defect in uterine receptivity.

Uterine receptivity is critically regulated by ER and PR. Though the progesterone signaling is not altered in uterus lacking *Msx1/2*, estrogen signaling is greatly altered. The expression of the transcriptionally active form of ESR1, phosphorylated at serine 118 [213], was markedly up-regulated in the luminal epithelial cells of *Msx1$^{d/d}$Msx2$^{d/d}$* uteri. It is well established that this phosphorylation event is critical for the transcriptional activation of ESR1 [213]. An elevated ERα signaling in the epithelium is, however, detrimental to the implantation process. For example, ERα promotes the expression of Muc-1, a well-known cell surface glycoprotein, which creates a barrier that prevents embryo attachment. In mice, high levels of MUC-1 are present in the non-receptive uterus on days 1 and 2 of pregnancy. As the pregnancy progresses, MUC-1 expression declines in the epithelium and it is drastically reduced on day 4 at the time of implantation [114]. Therefore, the reduction of MUC-1 expression is considered a sign of uterine receptivity in mice. The persistence of high levels of MUC-1 in the *Msx1$^{d/d}$Msx2$^{d/d}$* uteri on day 4 of pregnancy is indicative of hyperestrogenic activity in the luminal epithelium and consequently, reflects a lack of uterine receptivity.

Another important parameter of receptive uterus is the membrane transformation of uterine epithelium at the time of implantation. The presence of long microvilli, containing a thick layer of glycoprotein known as the glycocalyx, on the uterine epithelium is indicative of the non-receptive stage. A marked flattening of these microvilli occurs in the receptive phase prior to implantation [37]. Transmission electron microscopy (TEM) revealed that, in contrast to the control epithelium, the epithelia of *Msx1$^{d/d}$Msx2$^{d/d}$* uteri fail to undergo appropriate remodeling to promote microvilli flattening, indicating impaired uterine receptivity in these mice. In addition to microvilli remodeling, the epithelium undergoes characteristic ultrastructural changes in its

polarity. During pre-receptive phase, the epithelium maintains its polarity through different cell junctional complexes. The well known marker of epithelium, E-cadherin, is calcium dependent molecule expressed abundantly in adherens junctions during pre-receptive period; however, its expression level is drastically reduced during receptive period [41]. The elevated level of E-cadherin in the $Msx1^{d/d}Msx2^{d/d}$ uteri on day 4 of pregnancy is indicative of persistent epithelial cell polarity, a characteristic feature of nonreceptive uterus.

In summary, the deletion of both *Msx1* and *Msx2* leads to infertility due to lack of uterine receptivity during embryo implantation. The lack of uterine receptivity was characterized by enhanced estrogen signaling, failure of microvilli remodeling and sustained epithelial cell polarity. In addition, we also observed that the uterine epithelium lacking *Msx1/2* exhibited persistent proliferation. A detailed analysis of the proliferation defect, which led to the identification of the mechanism of action of *Msx* homeobox genes in mouse uterus, is discussed in detail in the next chapter.

2.6 FIGURES-Figure 1 Expression of *Msx*1 and *Msx*2 in the uterus during early pregnancy
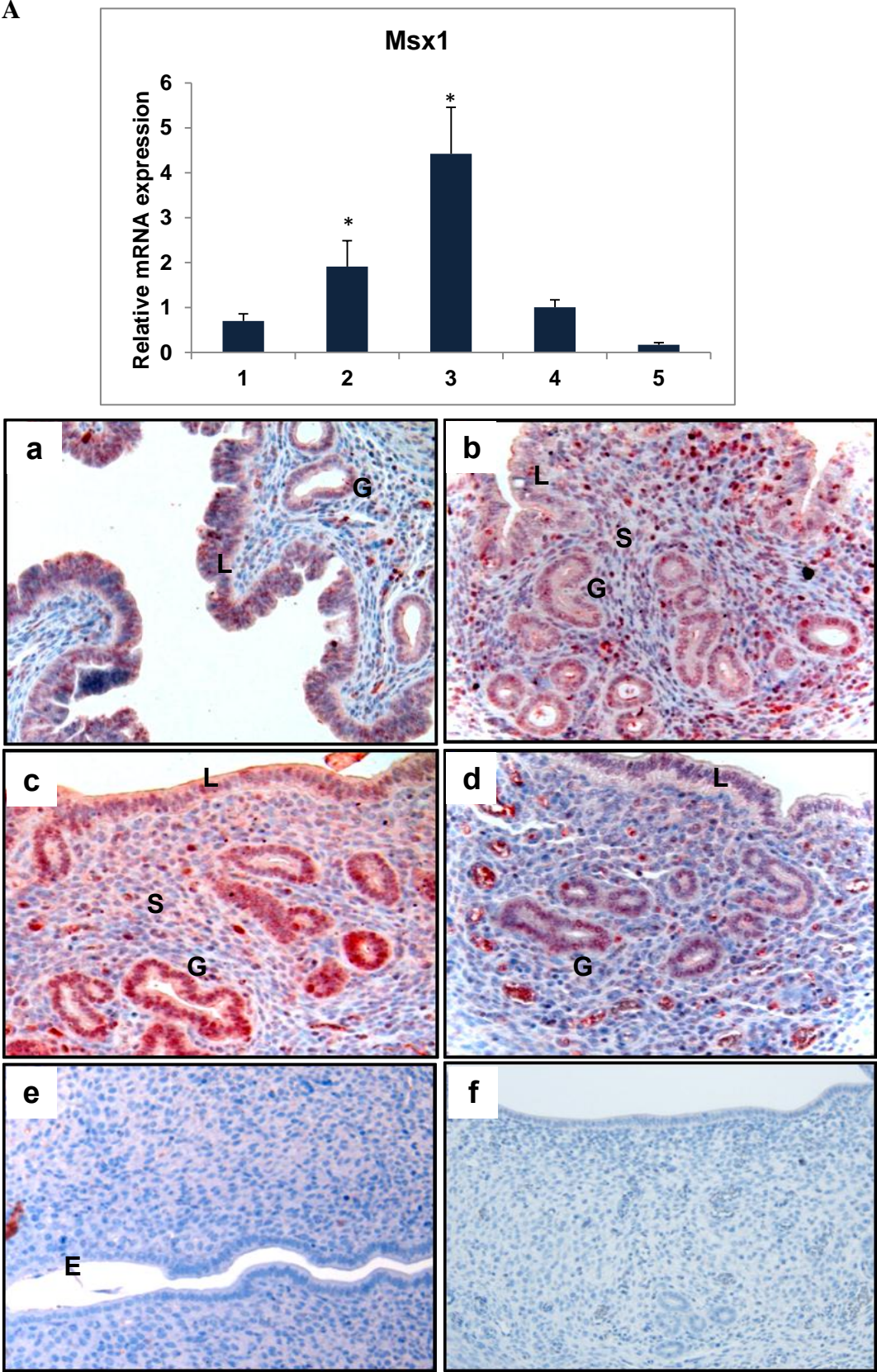
A

Figure 1 (Contd.) Expression of *Msx*1 and *Msx*2 in the uterus during early pregnancy
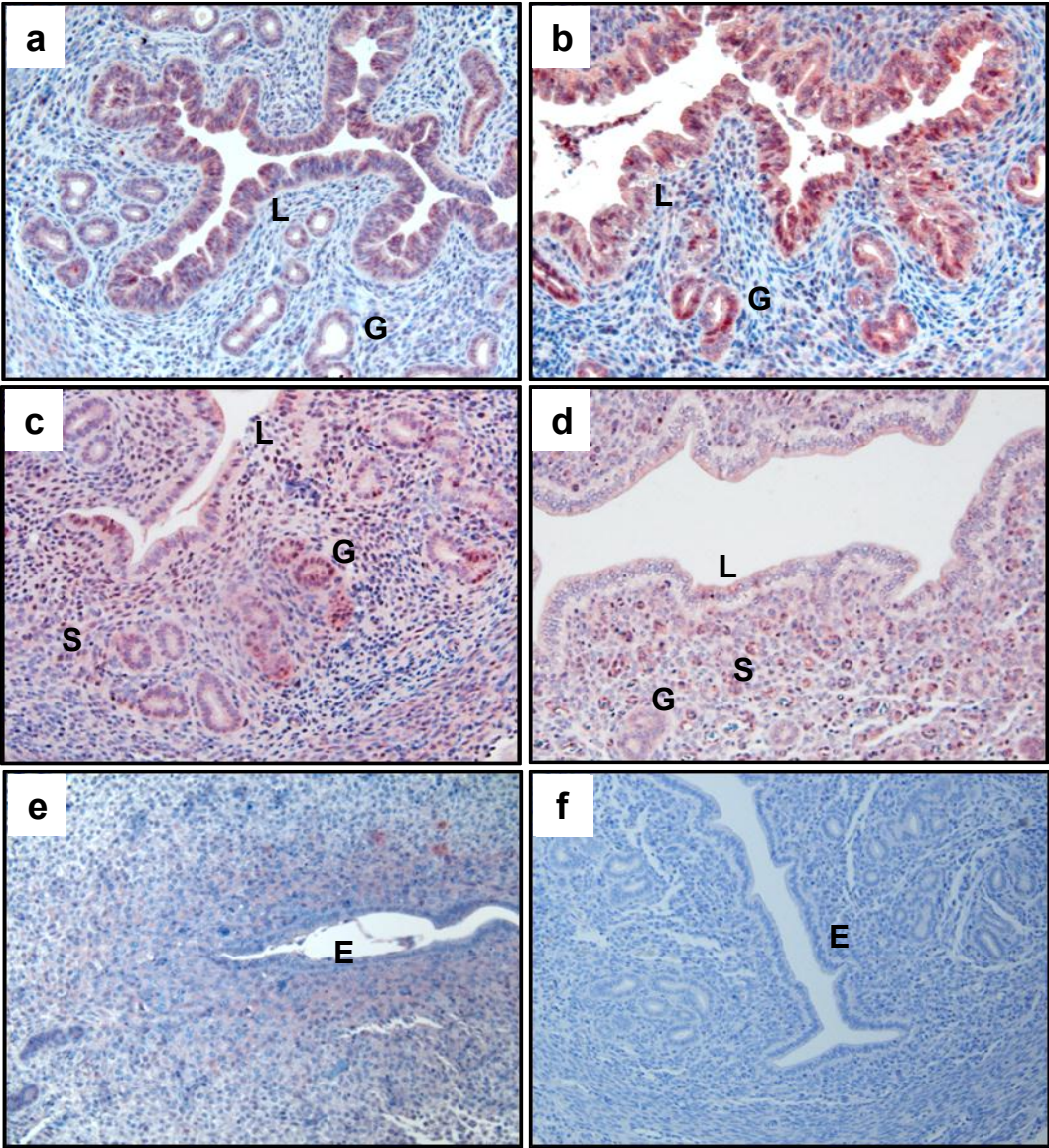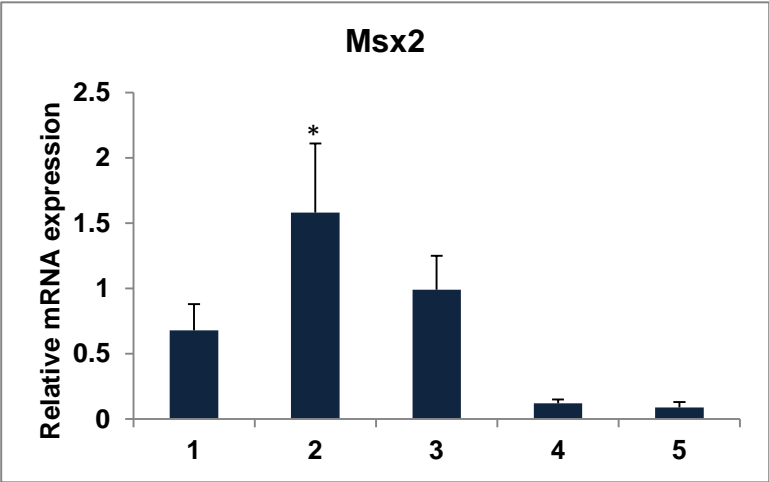
C
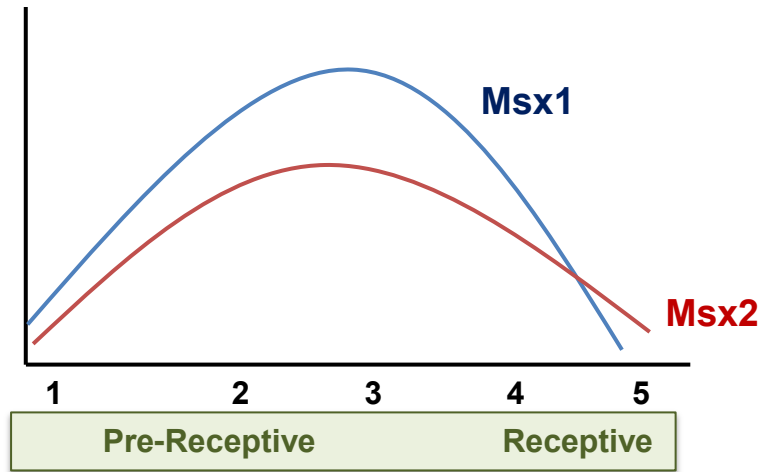
Figure 1 (Contd.) Expression of *Msx*1 and *Msx*2 in the uterus during early pregnancy

Real-time PCR was performed to monitor the expression of mRNAs corresponding to *Msx1* (A,Upper panel) and *Msx2* (B, Upper panel) in uterus on days 1 to 5 of gestation. The relative levels of gene expression on different days of pregnancy were determined by setting the expression level of *Msx1* mRNA on day 1 of pregnancy at 1.0. *Rplp0,* encoding a ribosomal protein, was used to normalize the level of RNA (* $p < 0.05$). Uterine sections from day 1 to day 5 (a-e) of pregnancy were subjected to immunohistochemical analysis using anti-MSX1 (A, Lower panel) and anti-MSX2 (B, Lower panel) antibodies. Panel f shows uterine sections from day 3 pregnant mice treated with non-immune IgG. L, G and S indicate luminal epithelium, glandular epithelium and stroma, respectively. C: The graphical representation of expression profile of *Msx1* and *Msx2* in uterus on days 1 to 5 of gestation showing the similar expression pattern.

Table 2 The compartment specific expression profile of MSX1 and MSX2 in uterus on days 1 to 5 of gestation
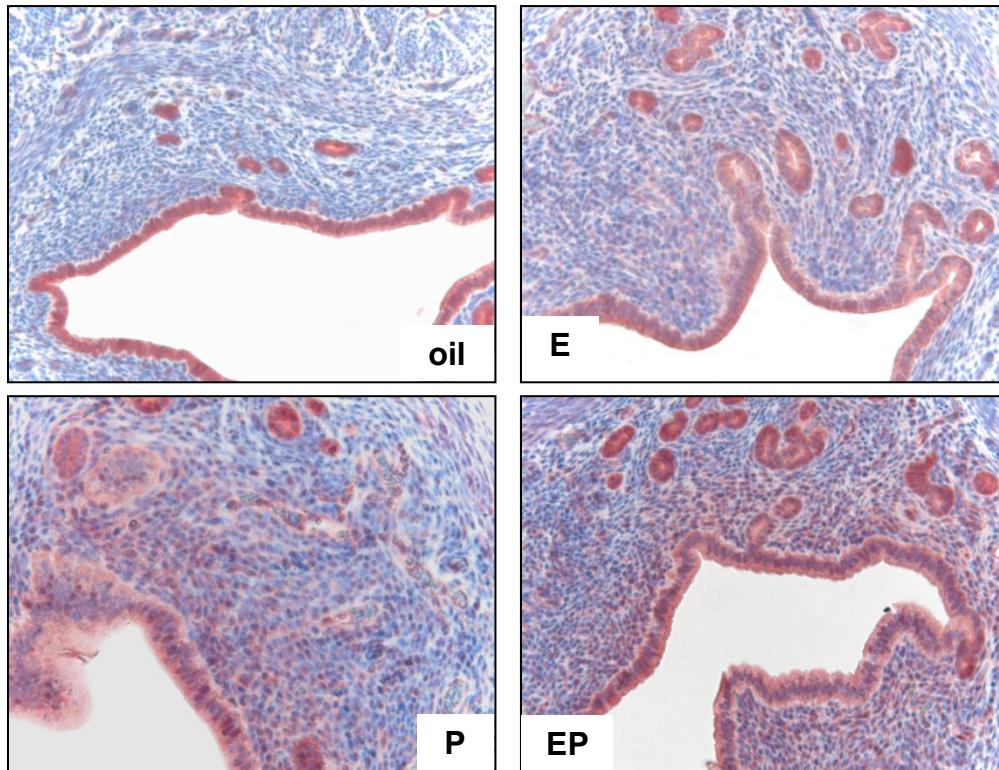
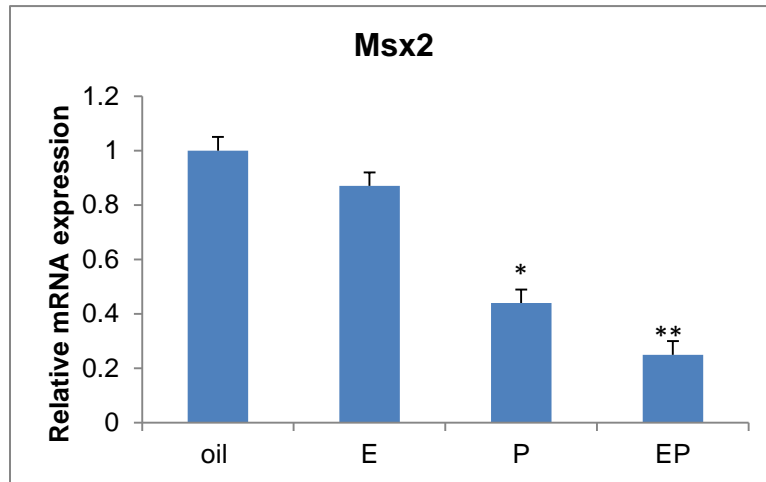| Protein	Uterine Compartment	Days of Pregnancy				
		1	2	3	4	5
MSX1	Epithelium	++	++	+++	+	-
	Stroma	-	+	++	+	-
MSX2	Epithelium	++	+++	++	+	-
	Stroma	-	-	++	++	+

41

Figure 2 Hormonal regulation of *Msx1* and *Msx2*

A
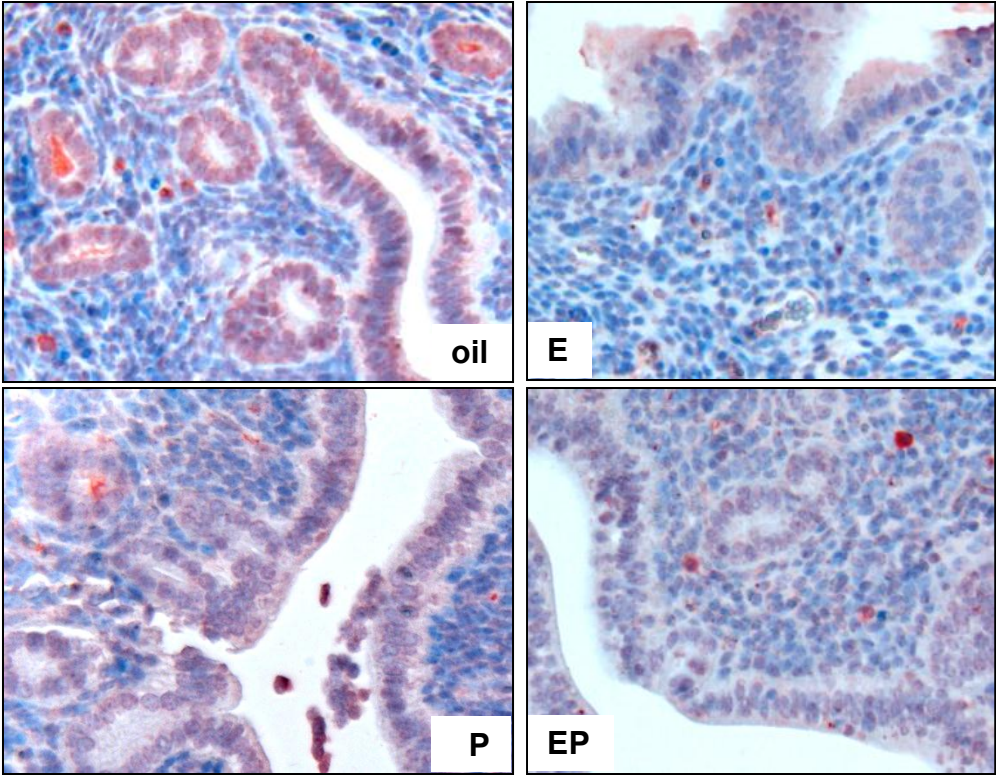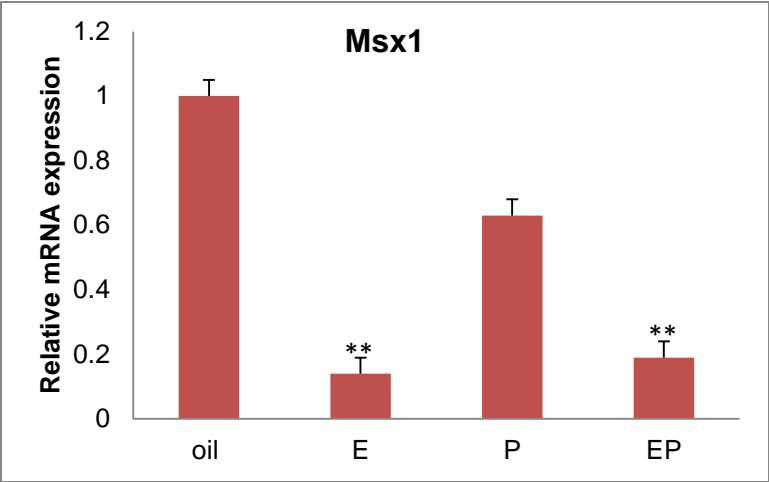
B

Figure 2 (Contd.) Hormonal regulation of *Msx1* and *Msx2*

Ovariectomized mice were treated with oil or steroid hormones as described in materials and methods. Real-time PCR was performed to monitor the expression of mRNAs corresponding to *Msx1* (A,Upper panel) and *Msx2* (B, Upper panel) in uterus (*p<0.05; **p<0.005). Uterine sections were subjected to immunohistochemical analysis using anti-MSX1 (A, Lower panel) and anti-MSX2 (B, Lower panel) antibodies.
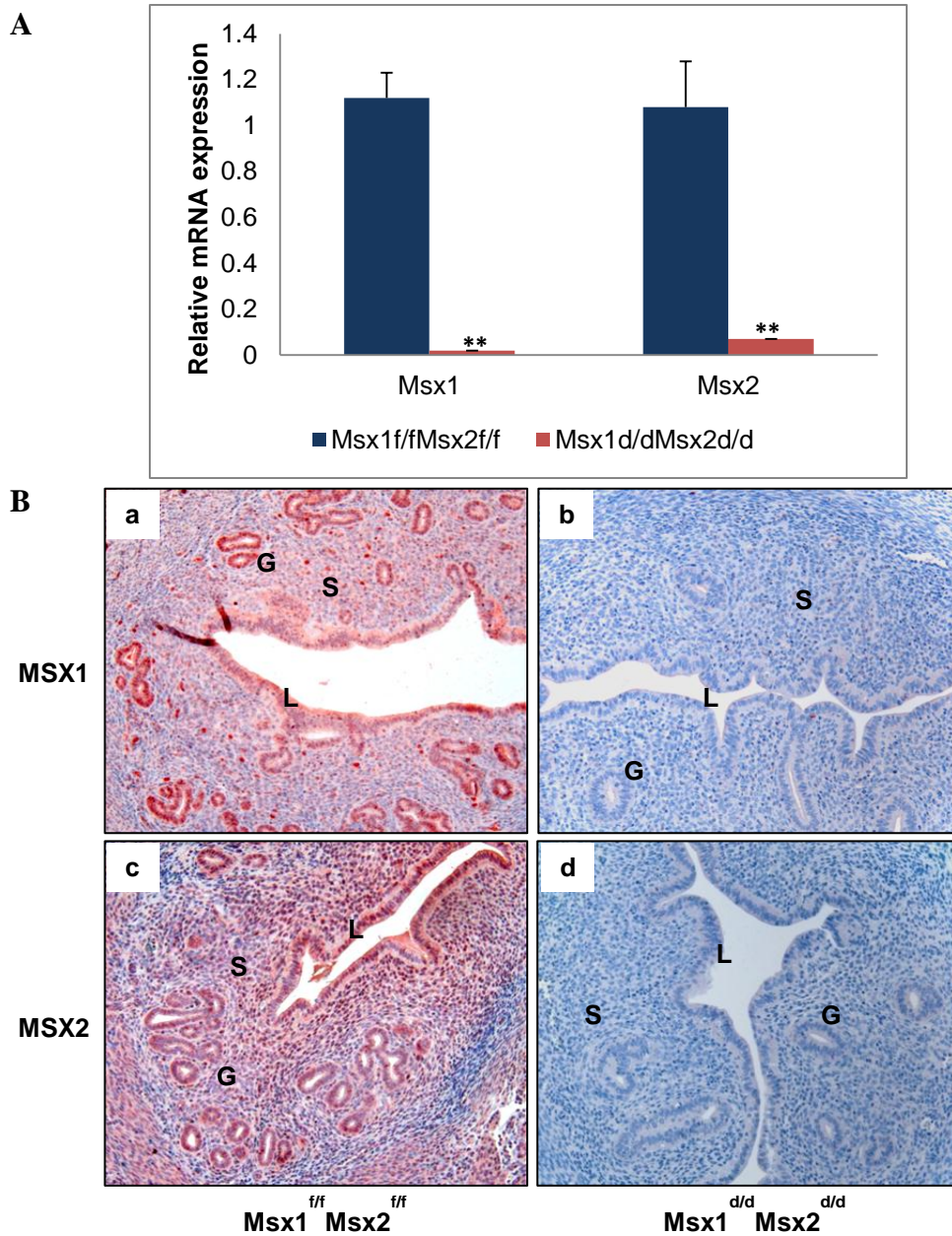
Figure 3 Loss of *Msx*1 and *Msx*2 expression in the uterus of *Msx*1$^{d/d}$*Msx*2$^{d/d}$ mice

A. Uterine RNA was purified from *Msx1*$^{f/f}$*Msx2*$^{f/f}$ and *Msx1*$^{d/d}$*Msx2*$^{d/d}$ mice on day 3 of pregnancy (n=3) and analyzed by real-time PCR. Relative levels of *Msx*1 and *Msx*2 mRNA expression in uteri of *Msx*1$^{d/d}$*Msx2*$^{d/d}$ mice are compared to those in *Msx1* $^{f/f}$*Msx2* $^{f/f}$ control mice. The data are represented as the mean fold induction ± SEM, **p<0.001. **B.** Uterine sections obtained from day 3 pregnant *Msx1*$^{f/f}$*Msx2*$^{f/f}$ (left panel) and *Msx1*$^{d/d}$*Msx2*$^{d/d}$ (right panel) mice were subjected to immunohistochemical analysis. Note the lack of MSX1 (upper panel) and MSX2 (lower panel) immunostaining in the uteri of the mutant mice. L, G and S indicate luminal epithelium, glandular epithelium and stroma respectively.

Table 3 Ablation of uterine *Msx*1 and *Msx*2 leads to female infertility

Genotype	No. of animals	No. of Litters born	No. of litters per animal (Mean ± SEM)	No. of pups born	No. of pups per litter (Mean ± SEM)
Msx1$^{f/f}$Msx2$^{f/f}$	6	32	5.3±0.2	261	8.1±0.4
Msx1$^{d/d}$	6	14	2.8±0.8	64	4.5±0.6
Msx2$^{d/d}$	6	22	3.6±0.6	132	6.0±0.5
Msx1$^{d/d}$Msx2$^{d/d}$	6	0	0	0	0

Figure 4 Ovarian functions and preimplantation events are unaffected in *Msx1$^{d/d}$Msx2$^{d/d}$* mice

A

B

C

Msx1$^{f/f}$Msx2$^{f/f}$ Msx1$^{d/d}$Msx2$^{d/d}$

D

E
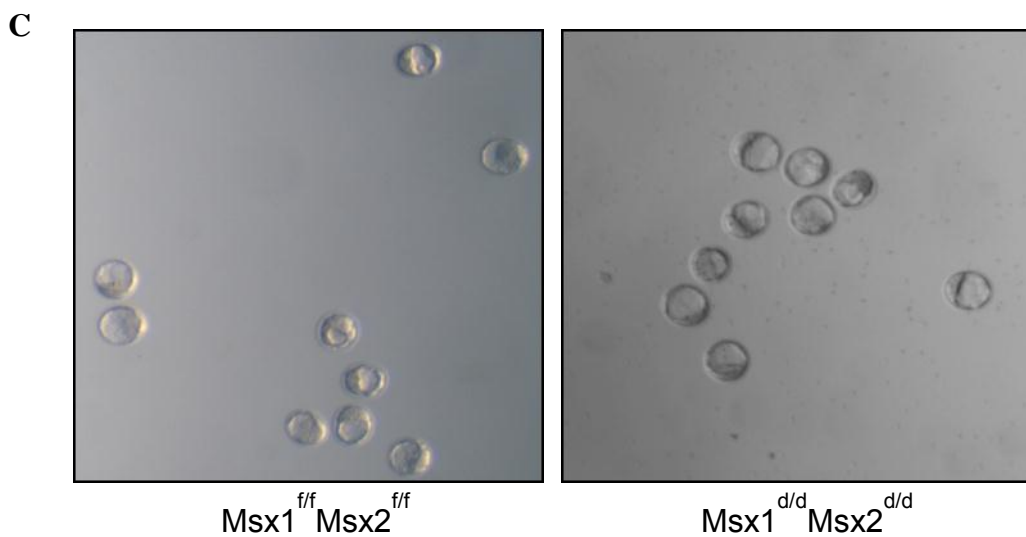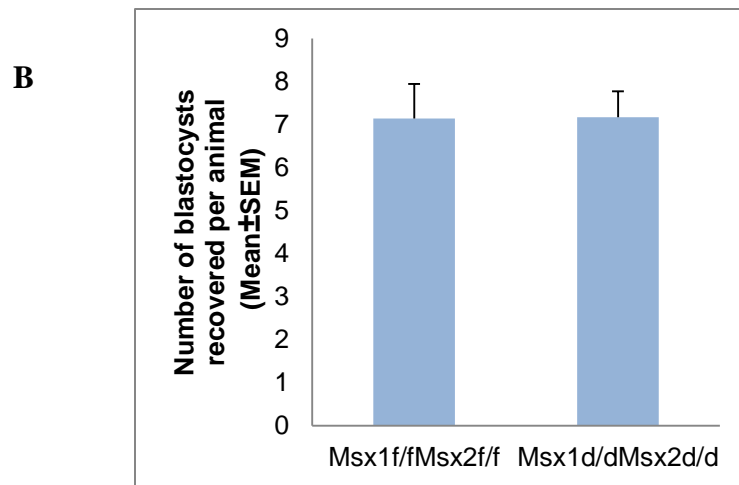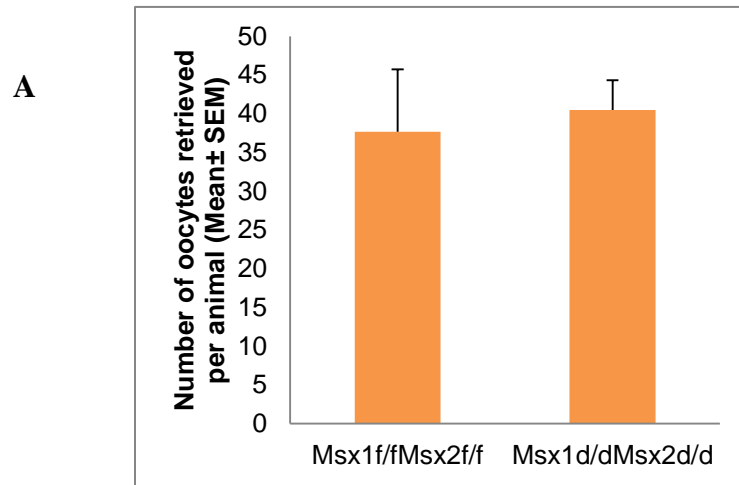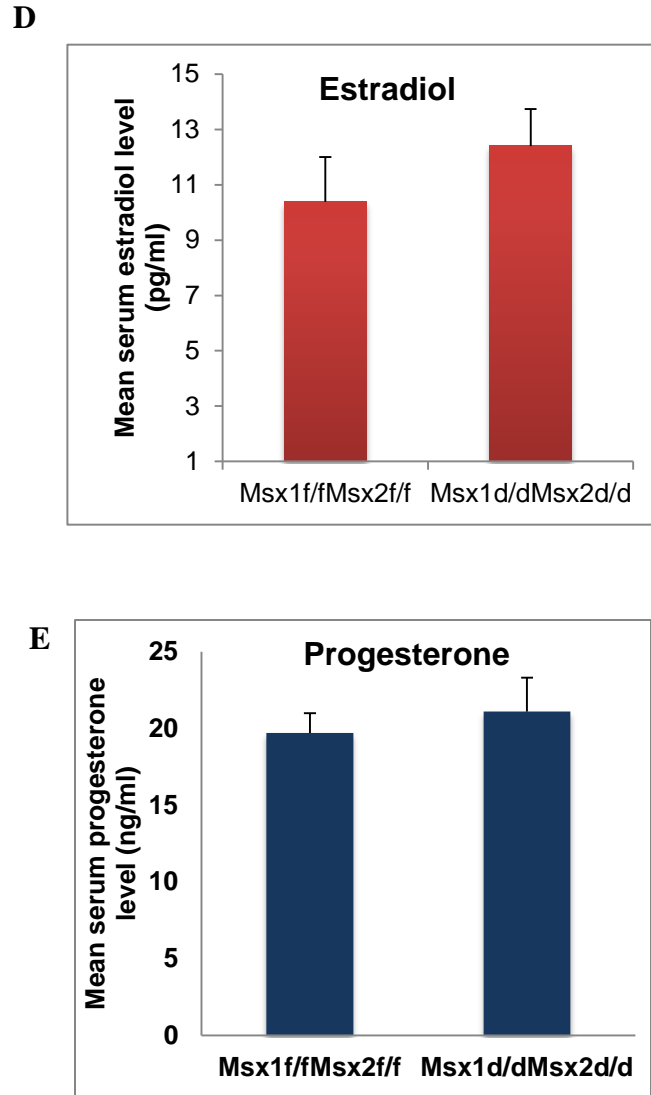
Figure 4 (Contd.) Ovarian functions and preimplantation events are unaffected in *Msx1$^{d/d}$Msx2$^{d/d}$* mice

A. Age-matched prepubertal *Msx1$^{f/f}$Msx2$^{f/f}$* (n=7) and *Msx1$^{d/d}$Msx2$^{d/d}$* mice (n=6) were subjected to superovulation. The oocytes were recovered and counted at 18h after hCG administration (values are mean ± SEM). **B.** Pre-implantation embryos were recovered from uteri of *Msx1$^{f/f}$Msx2$^{f/f}$* (n=7) and *Msx1$^{d/d}$Msx2$^{d/d}$* mice (n=12) in the morning of day 4 of pregnancy, counted (values are mean ± SEM) and photographed. **C.** Representative morphology of blastocysts recovered from uteri of *Msx1$^{f/f}$Msx2$^{f/f}$* and *Msx1$^{d/d}$Msx2$^{d/d}$* mice. **D & E:** E and P levels in serum of *Msx1$^{f/f}$Msx2$^{f/f}$* (n=6) and *Msx1$^{d/d}$Msx2$^{d/d}$* (n=10) mice on day 4 of pregnancy. Values are represented as means ± SEM.

47

Figure 5 Lack of uterine *Msx*1 and *Msx*2 causes implantation failure

D7

Msx1^{f/f} Msx2^{f/f}   Msx1^{d/d} Msx2^{d/d}

B

D5

a   b

L   L

E   E

Msx1^{f/f} Msx2^{f/f}   Msx1^{d/d} Msx2^{d/d}
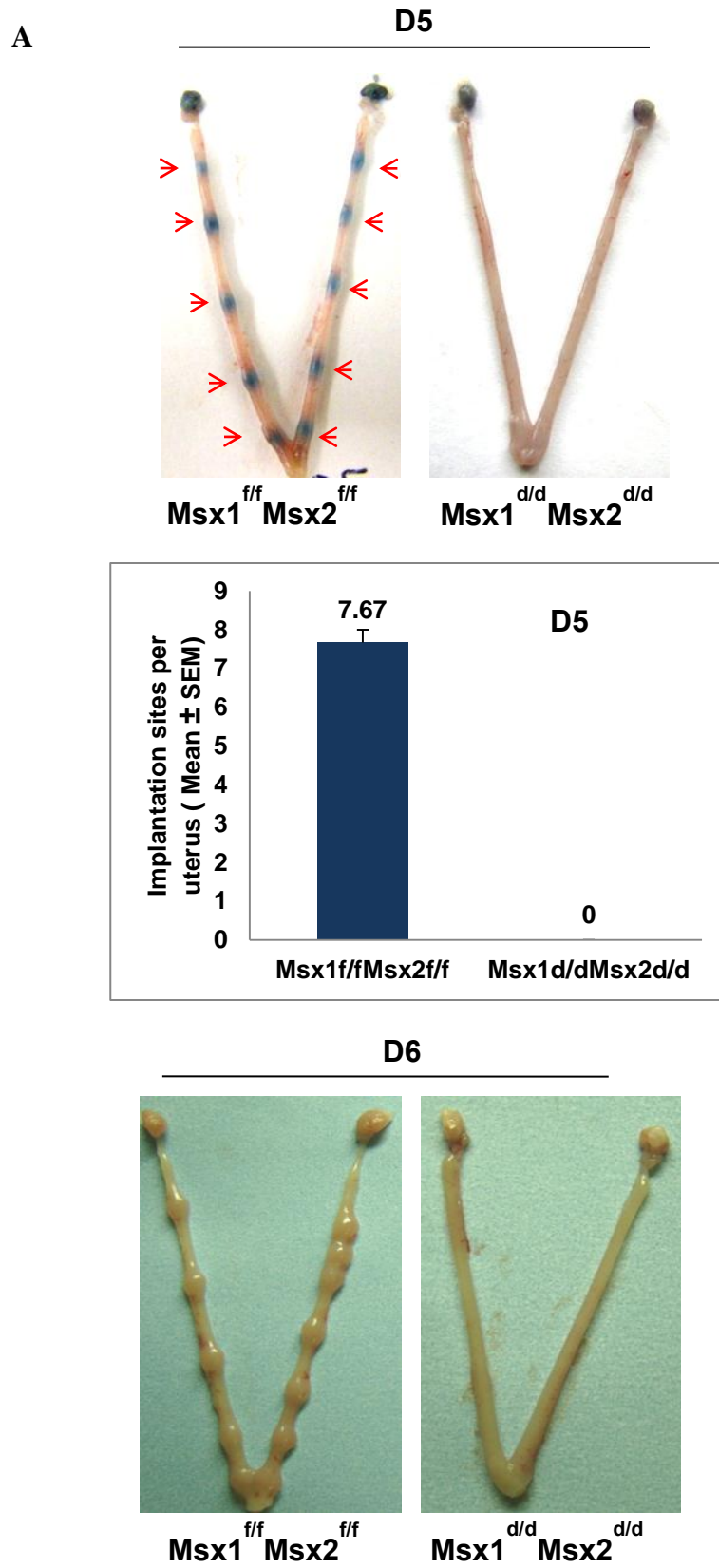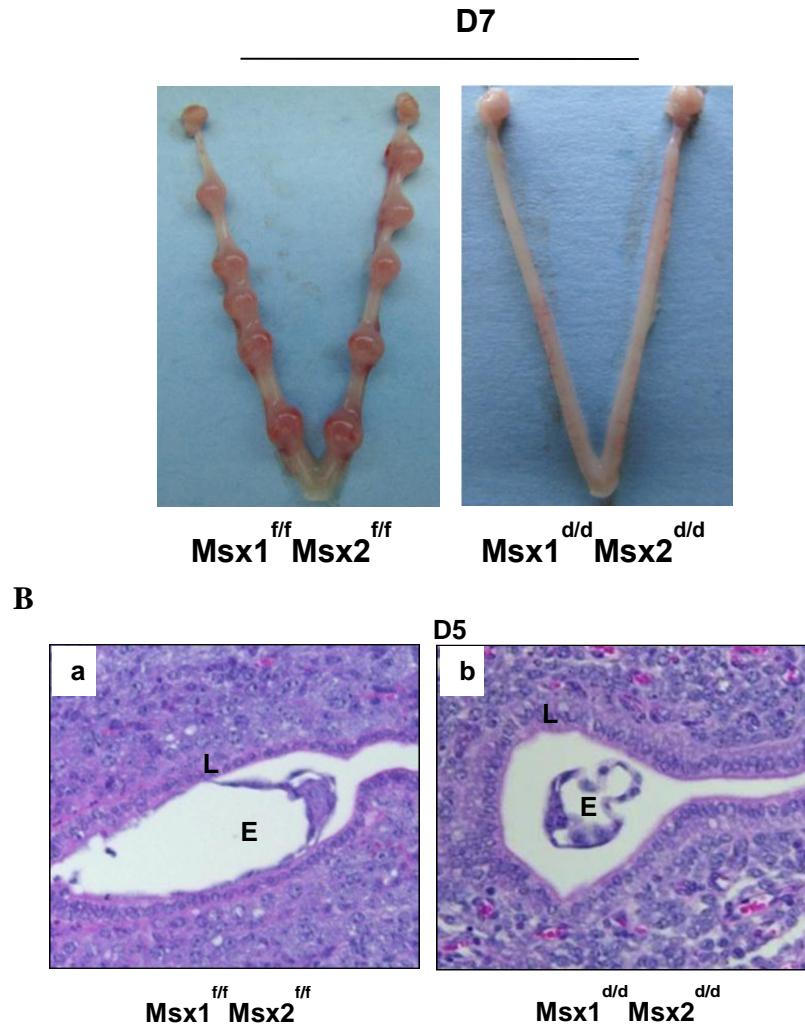
Figure 5 (Contd.) Lack of uterine *Msx*1 and *Msx*2 causes implantation failure

A. Embryo implantation sites were examined in *Msx1^{f/f}Msx2^{f/f}* and *Msx1^{d/d}Msx2^{d/d}* mice by the vascular permeability assay, which can be scored as distinct blue bands (red arrows) following an injection of Chicago blue dye on day 5 of pregnancy (D5, n=6) or direct eye-visualization of implanted embryo on day 6 (D6, n=4) and on day 7 (D7, n=4) of pregnancy. The graph represents the quantification of implantation sites in *Msx1^{f/f}Msx2^{f/f}* and *Msx1^{d/d}Msx2^{d/d}* mice on day 5 of pregnancy. **B.** Failure of embryo attachment in *Msx1^{d/d}Msx2^{d/d}* uteri. Histological analysis of uterine sections obtained from *Msx1^{f/f}Msx2^{f/f}* (a) and *Msx1^{d/d}Msx2^{d/d}* (b) mice on day 5 (n=3) of pregnancy by Hematoxylin and Eosin staining. Note the intimate contact between embryo and luminal epithelium in *Msx1^{f/f}Msx2^{f/f}* mice and the free floating embryo in the uterine lumen of *Msx1^{d/d}Msx2^{d/d}* mice. L and E indicate luminal epithelium and embryo respectively.

49

**Figure 6 Enhanced ERα activity in the luminal epithelium of *Msx1^{d/d}Msx2^{d/d}* uteri**

A

Msx1^{f/f}Msx2^{f/f}   Msx1^{d/d}Msx2^{d/d}

PR

ER

pERα
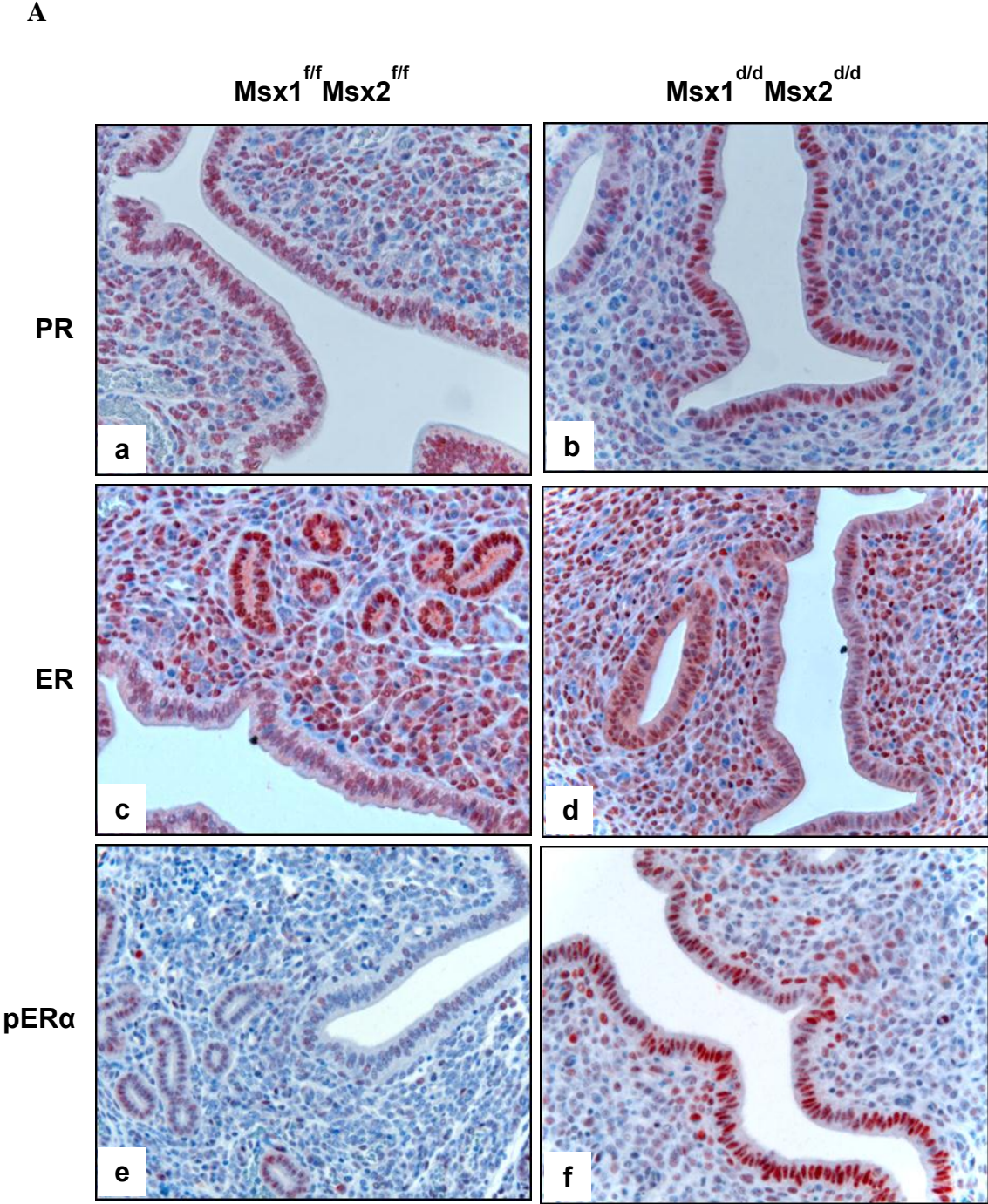
B
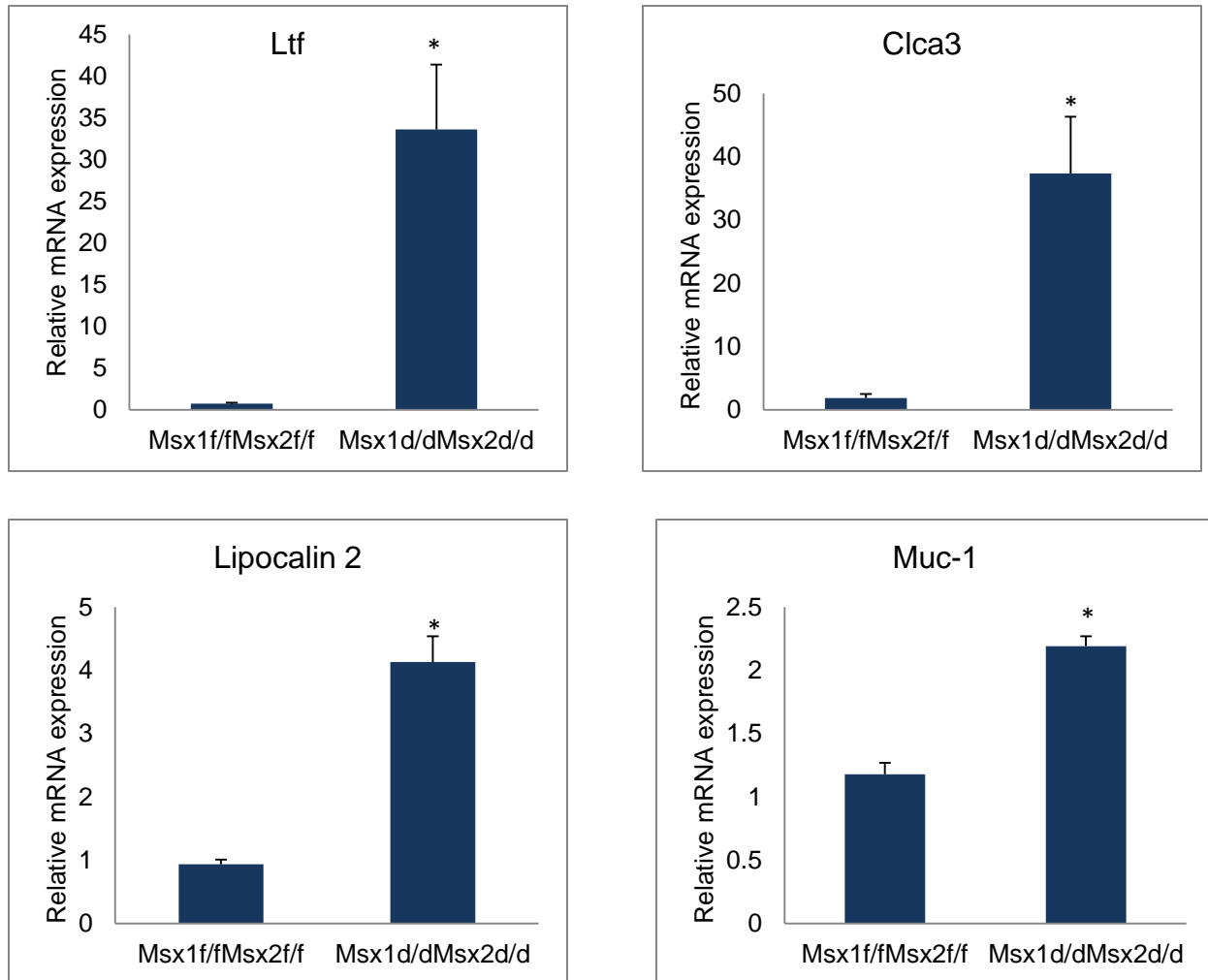
Figure 6 (Contd.) Enhanced ERα activity in the luminal epithelium of *Msx1$^{d/d}$Msx2$^{d/d}$* uteri

A. Uterine sections obtained from *Msx1$^{f/f}$ Msx2$^{f/f}$* (left panel) and *Msx1$^{d/d}$Msx2$^{d/d}$* (right panel) mice on day 4 of pregnancy were subjected to IHC using antibodies against PGR (top panel, a and b), ESR1 (middle panel, c and d) and phospho-ESR1 (lower panel, e and f). **B.** Real-time PCR was performed to analyze the expression of E-regulated genes, lactotransferrin *(Ltf)*, Clca3, lipocalin2 and Muc-1 in uteri of *Msx1$^{f/f}$Msx2$^{f/f}$* and *Msx1$^{d/d}$Msx2$^{d/d}$* mice on day 4 of pregnancy. The level of *Ck18* was used as internal control to normalize gene expression. The data are represented as the mean fold induction ± SEM, *p<0.05.
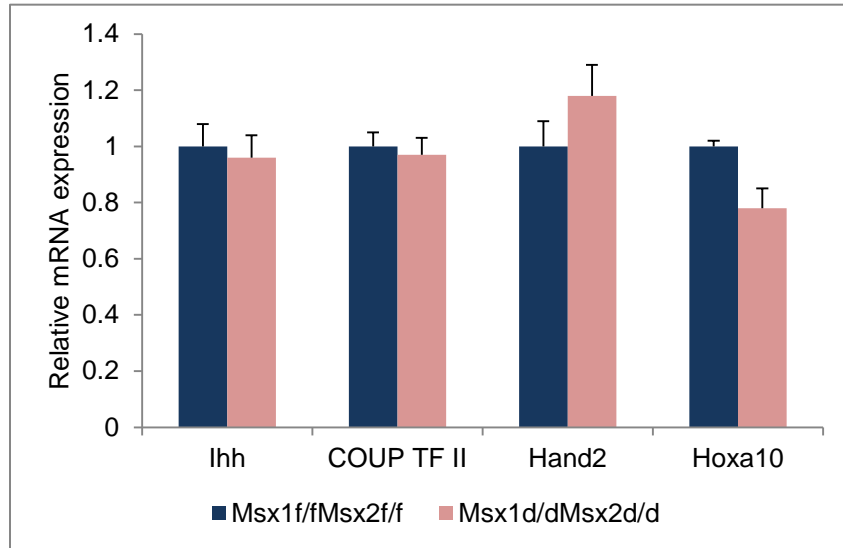
Figure 7 Progesterone signaling is not altered in Msx1^{d/d}Msx2^{d/d} mice uteri

Real-time PCR was performed to analyze the expression of P-regulated genes, Ihh, COUP-TF II, Hand2 and Hoxa10, in uteri of *Msx1^{f/f}Msx2^{f/f}* and *Msx1^{d/d}Msx2^{d/d}* mice on day 4 of pregnancy. The level of *Rplp0* or *Ck18* was used as internal control to normalize gene expression.

Figure 8 Lack of uterine receptivity in *Msx1$^{d/d}$Msx2$^{d/d}$* mice

A

Msx1$^{f/f}$Msx2$^{f/f}$ Msx1$^{d/d}$Msx2$^{d/d}$

D4
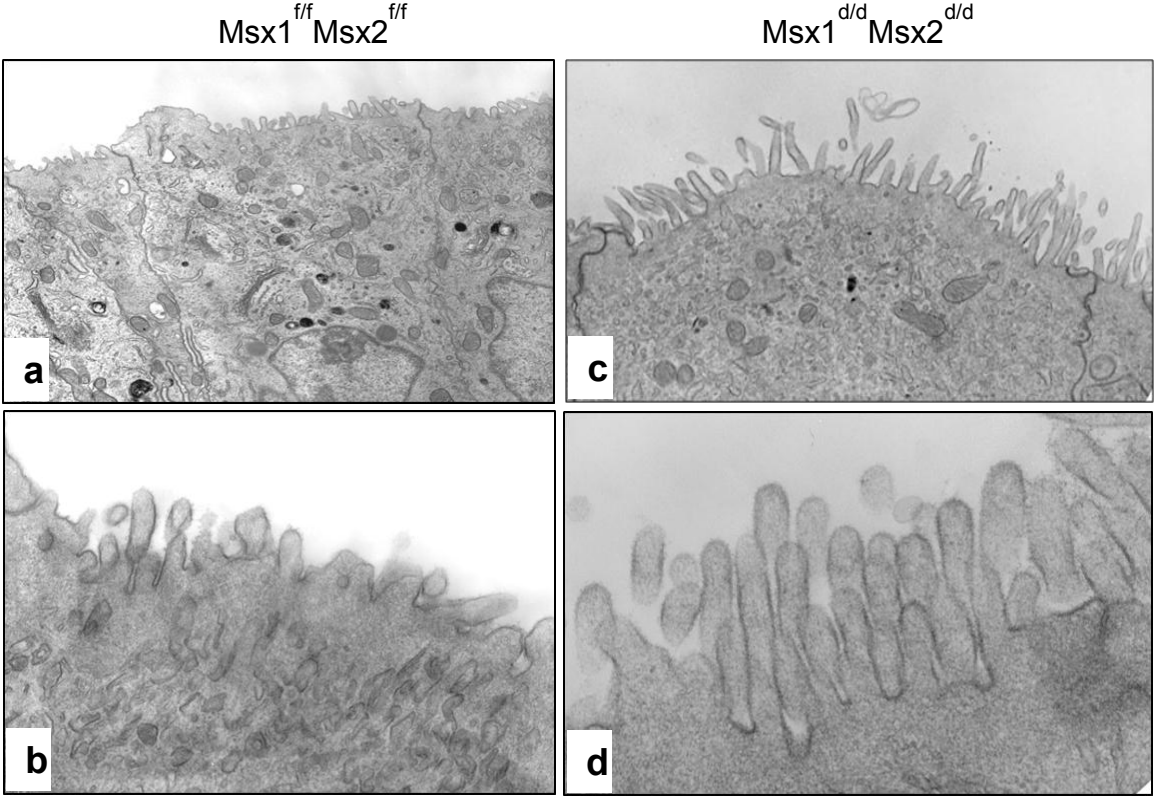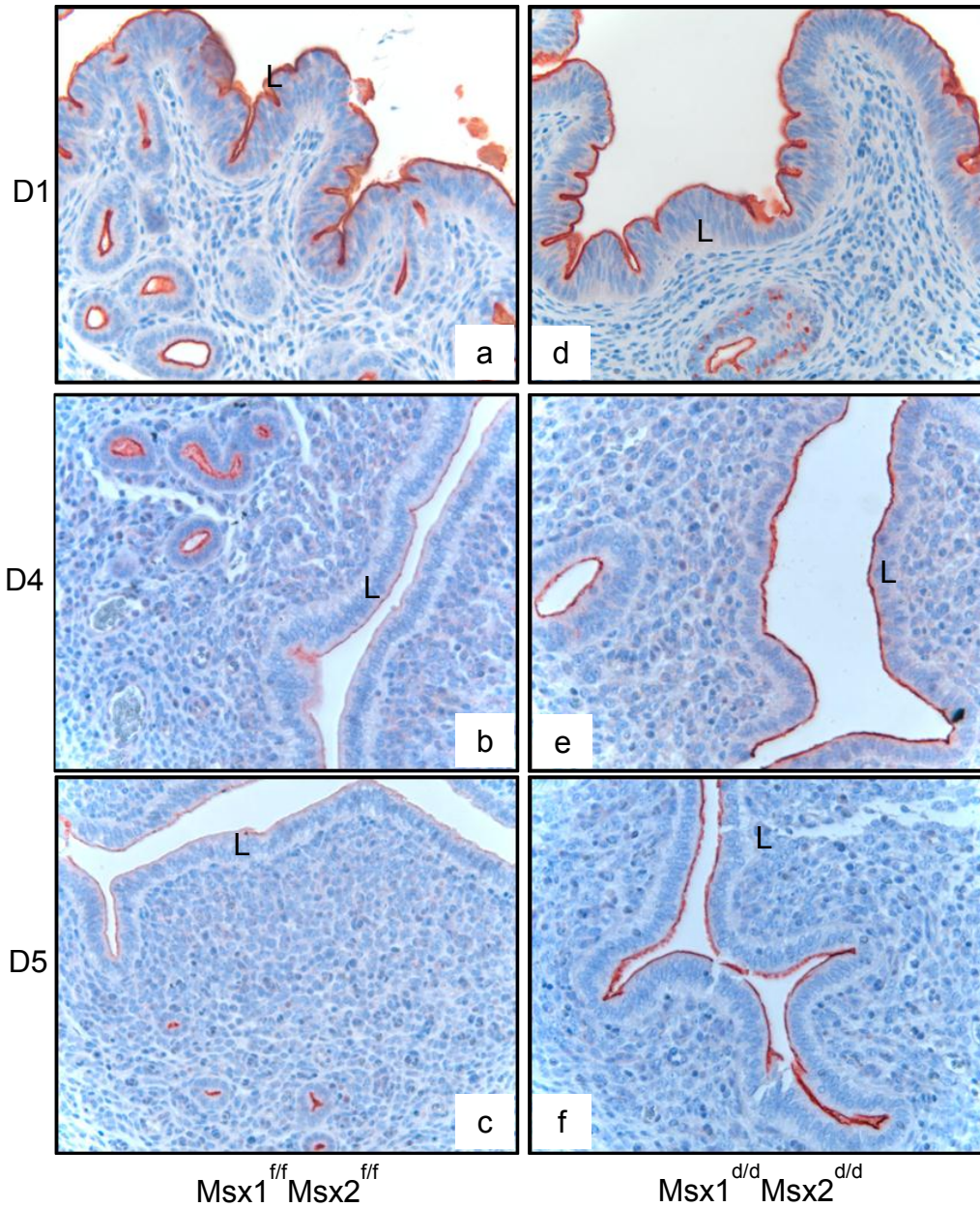
Figure 8 (Contd.) Lack of uterine receptivity in *Msx1^{d/d}Msx2^{d/d}* mice

A. Transmission electron microscopy of uterine sections obtained from *Msx1^{f/f}Msx2^{f/f}* (left panel, a and b) and *Msx1^{d/d}Msx2^{d/d}* (right panel, c and d) mice on day 4 of pregnancy. Panels a and c indicate lower magnification (5Kx) and b and d indicate higher magnification (30Kx). **B.** Immunohistochemical analysis of Muc-1 expression in the uterine sections of *Msx1^{f/f}Msx2^{f/f}* (Left panel) and *Msx1^{d/d}Msx2^{d/d}* Right panel) mice on day 1 (a and d), day 4 (b and e) and day 5 (c and f) of pregnancy. L indicates luminal epithelium.

E-cadherin

Msx1$^{f/f}$Msx2$^{f/f}$ D4   Msx1$^{d/d}$Msx2$^{d/d}$
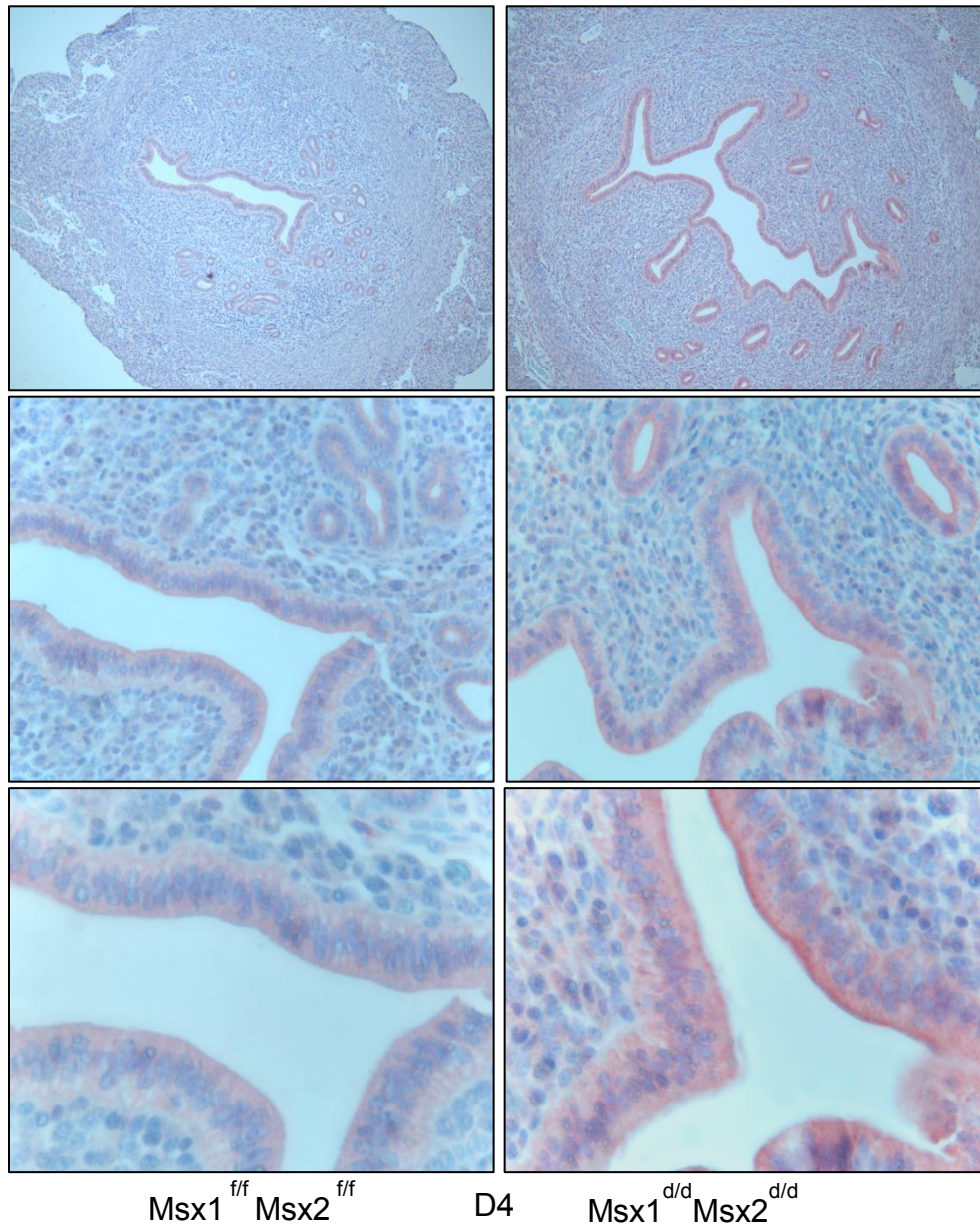
Figure 9 Sustained epithelial cell polarity in Msx1$^{d/d}$Msx2$^{d/d}$ mice

The level of E - cadherin was examined in the uterine sections of *Msx1$^{f/f}$Msx2$^{f/f}$* (left panel) and *Msx1$^{d/d}$Msx2$^{d/d}$* (right panel) mice on day 4 of pregnancy by immunohistochemistry. Magnification: upper panel: 10x, middle panel: 20x and lower panel: 40x.

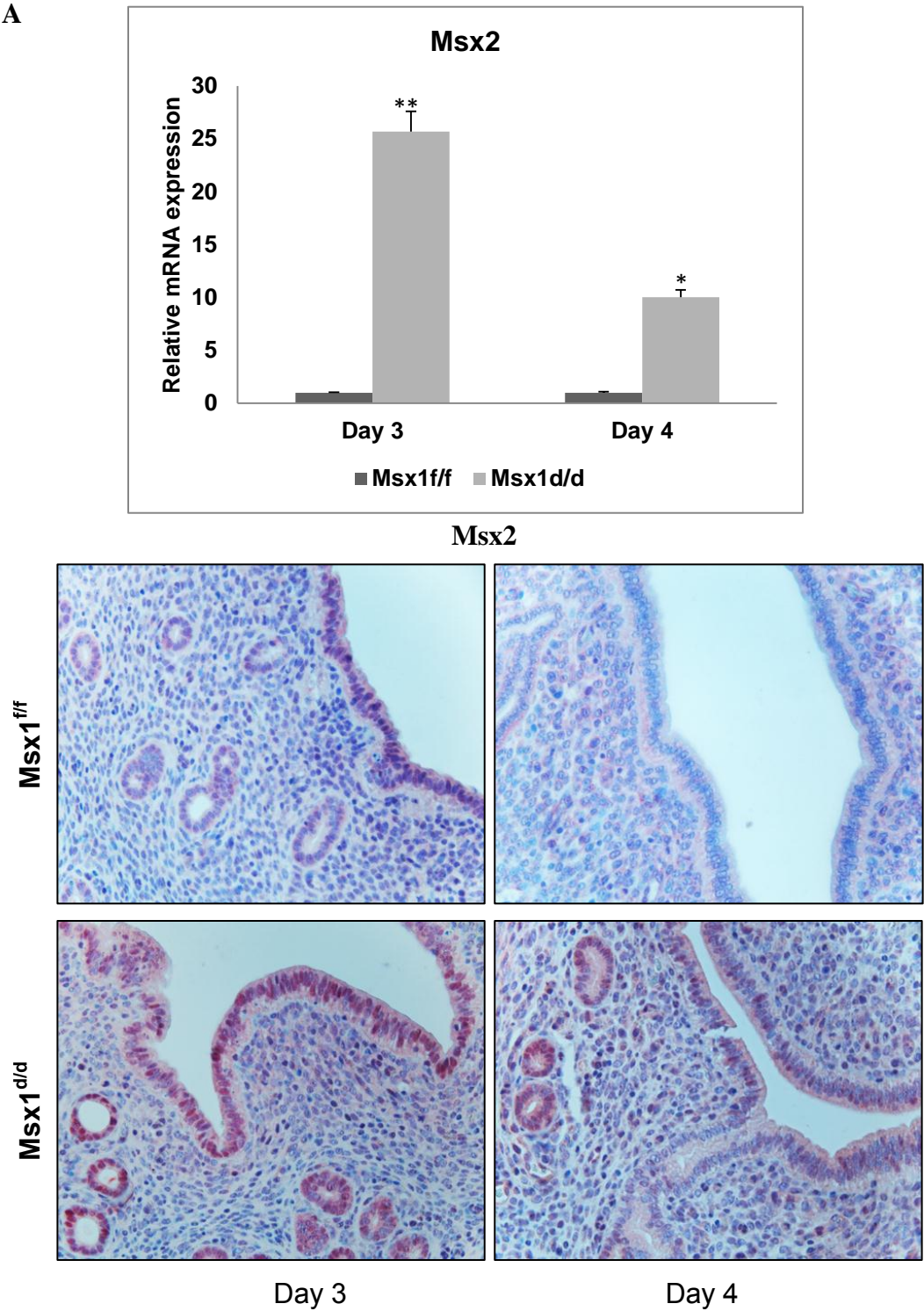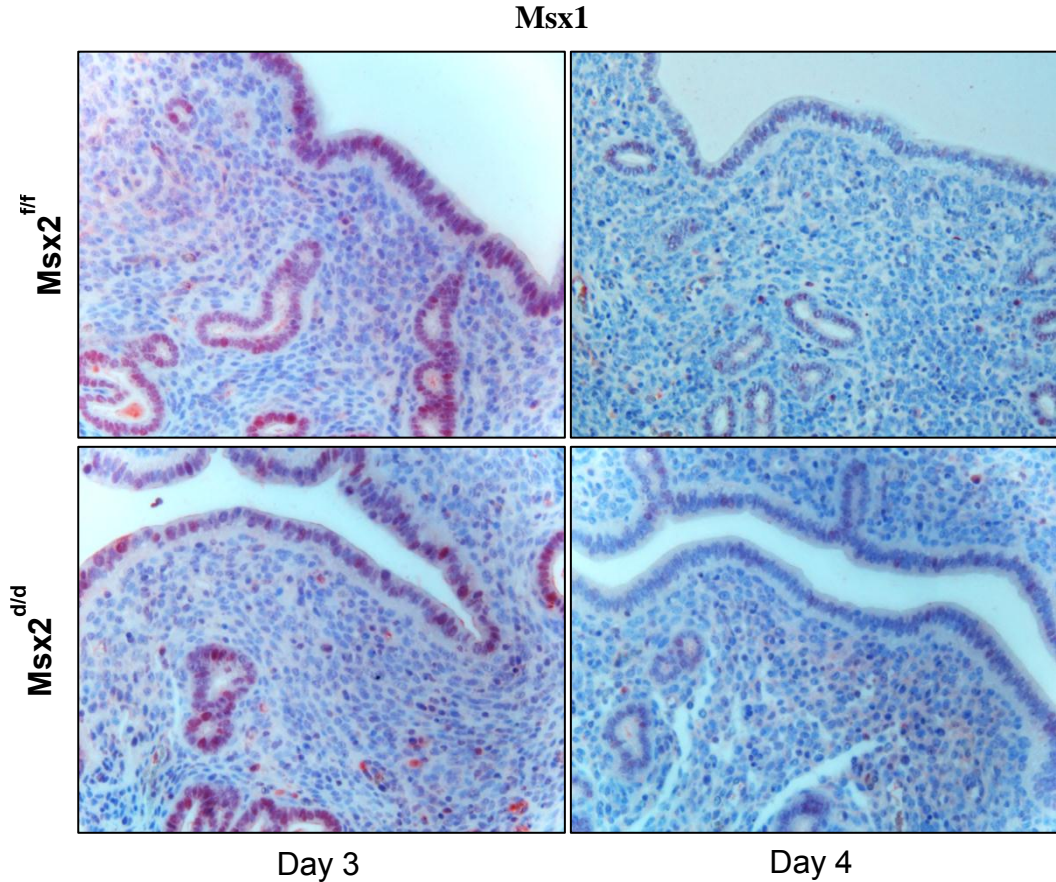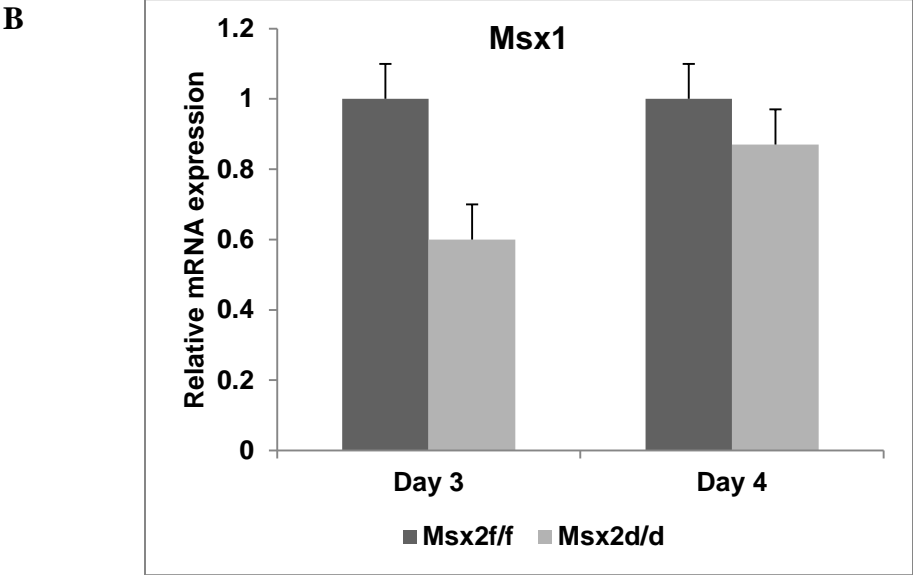**Figure 10 Functional redundancy of Msx genes during uterine receptivity**

A

Msx2

Day 3   Day 4

Figure 10 (Contd.) Functional redundancy of Msx genes during uterine receptivity

B

Msx1

Msx1

Figure 10 Functional redundancy of Msx genes during uterine receptivity

A. Upper Panel: Uterine RNA was purified from $Msx1^{f/f}$ and $Msx1^{d/d}$ mice on day 3 and day 4 of pregnancy and analyzed by real-time PCR. Relative levels of $Msx2$ mRNA expression in uteri of $Msx1^{d/d}$ mice are compared to those in $Msx1^{f/f}$ control mice. Lower Panel: Uterine sections obtained from day 3 and day pregnant $Msx1^{f/f}$ (upper panel) and $Msx1^{d/d}$ (lower panel) mice were subjected to immunohistochemical analysis to detect MSX2. Note the elevated levels of MSX2 immunostaining in the uteri of $Msx1^{d/d}$ mice (*p<0.05; **p<0.005).

B. Upper Panel: Uterine RNA was purified from $Msx2^{f/f}$ and $Msx2^{d/d}$ mice on day 3 and day 4 of pregnancy and analyzed by real-time PCR. Relative levels of $Msx1$ mRNA expression in uteri of $Msx2^{d/d}$ mice are compared to those in $Msx2^{f/f}$ control mice. Lower Panel: Uterine sections obtained from day 3 and day pregnant $Msx2^{f/f}$ (upper panel) and $Msx2^{d/d}$ (lower panel) mice were subjected to immunohistochemical analysis to detect MSX1. Note the elevated levels of MSX1 immunostaining in the uteri of $Msx1^{d/d}$ mice.

CHAPTER III

MSX GENES REGULATE UTERINE RECEPTIVITY BY CONTROLLING PARACRINE SIGNALING BETWEEN UTERINE STROMA AND EPITHELIUM

3.1 ABSTRACT

The mammalian *Msx* homeobox genes, *Msx1* and *Msx2,* encode transcription factors that control organogenesis and tissue interactions during embryonic development. Conditional ablation of both *Msx1* and *Msx2* in the uterus resulted in female infertility due to lack of uterine receptivity during embryo implantation. In these mutant mice ($Msx1^{d/d}Msx2^{d/d}$), the uterine epithelium exhibited persistent proliferative activity. Gene expression profiling of uterine epithelium and stroma of $Msx1^{d/d}Msx2^{d/d}$ mice revealed an elevated expression of several members of the *Wnt* gene family in the pre-implantation uterus. Increased canonical Wnt signaling in the stromal cells activated β-catenin, stimulating the production of a subset of fibroblast growth factors (FGFs) in these cells. The secreted FGFs acted in a paracrine manner via the FGF receptors in the epithelium to promote epithelial proliferation, thereby preventing differentiation of this tissue and creating a non-receptive uterus refractory to implantation. Collectively, these findings delineate a unique signaling network, involving *Msx1/2*, Wnts, and FGFs, which operates in the uterus at the time of implantation to control the mesenchymal-epithelial dialogue critical for successful establishment of pregnancy.

59

3.2 INTRODUCTION

Successful implantation is dependent on a timely progression of a series of biological events during which the embryo undergoes functional interactions with the uterus [1,4,90,118]. Various tissue compartments within the uterus, including luminal epithelium, glandular epithelium, and stroma, undergo sequential proliferation and differentiation as the embryo attaches to the luminal epithelium and invades into the stroma. In mice, the luminal and glandular epithelial cells are proliferative on days 1 and 2 of pregnancy. As pregnancy proceeds, these cells exit from the cell cycle and enter a differentiation program that allows their transition to a receptive state. The stromal cells underneath the epithelium begin to proliferate on day 3 and this proliferation becomes widespread following embryo attachment to the receptive luminal epithelium on day 4 of pregnancy [1,4,90,118]. As the embryo invades through the luminal epithelium into the stromal compartment, the stromal cells differentiate into secretory decidual cells, which support further growth and development of the implanted embryo until placentation ensues [1,4,90,118].

Extensive research over the past decade, using genetically altered mutant mouse models, has identified several factors that critically regulate uterine function in the pre-implantation or post-implantation phases of pregnancy [2,50,52-54,120,123]. However, there is only limited insight into the molecular mechanisms and signaling pathways that interconnect the various cellular compartments of the uterus to achieve receptivity to embryo implantation. Recent studies in our laboratory indicated that a subset of fibroblast growth factors (FGFs) produced by the stromal cells act in a paracrine manner to promote luminal epithelial proliferation [54]. The transcription factor Hand2 suppresses the production of these FGFs and inhibits luminal epithelial

60

proliferation at the time of implantation [54]. Studies by Lee *et al* identified Indian hedgehog (IHH) as an epithelial paracrine factor that acts on the stromal cells to regulate their differentiation [52]. These studies support the concept that maternal competency for implantation is determined by a critical exchange of diffusible signals between the epithelial and stromal compartments, allowing transition of these tissues to proper functional states that permit embryo attachment and invasion. Identification of epithelial or stromal transcription factors and their downstream molecular pathways that control these signals is essential for a clear understanding of the molecular basis of implantation.

In the previous chapter, we described in detail the infertility phenotype of mice lacking uterine *Msx1* and *Msx2*. In this chapter, we provide the molecular mechanism that explains the cause of this infertility in *Msx1*$^{d/d}$*Msx2*$^{d/d}$ mice. Our studies revealed that *Msx*1 and *Msx*2 function by suppressing the expression of several members of the *Wnt* family. In *Msx1/Msx2*-null uterus, continued expression of a subset of WNTs enhances β-catenin signaling in the stroma, which in turn induces the expression of specific members of the fibroblast growth factor (FGF) family in this compartment. One or more of these FGFs act via the FGF receptors in the glandular and luminal epithelial tissues to promote proliferation and prevent differentiation. Lack of differentiation of the glandular epithelial cells results in the failure to express critical factors, such as the leukemia inhibitory factor (LIF), which are critical for implantation. This study, therefore, delineated a novel signaling network downstream of *Msx*1 and *Msx*2, mediating the stromal-epithelial crosstalk critical for successful establishment of pregnancy.

3.3 MATERIALS AND METHODS

Animals

Mice were maintained in the designated animal care facility at the College of Veterinary Medicine of the University of Illinois, Urbana-Champaign, according to the institutional guidelines for the care and use of laboratory animals.

Isolation of uterine epithelial and stromal cells

Uterine epithelial cells were isolated as previously described [219]. Briefly, uterine horns were dissected into 3-4 mm pieces and incubated in a solution of 1% trypsin (Difco, Dertroit, MI) in Hank's balanced salt solution (HBSS) for 90 min at 4^0C and then for 30 min at room temperature. The tissues were then rinsed with 10% FBS. Under a dissecting microscope, each enzyme treated piece of uterus was squeezed by forceps to separate the epithelium from the rest of the uterine tissue. Uterine stromal cells were isolated as previously described [121]. Briefly, uterine horns of pregnant mice were dissected and placed in HBSS containing 6 g/liter dispase and 25g/liter pancreatin for 1 h at room temperature and then 15 min at 37°C to remove the endometrial epithelial clumps. The tissues were then placed in HBSS containing 0.5 g/liter collagenase for 45 min at 37 °C to disperse the stromal cells. After vortexing, the contents were passed through a 70-μm gauze filter (Millipore). The filtrate contained the stromal cells.

Culture of uterine stromal cells

The uterine stromal cells were diluted in Dulbecco's modified Eagle's Medium-F12 medium (DMEM-F12; with 100 unit/liter penicillin, 0.1 g/liter streptomycin, 1.25 mg/liter Fungizone)

with 2% heat-inactivated fetal calf serum. The live cells were counted by trypan blue staining using a hemocytometer. Cells were then seeded in 6-well cell culture plates. The unattached cells were removed by washing several times with HBSS after 2 h, and cell culture was continued after addition of fresh medium supplemented with P (1 μm) and E (10 nm).

Quantitative real time PCR analysis (qPCR)

Uterine tissue was homogenized and total RNA was extracted by using TRIZOL reagent, according to the manufacturer's protocol. cDNA was prepared by standard protocols. The cDNA was amplified to quantify gene expression by quantitative PCR, using gene-specific primers and SYBR Green (Applied Biosystems, Warringtom, UK). The expression level of *RPLP0* (*36B4*) or cytokeratin 18 (*Ck18*) was used as the internal control. For each treatment, the mean Ct and standard deviation were calculated from individual Ct values obtained from three replicates of a sample. The normalized ∆Ct in each sample was calculated as mean Ct of target gene subtracted by the mean Ct of internal control gene. ∆∆Ct was then calculated as the difference between the ∆Ct values of the control and treatment sample. The fold change of gene expression in each sample relative to a control was computed as $2^{-\Delta\Delta Ct}$. The mean fold induction and standard errors were calculated from three or more independent experiments.

Immunohistochemistry

Uterine tissues were processed and subjected to immunohistochemistry as described previously [212]. Briefly, paraffin-embedded tissues were sectioned at 5 μm and mounted on microscopic slides. Sections were deparaffinized in xylene, rehydrated through a series of ethanol washes, and rinsed in water. Antigen retrieval was performed by immersing the slides in 0.1M citrate

buffer solution, pH 6.0, followed by microwave heating for 25 min. The slides were allowed to cool and endogenous peroxidase activity was blocked by incubating sections in 0.3% hydrogen peroxide in methanol for 15 min at room temperature. After washing with PBS for 15 min and the slides were incubated in a blocking solution for 1 h before incubating them in primary antibody overnight at 4°C with antibodies specific for *MSX*1 (Abcam, ab73883), *MSX*2 (Santa Cruz, sc-15396), MUC1 (Novus biological, NB120-15481), Ki67 (BD Pharmingen, 550609), HAND2 (Santa Cruz, sc-9409), phospho-FRS2 (R&D systems, AF5126), phospho-ERK1/2 (Santa Cruz, sc-23759-R), phosphor-AKT (Cell Signaling, 4060s) and active β-catenin (PY489, Developmental Studies Hybridoma Bank, Iowa City, IA 52242). The slides were incubated with the biotinylated secondary antibodies at room temperature for 1h, followed by incubation with horseradish peroxidase-conjugated streptavidin (Invitrogen Corp., MD 21704). The sections were stained in 3-amino-9-ethylcarbazole chromogen (AEC) solution until optimal signal was developed. Sections were counterstained with Mayer's Hematoxylin and examined by bright field microscopy.

siRNA transfection

Control (scrambled) siRNA and siRNA targeted to β-catenin (s438) were purchased from Ambion Inc. The transfection was performed using SilentFect™ Reagent (Bio-Rad), according to the manufacturer's protocol. The stromal cells were isolated from uteri of $Msx1^{f/f}Msx2^{f/f}$ and $Msx1^{d/d}Msx2^{d/d}$ mice on day 3 of pregnancy and transfected with siRNA after 5 − 6 h of culture. The cells were harvested 24 h following transfection and RNA was isolated.

DNA Microarray Analysis

Uterine epithelial and stromal cells were isolated from $Msx1^{f/f}Msx2^{f/f}$ and $Msx1^{d/d}Msx2^{d/d}$ mice on day 4 of pregnancy. Total RNA was prepared from these cells, and hybridized to Affymetrix GeneChip Mouse Genome 430 2.0 array as previously described [50]. They were processed and analyzed according to the Affymetrix protocol.

Statistical Analysis

Statistical analysis was performed by t-test or ANOVA. The values were expressed as mean ± SEM and considered significant if $p < 0.05$.

3.4 RESULTS

Persistent proliferation of luminal epithelium in $Msx1^{d/d}Msx2^{d/d}$ mouse uterus

A hallmark of the receptive state of normal pregnant uterus is the cessation of epithelial cell proliferation prior to implantation (Fig. 11A) [1,4,90,118,220]. Therefore, in $Msx1^{f/f}Msx2^{f/f}$ mice, immunostaining of Ki67, a cell proliferation marker, was undetectable in the uterine luminal and glandular epithelium on day 4 of pregnancy (Fig.11B, panels a and c). However, uterine sections of $Msx1^{d/d}Msx2^{d/d}$ mice exhibited robust immunostaining for Ki67 in the luminal and glandular epithelia (Fig.11B, panels' b and d), indicating persistent epithelial cell proliferation on day 4 in the absence of *Msx1* and *Msx2*.

Endometrial glandular dysfunction in $Msx1^{d/d}Msx2^{d/d}$ mouse uterus

Previous studies indicated that the ability of the glandular epithelium to undergo differentiation and produce factors, including leukemia inhibitory factor (LIF) [44], Foxa2 [80], and Spink3 [81], is critical for implantation. As shown in Fig.12, the expression of these factors was drastically reduced in uteri deficient of *Msx*1 and *Msx*2.

Collectively, these findings indicated that persistent proliferation of luminal and glandular epithelia results in impaired epithelial transition from a proliferative to a non-proliferative state that allows proper differentiation. This impairment is a major contributor to implantation failure in $Msx1^{d/d}Msx2^{d/d}$ mice.

Enhanced WNT/β-catenin signaling in the *Msx1$^{d/d}$Msx2$^{d/d}$* mouse uterus

To gain insights into the mechanisms underlying the implantation defect of uteri lacking *Msx1* and *Msx2*, we isolated luminal epithelial and stromal cells from *Msx1$^{f/f}$Msx2$^{f/f}$* and *Msx1$^{d/d}$Msx2$^{d/d}$* uteri on day 4 of pregnancy and performed compartment-specific gene expression profiling, using Affymetrix Mouse GeneChip arrays. Interestingly, our study revealed up-regulation of WNTs in *Msx1$^{d/d}$Msx2$^{d/d}$* uteri compared to *Msx1$^{f/f}$Msx2$^{f/f}$* uteri. The microarray data (GEO accession #GSE30969) were validated by real-time PCR analysis. In the epithelial compartment of *Msx1$^{d/d}$Msx2$^{d/d}$* uteri, we observed stimulated expression of mRNAs corresponding to several Wnts, including *Wnt4*, *Wnt7a* and *Wnt7b* (Fig.13A). In the stromal cells of *Msx1$^{d/d}$Msx2$^{d/d}$* uteri, we observed marked up-regulation of *Wnt4* and *Wnt5a* mRNAs (Fig.13B).

We next investigated whether the increased expression of the Wnt ligands in the uteri of *Msx1$^{d/d}$Msx2$^{d/d}$* mice is translated into increased activation of the Wnt signaling pathway. Wnt signals are transduced via the canonical Wnt/β-catenin-dependent pathway (Fig. 13C) or the non-canonical β-catenin-independent pathways [221-223]. When we examined the expression of active β-catenin in uterine sections of *Msx1$^{f/f}$Msx2$^{f/f}$* and *Msx1$^{d/d}$Msx2$^{d/d}$* mice on day 4 of pregnancy, we noted comparable levels of nuclear expression of active β-catenin in luminal and glandular epithelium in both genotypes (Fig.13D). However, a marked increase in the level of nuclear β-catenin was observed in the stromal cells of *Msx1Msx2*-null uteri, indicating that canonical β-catenin signaling is markedly enhanced in the *Msx1Msx2*-ablated stroma (Fig.13D).

Enhanced expression of FGF growth factors in the *Msx1^{d/d}Msx2^{d/d}* uterine stromal cells

In addition to Wnts, gene expression profiling of stromal cells from *Msx1^{f/f}Msx2^{f/f}* and *Msx1^{d/d}Msx2^{d/d}* uteri on day 4 of pregnancy also revealed that the levels of mRNAs encoding several members of the FGF family, such as *Fgf1*, *Fgf10*, *Fgf18* and *Fgf21*, were elevated as a consequence of *Msx1* and *Msx2* deletion (Fig.14A). However, the mRNA levels of these FGFs were not altered in the epithelial cells. The expression of mRNAs corresponding to several other FGF family members as well as other growth factors, such as TGFβ, EGF, IGF-1, and HBEGF, which are expressed in the uterus during pregnancy, was not significantly altered in the uterine stroma of *Msx1^{d/d}Msx2^{d/d}* mice (Fig.14A and 14B).

WNT regulates FGF in the *Msx1^{d/d}Msx2^{d/d}* mouse uterus

Interestingly, previous studies indicated that the production of FGFs, particularly FGF10 and FGF18, is stimulated downstream of canonical Wnt signaling during certain cellular processes, such as chick embryo development, bone development and human hepatocellular carcinoma [193,195,224], raising the possibility that the enhanced β-catenin signaling seen in uterine stromal cells of *Msx1^{d/d}Msx2^{d/d}* mice may drive the increased FGF synthesis in these cells. To test this possibility, primary stromal cells were isolated from uteri of *Msx1^{f/f}Msx2^{f/f}* and *Msx1^{d/d}Msx2^{d/d}* mice on day 3 of pregnancy and transfected with siRNA targeted specifically to the β-catenin mRNA. We observed that treatment with this siRNA resulted in more than 80% reduction in β-catenin mRNA expression compared to cells transfected with control (scrambled) siRNA (Fig.15). Most importantly, as shown in Fig.15, siRNA-mediated down regulation of β-catenin in the stromal cells led to a significant reduction in expression of FGF10, FGF18, and FGF21. However, the expression of FGF1 remained unaltered in cells treated with β-catenin

siRNA. These results indicated that canonical Wnt signaling via β-catenin regulates the expression of a specific subset of FGF family members in the uterine stromal cells.

Enhanced FGF receptor (FGFR) signaling in the uterine epithelium of *Msx1$^{d/d}$Msx2$^{d/d}$* mice

We next investigated whether the increased production of FGFs downstream of Wnt signaling leads to enhanced FGF receptor (FGFR) signaling in the uteri of *Msx1$^{d/d}$Msx2$^{d/d}$* mice. Stimulation of the cell surface FGFRs by FGF ligands leads to phosphorylation of specific tyrosine residues in a critical docking protein, FGFR substrate 2 (FRS2), which guides the assembly of distinct multi-protein complexes, leading to the activation of either MAP kinase or AKT signaling cascades (Fig. 16A) [225-227]. We, therefore, investigated the state of activation of the FGFR signaling pathway in the uteri of *Msx1$^{f/f}$Msx2$^{f/f}$* and *Msx1$^{d/d}$Msx2$^{d/d}$* mice by monitoring the level of phospho-FRS2. We observed only low level of phospho-FRS2 in the uterine luminal or glandular epithelium or stroma of *Msx1$^{f/f}$Msx2$^{f/f}$* mice on day 4 of pregnancy (Fig.16B, panels a-c). In contrast, a marked elevation in the level of phospho-FRS2 was observed specifically in the luminal and glandular epithelium, but not in the stroma (Fig.16B, panels d-f) of *Msx1Msx2*-null uteri, indicating that FGFR signaling is increased in uterine epithelium in the absence of *Msx*1/*Msx*2. Since the FGFs are produced in the stroma of these mutant uteri, this finding suggests that they act in a paracrine fashion via the FGFRs on the epithelial cells.

The kinases ERK1/2 and/or PI3K/AKT are known to be activated downstream of FGF receptor signaling [225]. We, therefore, investigated whether these pathways were activated in the epithelia of *Msx1Msx2*-ablated uteri. As shown in Fig.16C, phospho-ERK1/2 (pERK) was undetectable in the uterine epithelium of *Msx1$^{f/f}$Msx2$^{f/f}$* mice on day 4 of pregnancy (panels a-c).

However, a dramatic increase in the immunostaining of pERK1/2 was seen in uterine epithelium of *Msx1Msx2*-null mice on day 4 of pregnancy (panels d-f). In contrast, the expression of phospho-AKT was undetectable in both of these genotypes (Fig.16D), suggesting that the ERK1/2 pathway, rather than the PI3K/AKT pathway, is the key downstream mediator of enhanced FGFR signaling in *Msx1Msx2*-null uteri.

To examine whether the elevated mitogenic activity in the luminal epithelium of $Msx1^{d/d}Msx2^{d/d}$ uteri on day 4 of pregnancy is indeed a result of the enhanced FGF signaling, we administered PD173074, a FGFR-specific inhibitor [228], or vehicle into uterine horns of $Msx1^{d/d}Msx2^{d/d}$ mice in the pre-implantation phase. As shown in Fig.16E, the epithelia of vehicle-treated uterine horns of these mice showed strong expression of phospho-FRS2 in on day 4 of pregnancy (panel a). Treatment with the FGFR inhibitor led to a marked reduction in the level of phospho-FRS2 in the uterine epithelium (Fig.16E, panel b). Concomitant with this down regulation of FGFR signaling, we observed a decline in the proliferative activity of *Msx1Msx2*-null uterine epithelia as well as down-regulation of MUC-1 expression (Fig.16E, panels c-f). Collectively, these results are consistent with the hypothesis that increased FGF production, downstream of Wnt-β-catenin pathway in *Msx1Msx2*-null uterine stroma, stimulates epithelial proliferation by activating FGFR-ERK1/2 signaling pathway. The proliferative epithelium fails to undergo differentiation, resulting in persistent expression of MUC-1, which acts as a major barrier to embryo attachment and implantation.

3.5 DISCUSSION

Msx1 and *Msx2* are critical regulators of the receptive state of the uterus during implantation. Particularly interesting is the finding that uterine expression of *Msx1Msx2* influences the activity of β-catenin in the stroma, which in turn regulates epithelial activity during early pregnancy. The identity of the factors that function downstream of *Msx1Msx2* to regulate stromal-epithelial cross-talk during implantation was revealed by compartment-specific gene expression profiling of epithelial and stromal cells collected from control and *Msx1Msx2*-ablated uteri. We found that, in the absence of *Msx1* and *Msx2* in the uterus, the expression of several WNT ligands was up-regulated in uterine epithelial and stromal cells. While the expression of WNT4, WNT7a, and WNT7b was elevated in the epithelium, that of WNT4 and WNT5a increased in the stroma. With the exception of WNT5a, these WNTs are known to signal via the canonical pathway to release β-catenin from a complex with GSK3β, leading to its stabilization and nuclear accumulation [221,222]. Nuclear β-catenin then associates with TCF/LEF family transcription factors to regulate cellular gene expression. Consistent with this scenario, a marked increase in the level of active β-catenin was observed in uterine stromal cells of *Msx1$^{d/d}$Msx2$^{d/d}$* uteri, while the active β-catenin levels remained unaltered in the surface epithelium. Our results indicated that canonical Wnt signaling is specifically enhanced in the stromal cells as a consequence of *Msx1Msx2* ablation. How does *Msx1Msx2* regulate the WNTs and whether the β-catenin activation in the stromal cells is driven by WNTs originating in the epithelium or stroma, is unclear.

An important finding of this paper is that, in addition to WNTs, the expression of several members of the FGF family is stimulated in the stromal cells of *Msx1$^{d/d}$Msx2$^{d/d}$* uteri. The FGFs belong to a large family of growth factors, comprising 23 distinct members [225-227]. We

71

observed that a subset of FGFs, including FGF1, FGF10, FGF18 and FGF21, exhibited marked up-regulation in uterine stroma of $Msx1^{d/d}Msx2^{d/d}$ mice, indicating that the expression of these growth factors are normally suppressed by $Msx1$/$Msx2$. Interestingly, previous studies have shown that TCF/LEF, activated downstream of WNT-β-catenin signaling in colorectal cancer cells, binds to the promoter regions of FGF18 and FGF20 [193,195,229]. Studies have also shown that, in the chick embryo, WNT-β-catenin signaling triggered the synthesis of FGF8 and FGF10, which control the initiation of limb development [193]. These previous findings suggested that WNT-activated β-catenin regulates the expression of a subset of FGFs [193]. In the present study, we provide direct evidence that active β-catenin regulates the synthesis of the FGFs, particularly FGF10, FGF18, and FGF21, in the stromal cells, uncovering a link between the WNT and FGF signaling pathways in the endometrium. The precise mechanism by which active β-catenin regulates the expression of these FGFs in uterine stromal cells remains to be determined.

The FGFs exert their paracrine responses by binding to FGFRs on the surface of the target cells and activating the receptor tyrosine kinase pathway. It is well documented that signaling via FGFRs leads to tyrosine phosphorylation of the docking protein FRS2, followed by the recruitment of multiple distinct complexes, which results in activation of Ras/ERK/MAP kinase and/or PI3 kinase/AKT signaling pathways in a variety of cell types [225,227]. In uteri lacking $Msx1$ and $Msx2,$ the accumulation in the uterine epithelium of phospho-FRS2, a key indicator of FGF signaling, indicated activation of FGFR signaling. Bazer and his coworkers have previously reported that the FGFRs are activated in ovine uterine epithelia of sheep in response to the secretion of FGF7 and FGF10 from the progesterone-primed mesenchyme and proposed that

these factors are potential regulators of the maternal-fetal interactions [230,231]. However, in the mouse uterus, the expression of FGF10, FGF18, and FGF21 is suppressed during the receptive phase of implantation. The expression of these factors is induced in the absence of *Msx*1 and *Msx*2, and the consequent increase in FGFR signaling is associated with the lack of uterine receptivity and implantation failure in *Msx1*$^{d/d}$*Msx2*$^{d/d}$ mice.

The central hypothesis of this chapter is that *Msx1Msx2* controls uterine receptivity at the time of embryo implantation by regulating epithelial function. During normal pregnancy in mice, the uterus attains receptive status on day 4 of gestation when the luminal and glandular epithelia cease to proliferate and begin to differentiate. Our study suggests that, in the absence of *Msx*1 and *Msx2*, the uterine stroma produces a subset of FGFs, which act via the FGFRs to stimulate the ERK1/2 kinase pathway in both luminal and glandular epithelia. As a consequence, the uterine epithelia of *Msx1*$^{d/d}$*Msx2*$^{d/d}$ mice remain proliferative and fail to undergo transformation to the receptive state that allows embryo attachment to initiate implantation. The activation of the ERK1/2 pathway in the epithelium also triggers phosphorylation of epithelial ESR1 at serine-118. It is well established that this phosphorylation event is critical for the transcriptional activation of ESR1 [213]. An elevated ERα signaling in the epithelium is, however, detrimental to the implantation process.

Pathways downstream of *Msx1* and *Msx2* also control the synthesis of glandular factors critical for uterine receptivity at the time of implantation. While the uterine luminal epithelium is the initial site of embryo attachment, the glandular epithelium is an important source of paracrine factors required for the establishment and maintenance of pregnancy [76]. As the uterus acquires

73

competency for implantation, the glandular epithelial cells cease to proliferate and undergo differentiation to express factors, such as LIF and FOXA2, which are critical for embryo implantation [44,80]. Presumably due to enhanced WNT and FGF signaling in $Msx1^{d/d}Msx2^{d/d}$ uteri, the glandular epithelial cells remain proliferative and fail to express LIF and FOXA2. Consistent with this hypothesis, a recent study has shown that expression of constitutively active β-catenin in mouse endometrium leads to enhanced proliferation and glandular hyperplasia [89].

We recently reported that the transcription factor HAND2 suppresses the production of a subset of FGFs, which act in a paracrine manner to stimulate the proliferation of the luminal epithelium [54]. Conditional deletion of *Hand2* in the uterus also results in the failure of implantation due to impaired uterine receptivity caused by increased production of FGFs in the stroma. The uterine phenotype of *Hand2* deletion is remarkably similar to those of *Msx1Msx2* ablation. We, therefore, examined whether *Hand2* is regulated by *Msx1Msx2* or vice versa. Surprisingly, our studies showed that the loss of *Msx1* or *Msx2* or both did not affect *Hand2* expression in the uterus during implantation (Fig.17). Similarly, *Msx1Msx2* expression is unaltered in *Hand2*–null uteri (Fig.18). Furthermore, while *Hand2* coordinately suppresses the expression of FGF1, FGF2, FGF9 and FGF18, *Msx1Msx2* inhibits the expression of FGF1, FGF10, FGF18, and FGF21. Although these results suggest that one or more of these FGFs act in a paracrine manner through the epithelial FGFRs to promote epithelial cell proliferation, the contribution of each these FGFs remain unclear and, therefore, it remains to be determined whether *Hand2* and *Msx1Msx2* function via similar or distinct mechanisms.

In summary, we have uncovered a novel mechanism by which *Msx1Msx2* regulates epithelial function at the time of implantation (Fig. 19). In normal pregnancy, these factors act to repress WNT and β-catenin signaling and inhibit FGF synthesis in the uterine stroma, thereby attenuating the paracrine mechanisms that promote epithelial proliferation. It is also evident that the activation of ERK1/2 kinase pathway downstream of FGFR signaling in the epithelium of *Msx1Msx2*-ablated uteri activates transcriptional function of ESR1, contributing to the non-receptive status of the uterus. Continued analysis of the mechanisms by which *Msx*1 and *Msx2* control the WNT-β-catenin-FGF pathway to direct uterine stromal-epithelial communication will clarify our understanding of the molecular events that underlie uterine receptivity.

3.6 FIGURES

Figure 11 Enhanced proliferation in the uterine epithelium of $Msx1^{d/d}Msx2^{d/d}$ mice
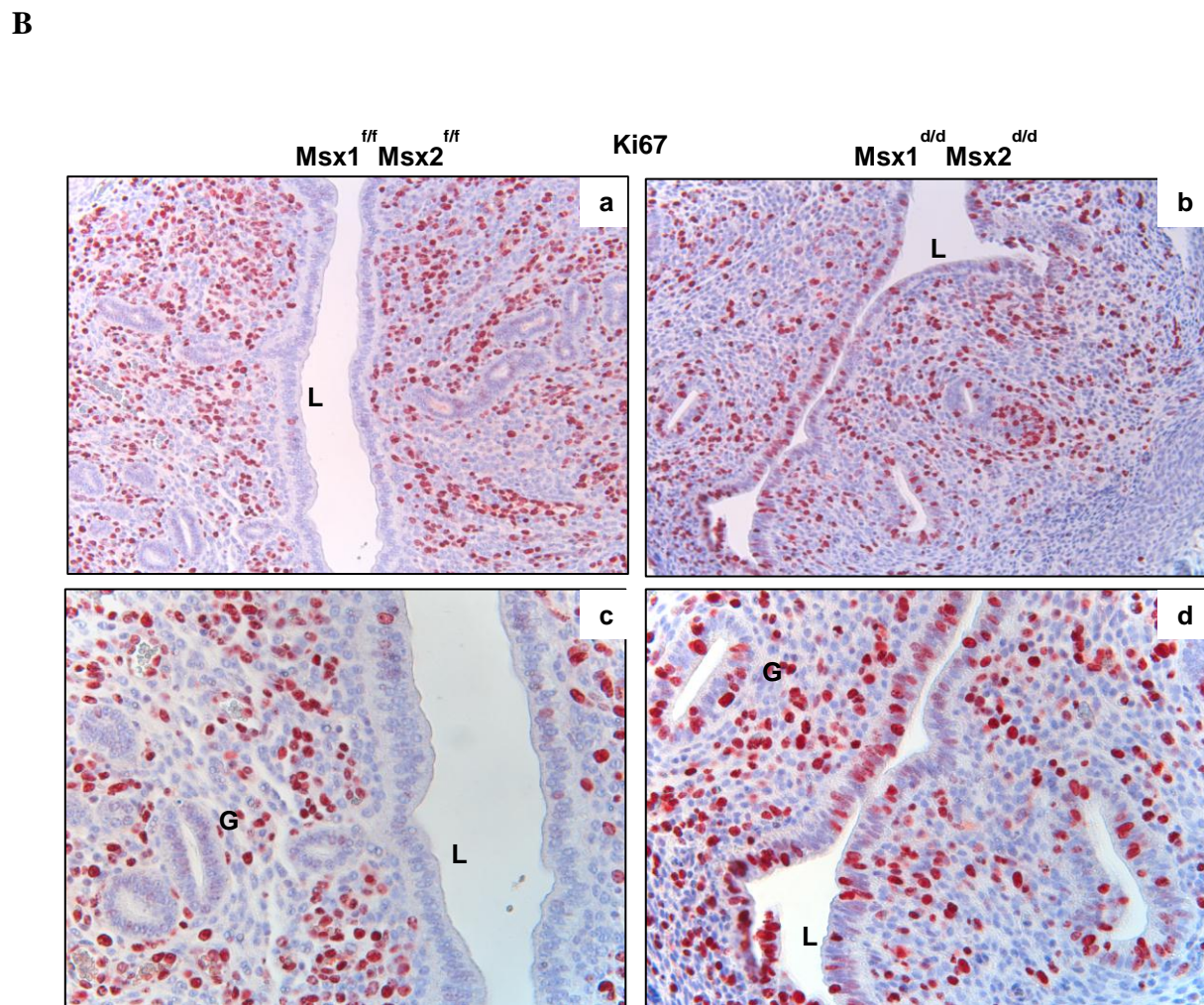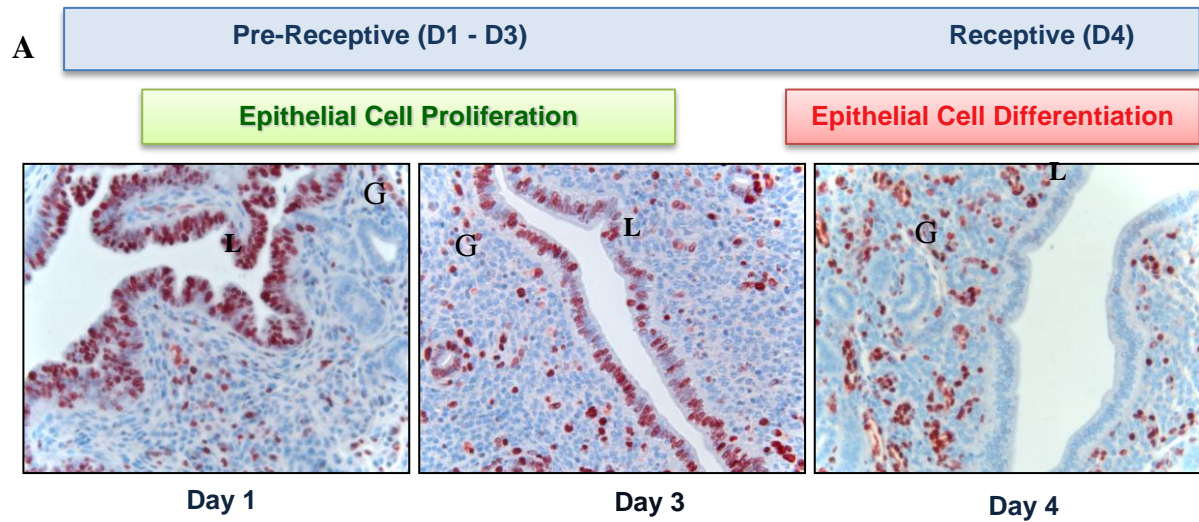
Figure 11 (Contd.) Enhanced proliferation in the uterine epithelium of *Msx1$^{d/d}$Msx2$^{d/d}$* mice

A. Immunohsitochemical localization of Ki67 in the uterine sections of *Msx1$^{f/f}$Msx2$^{f/f}$* mice on days 1, 3 and 4 of pregnancy. L and G indicate luminal epithelium and glandular epithelium respectively. B. Immunohsitochemical localization of Ki67 in the uterine sections of *Msx1$^{f/f}$Msx2$^{f/f}$* (n=5) (left panel, a and c) and *Msx1$^{d/d}$Msx2$^{d/d}$* (n=5) (right panel, b and d) mice on day 4 of pregnancy. Panels a and b indicate lower magnification (20x) and c and d indicate higher magnification (40x). L and G indicate luminal epithelium and glandular epithelium respectively.
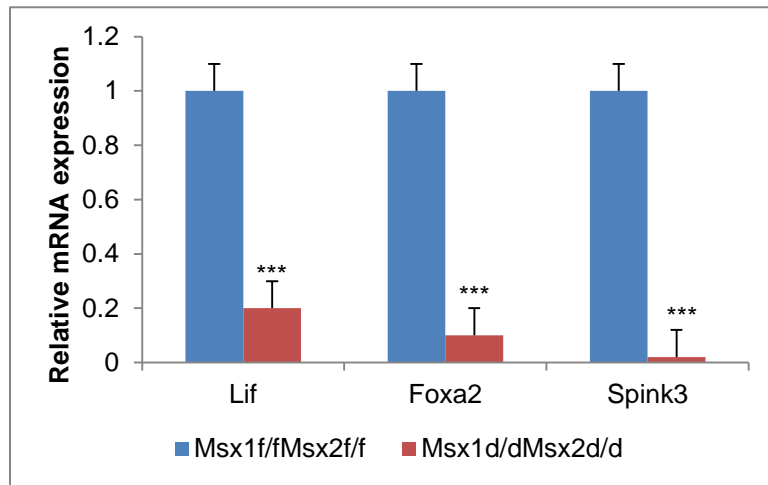
Figure 12 Endometrial glandular dysfunction in *Msx1$^{d/d}$Msx2$^{d/d}$* mice

Real-time PCR was performed to analyze the expression of glandular factors, *Lif*, *Foxa2* and *Spink3* in uteri of *Msx1$^{f/f}$Msx2$^{f/f}$* and *Msx1$^{d/d}$Msx2$^{d/d}$* mice on day 4 of pregnancy. The level of *Ck18* was used as internal control to normalize gene expression. The data are represented as the mean fold induction ± SEM, ***p<0.0001.

Figure 13 Enhanced Wnt/β-catenin signaling in *Msx1$^{d/d}$Msx2$^{d/d}$* mouse uterus

A   **Epithelial cells**
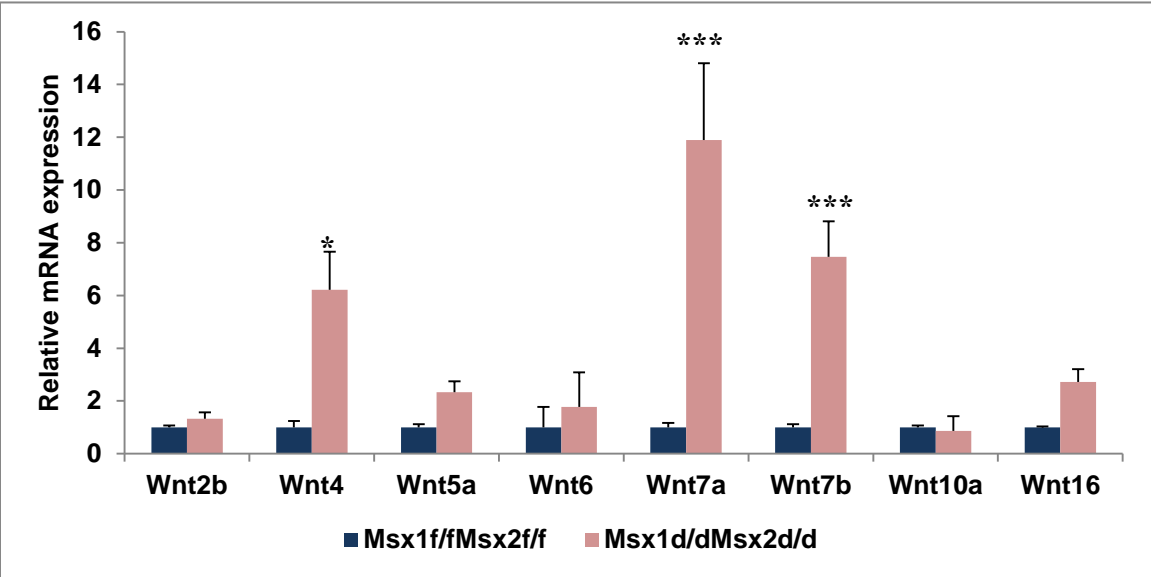
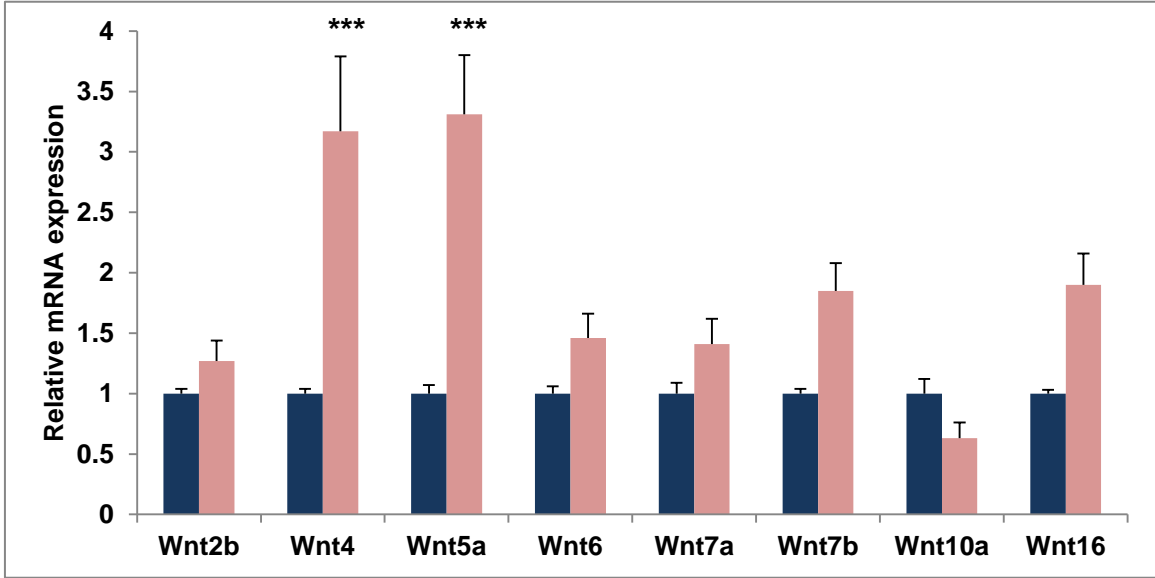**B**   **Stromal cells**

Figure 13 (Contd.) Enhanced Wnt/β-catenin signaling in *Msx1$^{d/d}$Msx2$^{d/d}$* mouse uterus

C

Wnt/β-catenin signaling pathway

D

Msx1^{f/f} **Msx2**^{f/f}

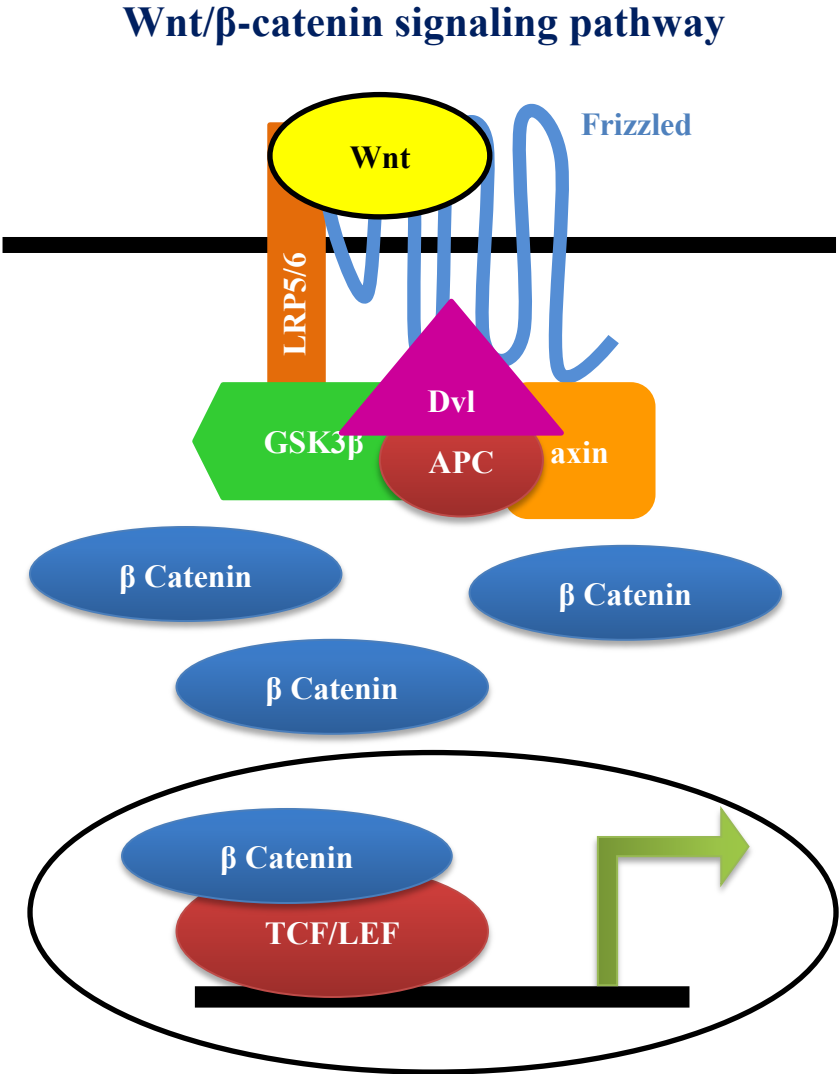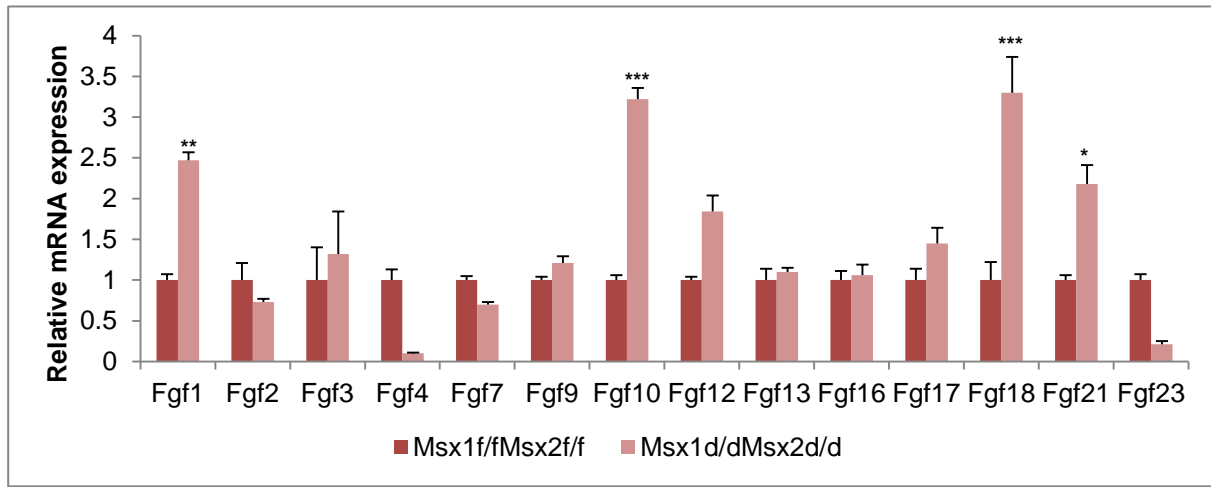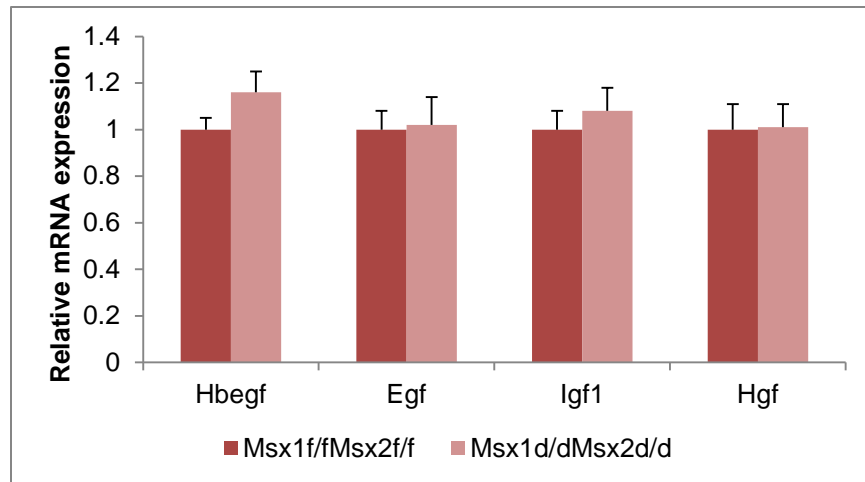**Msx1**^{d/d} **Msx2**^{d/d}

D4

Active β-catenin
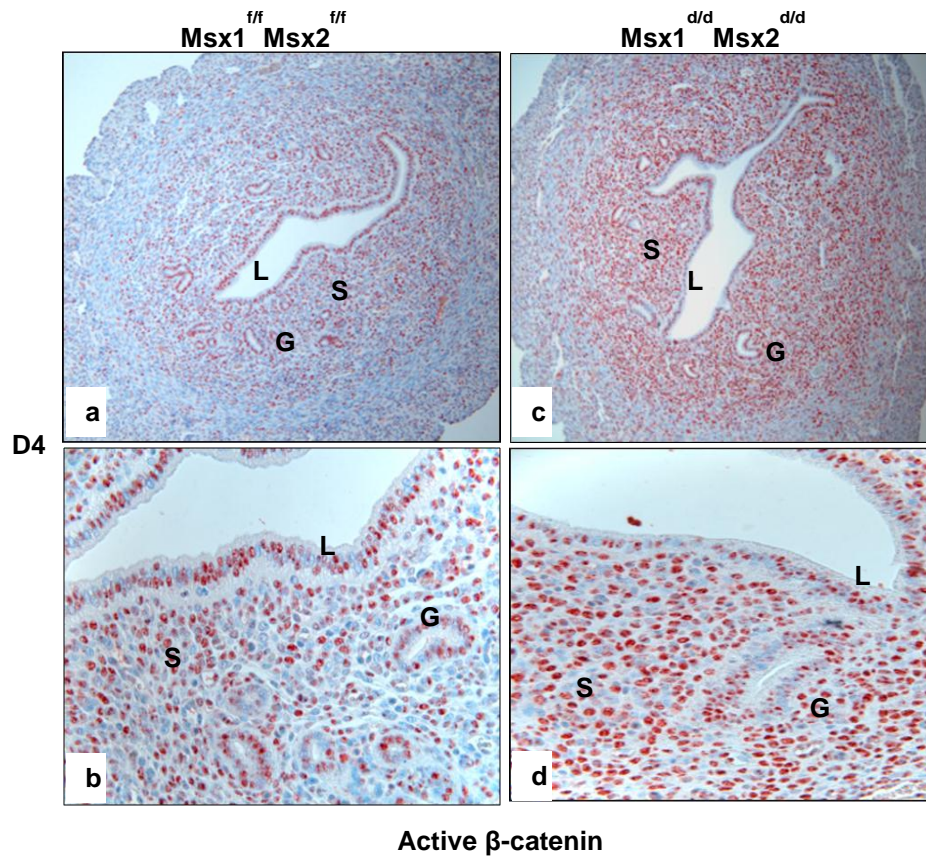
**Figure 13 (Contd.) Enhanced Wnt/β-catenin signaling in $Msx1^{d/d}Msx2^{d/d}$ mouse uterus**

A. Schematic representation of Wnt/β-catenin signaling pathway **B.** Real-time PCR was performed to analyze the expression of Wnt ligands in uterine epithelial cells of $Msx1^{f/f}Msx2^{f/f}$ and $Msx1^{d/d}Msx2^{d/d}$ mice on day 4 of pregnancy. The level of $Ck18$ was used as internal control to normalize gene expression. The data are represented as the mean fold induction ± SEM, *p<0.01, ***p<0.0001. **C.** Real-time PCR was performed to analyze the expression of Wnt ligands in uterine stromal cells of $Msx1^{f/f}Msx2^{f/f}$ and $Msx1^{d/d}Msx2^{d/d}$ mice on day 4 of pregnancy. The level of $Rplp0$ was used as internal control to normalize gene expression. The data are represented as the mean fold induction ± SEM, *p<0.01, **p<0.001, ***p<0.0001. **D.** The level of active β-catenin in uterine sections of $Msx1^{f/f}Msx2^{f/f}$ (left panel) and $Msx1^{d/d}Msx2^{d/d}$ (right panel) mice on day 4 of pregnancy was analyzed by IHC. (Magnification: a and c: 10x, b and d: 40x)

Figure 14 Enhanced expression of FGFs in uterine stromal cells of $Msx1^{d/d}Msx2^{d/d}$ mouse

A. Schematic representation of FGF signaling pathway **B**. Real-time PCR was performed to analyze the expression of Fgf family members in uterine stromal cells of $Msx1^{f/f}Msx2^{f/f}$ and $Msx1^{d/d}Msx2^{d/d}$ mice on day 4 of pregnancy. The level of *Rplp0* was used as internal control to normalize gene expression. The data are represented as the mean fold induction ± SEM, *p<0.01, **p<0.001, ***p<0.0001. **C**. Real-time PCR was performed to monitor the expression of *Egf* family of growth factors in the uterine stroma of $Msx1^{f/f}Msx2^{f/f}$ and $Msx1^{d/d}Msx2^{d/d}$ mice on day 4 of pregnancy.

82
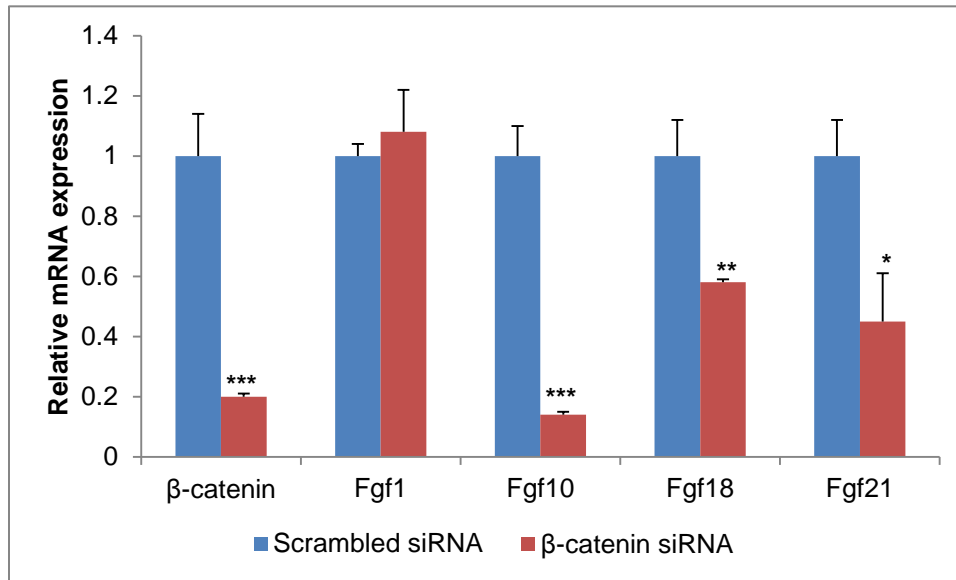
Figure 15 Wnt/β-catenin signaling controls FGF synthesis in uterine stromal cells

Primary stromal cells were isolated from uteri of $Msx1^{f/f}Msx2^{f/f}$ mice on day 3 of pregnancy and transfected with siRNA targeted to the β-catenin mRNA. Total RNA was isolated 24 h after transfection to analyze the expression of Fgf family members by real-time PCR. The level of $Rplp0$ was used as an internal control to normalize gene expression. The data are represented as the mean fold induction ± SEM, *p<0.01, **p<0.001, ***p<0.0001.

Figure 16 Enhanced FGFR signaling in the epithelium of *Msx1$^{d/d}$Msx2$^{d/d}$* uteri

A   **FGF and FGFR Signaling Pathway**
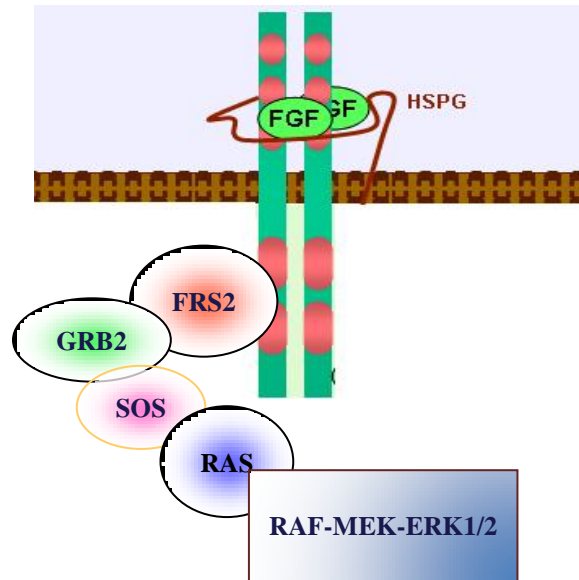
B

Figure 16 (Contd.) Enhanced FGFR signaling in the epithelium of *Msx1^{d/d}Msx2^{d/d}* uteri

pERK

D4

pAKT

E
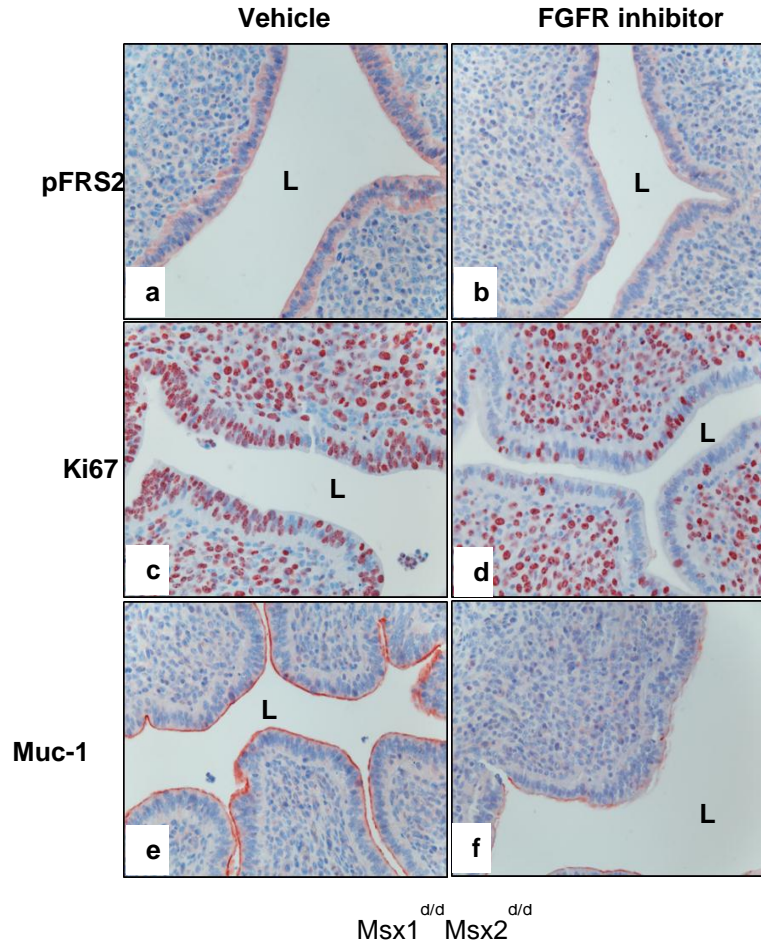
Figure 16 (Contd.) Enhanced FGFR signaling in the epithelium of $Msx1^{d/d}Msx2^{d/d}$ uteri
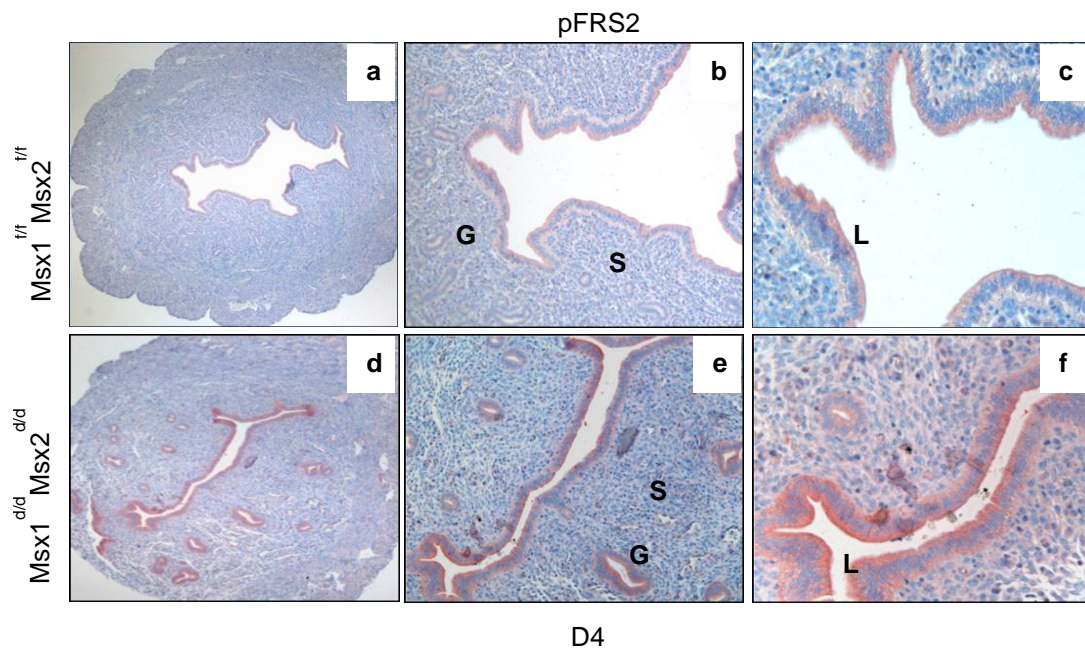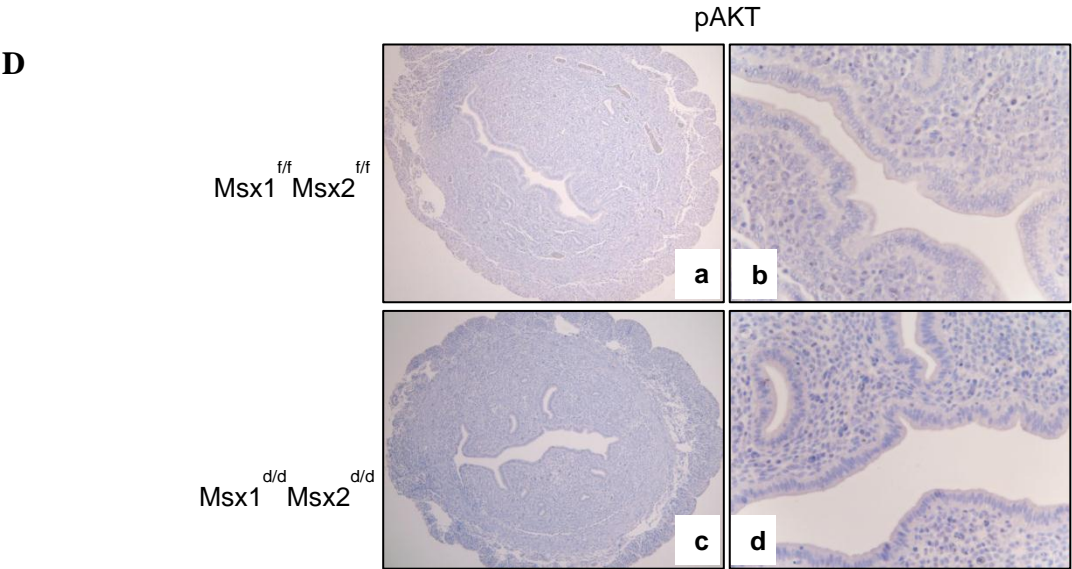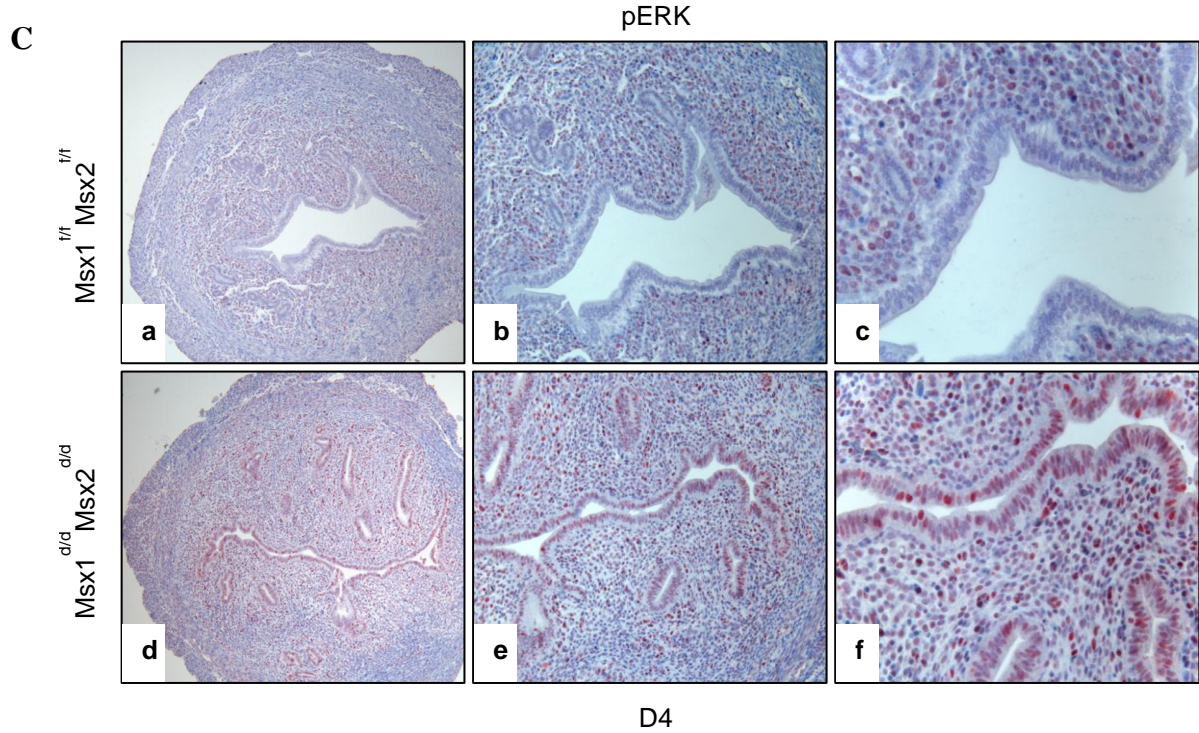
A. The schematic representation of FGF-FGFR signaling pathway **B**. The level of p-FRS2 was examined in the uterine sections of $Msx1^{f/f}Msx2^{f/f}$ (upper panel) and $Msx1^{d/d}Msx2^{d/d}$ (lower panel) mice on day 4 of pregnancy by immunohistochemistry. Magnification: a and d: 10x, b and e: 20x, c and f: 40x. **C**. The level of p-ERK was examined in the uterine sections of $Msx1^{f/f}Msx2^{f/f}$ (upper panel) and $Msx1^{d/d}Msx2^{d/d}$ (lower panel) mice on day 4 of pregnancy by immunohistochemistry. Magnification: a and d: 10x, b and e: 20x, c and f: 40x. L, G and S indicate luminal epithelium, glandular epithelium, and stroma respectively. **D.** The level of p-AKT was examined in the uterine sections of $Msx1^{f/f}Msx2^{f/f}$ (upper panel) and $Msx1^{d/d}Msx2^{d/d}$ (lower panel) mice on day 4 of pregnancy by immunohistochemistry. Magnification: a and c: 10x, b and d: 40x. **E.** FGFR-specific inhibitor PD173074 was applied to one uterine horn of $Msx1^{d/d}Msx2^{d/d}$ (n=3) mice on day 3 of pregnancy. The other horn served as vehicle-treated control. Uterine horns were collected on day 4 morning and sections were subjected to immunohistochemistry to detect p-FRS2, Ki67, and Muc-1.
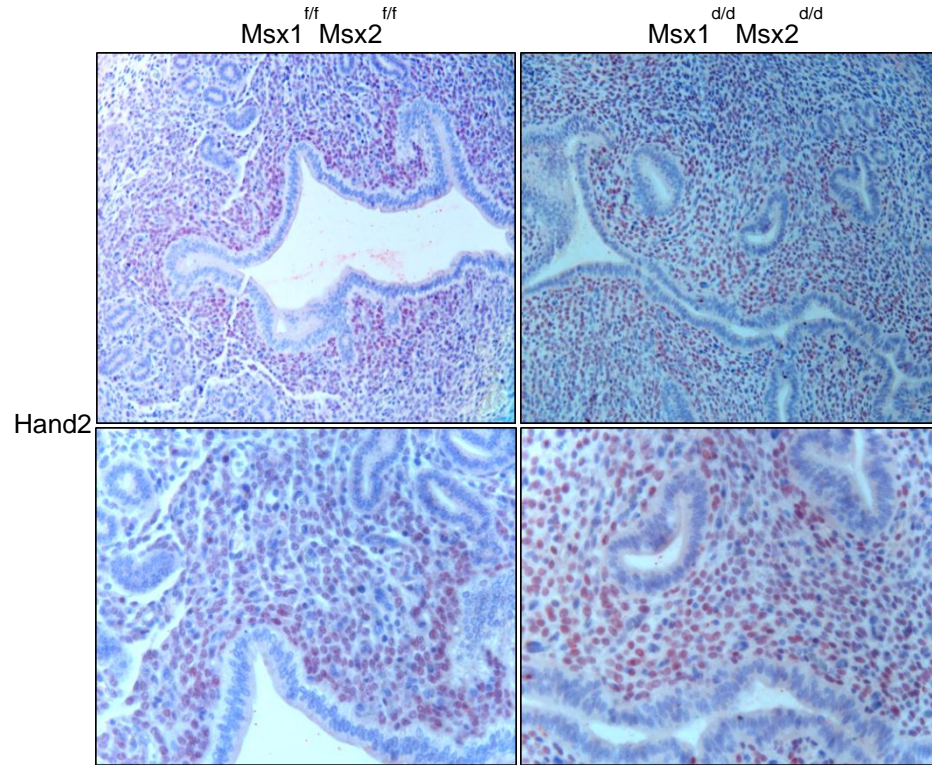
Figure 17 Hand2 expression in _Msx1$^{d/d}$Msx2$^{d/d}$_ uteri

The level of Hand2 in uterine sections of _Msx1$^{f/f}$Msx2$^{f/f}$_ (left panel) and _Msx1$^{d/d}$Msx2$^{d/d}$_ (right panel) mice on day 4 of pregnancy was analyzed by IHC (Magnification: upper panel: 20x, lower panel: 40x).
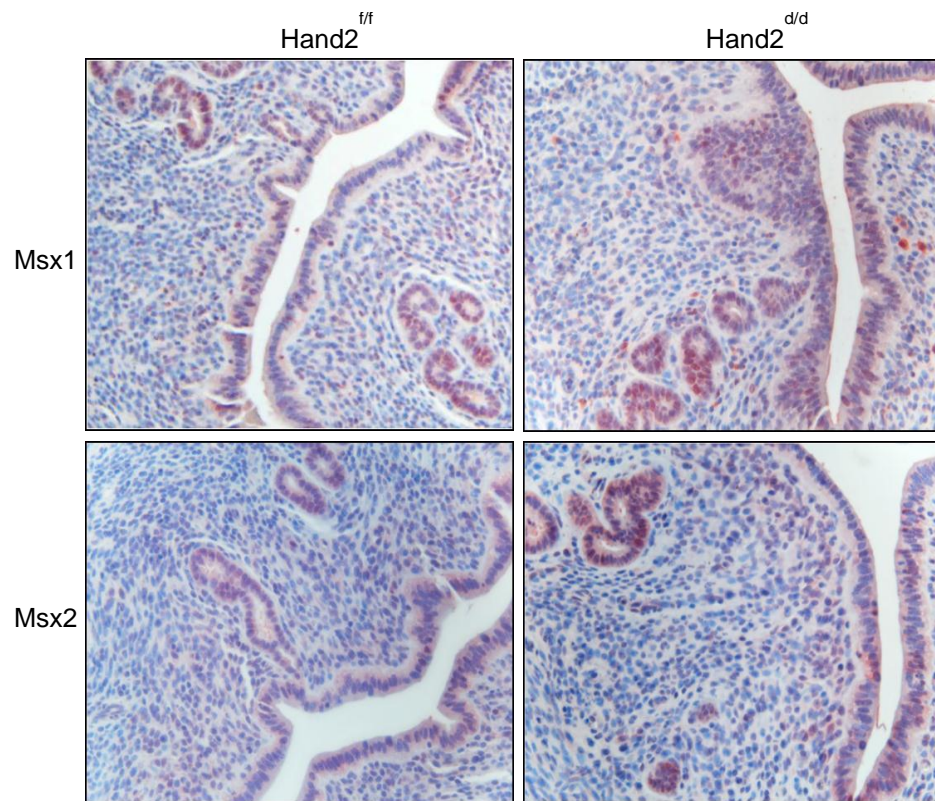
Figure 18 Msx1 and Msx2 expression in *Hand2^{d/d}* uteri

The levels of MSX1 (upper panel) and MSX2 (lower panel) were examined in the uterine sections of Hand2*^{f/f}* (left panel) and Hand2*^{d/d}* (right panel) mice on day 3 of pregnancy by IHC.
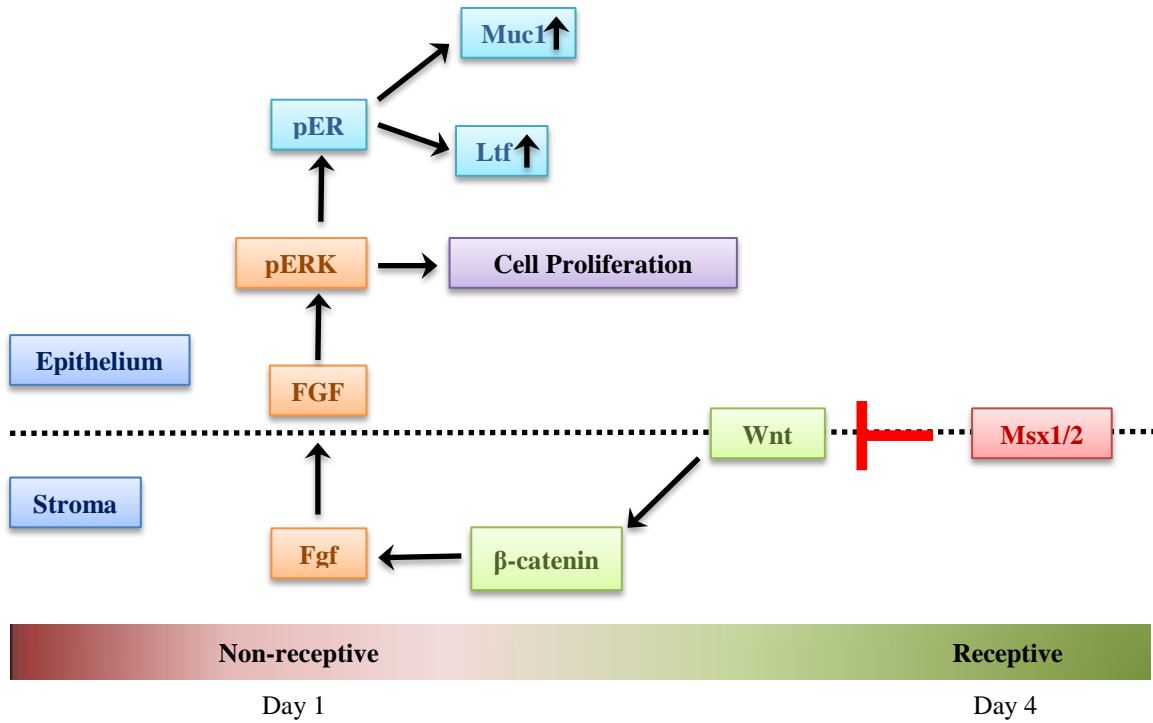
Figure 19 Mechanism of Msx1 and Msx2 action in mouse uterus

In normal pregnancy, MSX1 and MSX2 act to repress WNT and β-catenin signaling and inhibit FGF synthesis in the uterine stroma, thereby suppressing stromal-epithelial cross-talk. In the absence of MSX1 and MSX2, FGFs are induced, activating the epithelial FGFR-ERK1/2 pathway, and promoting epithelial proliferation. Activated ERK1/2 then phosphorylates epithelial ESR1. This triggers transcriptional activation of ESR1 and expression of its target genes, such as *Muc-1*, which prevent the functional transformation of the luminal epithelium to receptive state, blocking embryo implantation.

CHAPTER IV

MSX HOMEOBOX GENES ACT DOWNSTREAM OF BMP2 TO REGULATE UTERINE DECIDUALIZATION IN THE MOUSE AND THE HUMAN

4.1 ABSTRACT

Differentiation of endometrial stromal cells to decidual cells in a process known as decidualization is critical for embryo implantation and successful establishment of pregnancy. We previously reported that bone morphogenetic protein 2 (BMP2) mediates uterine stromal cell differentiation in the mouse and the human. To identify the downstream target(s) of BMP2 signaling during decidualization, we performed gene expression profiling of mouse uterine stromal cells treated with or without recombinant BMP2. Our studies revealed that the expressions of *Msx* homeobox genes, *Msx1* and *Msx2*, were markedly altered in response to exogenous BMP2. To investigate their role during decidualization, we created a conditional knockout of the *Msx1* and *Msx2* gene in the uterus of adult mice by employing the Cre-LoxP strategy. Our studies revealed that mice lacking *Msx1* and *Msx2* fail to elicit a decidual response. Further analysis indicated that the uterine stromal cells in the absence of *Msx*1 and *Msx*2 are able to proliferate but fail to undergo terminal differentiation. We also observed that addition of BMP2 to human endometrial stromal cell cultures led to a robust enhancement of *Msx1* and *Msx2* expression and stimulated the differentiation process. Attenuation of *Msx1* or *Msx2* expression by siRNAs greatly reduced human stromal differentiation *in vitro*, indicating that it is a key mediator of BMP2-induced decidualization in the mouse and the human.

4.2 INTRODUCTION

In murine and human pregnancies, embryos implant by attaching to the luminal epithelium and invading into the stroma of the endometrium. Under the influence of the steroid hormones, estrogen and progesterone, the stromal cells surrounding the implanting embryo undergo a remarkable transformation event. This process, known as decidualization, is an essential prerequisite for implantation. In mice, decidualization is initiated at the time of embryo attachment to the uterine epithelium on day 4.5 of pregnancy. The attachment reaction is followed by the proliferation and differentiation of the stromal cells surrounding the implanting embryo to form the decidual bed [1,4]. The decidual cells are thought to produce hormones and cytokines that are critical for embryo development, secrete factors that control trophoblast invasion and serve an immunoregulatory function during pregnancy [118]. The current challenge is to understand the complex process by which steroid hormones regulate the formation and function of the decidual tissue. To this end, it is critical to identify and characterize the factors induced by the maternal hormones that regulate the proliferation and differentiation of uterine stromal cells during the decidualization process.

Our previous studies revealed that progesterone induces the synthesis of bone morphogenetic protein-2 (BMP2), a member of the TGFβ superfamily in the uterus during decidualization [121]. BMPs are well-known mediators of cell differentiation and development in a variety of tissues [232-235]. We observed that addition of recombinant BMP2 to primary cultures of stromal cells isolated from pregnant mouse uterus markedly accelerated the decidualization program. Conversely, siRNA-mediated downregulation of BMP2 expression in these cells efficiently

blocked the differentiation process [121]. Consistent with these *in vitro* results, it was observed that mice deficient in uterine BMP2 are infertile and exhibit a severe defect in stromal differentiation [120]. We also observed a remarkable induction in the expression of BMP2 in human endometrial stromal cells undergoing decidualization *in vitro* in response to steroid hormones and cAMP. Addition of exogenous BMP2 to these cultures stimulated the differentiation process indicating an important role for this signaling molecule in the mouse and the human endometrium [121].

In this study, we used microarray-based gene expression profiling and identified *Msx* homeobox genes including *Msx1* and *Msx2* as downstream targets of BMP2 regulation in stromal cells undergoing decidualization. *Msx* homeobox genes are transcription factors that regulate cellular proliferation and differentiation during embryonic development [146,147]. Interestingly, *Bmp*2 and *Msx*1/2 are often co-localized during embryonic development at distinct sites including the primitive streak, limb bud, myocardium, and the mammary gland [141,167,185,236]. Furthermore, BMP-MSX axis is known to regulate a variety of differentiation systems including osteoblast differentiation [237-239]. These findings raised the possibility that the MSX factors functioning downstream of BMP2 regulate the uterine differentiation program during embryo implantation.

Global deletion of *Msx1* or *Msx2* gene is embryonic lethal, necessitating the development of conditional deletion of these genes to study their functions during decidualization. Conditional ablation of either *Msx1* or *Msx2* showed only modest impairment in decidualization, most likely due to compensation of the function of one *Msx* gene by the other. Indeed, in *Msx2*-null uteri, the

level of *Msx1* expression in the uterus was markedly elevated and vice versa. On the other hand, conditional ablation of both *Msx1* and *Msx2* in mouse uterus led to a severe defect in decidualization. Our studies further showed that in the absence of MSX1 and MSX2, the uterine stromal cells are able to proliferate but are not competent to undergo differentiation, indicating that MSX factors are key mediators of BMP2-induced decidualization.

Although evolutionarily very different, humans and rodents have a similar hemochorial type of placenta and exhibit similarities in terms of hormonal regulation of gene expression in the uterus. In preparation for implantation, the human endometrial stromal cells also undergo a differentiation process, known as "predecidualization", during the progesterone-dominated secretory phase of the menstrual cycle [118, 240-242]. Our previous studies have shown that BMP2 is strongly induced in human endometrial stromal cells during predecidualization. Addition of recombinant BMP2 to human stromal cultures greatly enhanced the differentiation process as indicated by the expression of decidual biomarkers [121]. In this study we now show a marked induction in the expression of *Msx1* and *Msx2* in response to BMP2 in human endometrial stromal cells during decidualization *in vitro*. More importantly, attenuation of *Msx1* or *Msx2* expression by siRNAs greatly reduced stromal differentiation, suggesting that it is a candidate mediator of BMP2-induced decidualization in the human. Collectively, our studies uncovered a unique conserved pathway involving BMP2 and MSX that mediates stromal decidualization in the mouse and the human.

4.3 MATERIALS AND METHODS

Materials

Recombinant human BMP2 was purchased from R&D systems (Minneapolis, MN).

Animals

Mice were maintained in the designated animal care facility at the College of Veterinary Medicine of the University of Illinois, Urbana-Champaign, according to the institutional guidelines for the care and use of laboratory animals. To generate the conditional *Msx1Msx2*-null mice (*Msx1$^{d/d}$Msx2$^{d/d}$*), *Msx1Msx2*-floxed (*Msx1$^{f/f}$Msx2$^{f/f}$*) [210] mice were mated with PR-Cre knock-in mice [211]. The presence of a vaginal plug after mating was designated as day 1 of pregnancy. Female mice were killed at various stages of gestation and the uteri collected.

Decidualization was experimentally induced in non-pregnant mice as described previously [123]. Ovariectomized mice were injected s/c with 100 ng of E in 0.1 ml of sesame oil for 3 consecutive days. This was followed by 2 days rest and then daily injections of 6.7 ng and 2 mg of P for 3 consecutive days. On day3, one uterine horn was infused with 50 μl oil and the other horn was not infused. The administration of E and P was continued for an additional 3 days and then killed to collect the uterine tissue.

In some experiments, animals were injected i.p. with bromodeoxyuridine (BrdU) (2 mg/animal; BD Pharmingen) 1 h prior to sacrifice. Uteri were collected and fixed in neutral buffered formalin prior to immunohistochemistry (IHC) analysis.

94

Our studies involving human endometrial cell cultures and endometrial biopsies adhere to the regulations set forth for the protection of human subjects participating in clinical research and are approved by the IRBs of Emory University and the University of Illinois. Endometrium samples from early proliferative stage of the menstrual cycle were obtained at the Emory University Medical Center from fertile volunteers by Pipelle biopsy.

Isolation and culture of mouse uterine stromal cells

Uterine stromal cells were isolated as previously described [121]. Briefly, uterine horns of pregnant mice were dissected and placed in HBSS containing 6 g/liter dispase and 25g/liter pancreatin for 1 h at room temperature and then 15 min at 37°C to remove the endometrial epithelial clumps. The tissues were then placed in HBSS containing 0.5 g/liter collagenase for 45 min at 37 °C to disperse the stromal cells. After vortexing, the contents were passed through a 70-μm gauze filter (Millipore). The filtrate containing uterine stromal cells were diluted in Dulbecco's modified Eagle's Medium-F12 medium (DMEM-F12; with 100 unit/liter penicillin, 0.1 g/liter streptomycin, 1.25 mg/liter Fungizone) with 2% heat-inactivated fetal calf serum. The live cells were counted by trypan blue staining using a hemocytometer. Cells were then seeded in 6-well cell culture plates. The unattached cells were removed by washing several times with HBSS after 2 h, and cell culture was continued after addition of fresh medium supplemented with P (1 μm) and E (10 nm).

Culture of human endometrial stromal cells

Human stromal cells were isolated from endometrial biopsy samples of fertile women. The cells were grown in Dulbecco's modified Eagle's medium/F-12 medium containing 5%charcoal

stripped fetal bovine serum. The cells were treated with a hormone mixture containing 0.5 mM 8-bromo-cAMP, 1 μM P and 10 nM E. Cells were harvested at indicated times after addition of hormone mixture. The day of hormones and cAMP treatment was designated as day 0.

Quantitative real time PCR analysis (qPCR)

The total RNA was extracted by using TRIZOL reagent from homogenized uterine tissue or cultured cells according to the manufacturer's protocol. cDNA was prepared by standard protocols. The cDNA was amplified to quantify gene expression by quantitative PCR, using gene-specific primers and SYBR Green (Applied Biosystems, Warringtom, UK). The expression level of *RPLP0* (*36B4*) was used as the internal control. For each treatment, the mean Ct and standard deviation were calculated from individual Ct values obtained from three replicates of a sample. The normalized ΔCt in each sample was calculated as mean Ct of target gene subtracted by the mean Ct of internal control gene. ΔΔCt was then calculated as the difference between the ΔCt values of the control and treatment sample. The fold change of gene expression in each sample relative to a control was computed as $2^{-\Delta\Delta Ct}$. The mean fold induction and standard errors were calculated from three or more independent experiments.

Immunohistochemistry

Uterine tissues were processed and subjected to immunohistochemistry as described previously [212]. Briefly, paraffin-embedded tissues were sectioned at 5 μm and mounted on microscopic slides. Sections were deparaffinized in xylene, rehydrated through a series of ethanol washes, and rinsed in water. Antigen retrieval was performed by immersing the slides in 0.1M citrate buffer solution, pH 6.0, followed by microwave heating for 25 min. The slides were allowed to

cool and endogenous peroxidase activity was blocked by incubating sections in 0.3% hydrogen peroxide in methanol for 15 min at room temperature. After washing with PBS for 15 min and the slides were incubated in a blocking solution for 1 h before incubating them in primary antibody overnight at 4°C with antibodies specific for mouse-MSX1 (Abcam, ab73883), human–MSX1 (Aviva systems biology, ARP31396_T100) and MSX2 (Santa Cruz, sc-15396). The slides were incubated with the biotinylated secondary antibodies at room temperature for 1h, followed by incubation with horseradish peroxidase-conjugated streptavidin (Invitrogen Corp., MD 21704). The sections were stained in 3-amino-9-ethylcarbazole chromogen (AEC) solution until optimal signal was developed. Sections were counterstained with Mayer's Hematoxylin and examined by bright field microscopy.

siRNA transfection

Control (scrambled) siRNA and siRNA targeted to *Msx1* or *Msx2* were purchased from Ambion Inc. The transfection was performed using SilentFect™ Reagent (Bio-Rad), according to the manufacturer's protocol. The human stromal cells were transfected with siRNA after reaching 70% confluency. The cells were harvested 24 h following transfection to extract the RNA.

Statistical Analysis

Statistical analysis was performed by *t*-test or ANOVA. The values were expressed as mean ± SEM and considered significant if $p < 0.05$.

4.4 RESULTS

Msx homeobox genes are downstream targets of BMP2 during decidualization

Our previous studies have shown that BMP2 plays a critical role in the regulation of stromal differentiation during implantation. To determine the function of BMP2 during this differentiation process, we employed a primary culture system in which undifferentiated stromal cells isolated from pregnant mouse uterus undergo decidualization. When recombinant BMP2 was added to these stromal cultures, it markedly advanced the differentiation program. To gain insight into the mechanisms by which BMP2 regulates decidualization, we performed gene expression profiling of RNA isolated from primary stromal culture system treated with or without recombinant BMP2 for 24 h. Total RNA was isolated from uterine stromal cells and subjected to microarray analysis using Affymetrix murine GeneChip arrays. Interestingly we observed that the expression of the homeobox gene *Msx1* was downregulated while that of *Msx2* was upregulated in the stromal cells in response to BMP2. We verified the results of the microarray analysis by performing real-time PCR analysis. Primary cultures of stromal cells isolated from pregnant uteri (preimplantation, day 4) were subjected to decidualization in the absence or presence of BMP2. As shown in Fig. 20, a marked increase in the expression of *Msx2* was observed when stromal cells were treated with BMP2. In contrast, the expression of *Msx1* declined signficantly in the BMP2-treated stromal cells.

Expression profile of *Msx*1 and *Msx*2 during stromal cell decidualization

We next examined the expression profile of *Msx*1 and *Msx*2 during *in vitro* stromal cell differentiation. As the duration of stromal cell culture progressed from 2 to 72 h, we noted a

dramatic decline in the level of *Msx1* while a steady enhancement in the expression of *Msx2* (Figs. 21A and 21B, upper panels). Immunocytochemical studies confirmed a similar temporal pattern of expression and prominent nuclear localization of *Msx1* and *Msx2* at 24 h and 72 h of decidualization (Figs. 21A and 21B, lower panels) consistent with the possibility that BMP2 differentially regulates *Msx1* and *Msx2* expression in the uterus during decidualization.

We next examined the spatio-temporal profiles of mRNAs and proteins corresponding to *Msx1* and *Msx2* in the mouse uterus on days 4 to 7 of pregnancy by real-time PCR and immunohistochemistry (IHC), respectively. Consistent with the expression profiles of *Msx1* and *Msx2* during *in vitro* stromal differentiation, we observed a sharp decline in the level of *Msx1* on day 5 at the onset of stromal differentiation and a marked increase in the level of *Msx2* on day 7 at the time of decidualization (Fig. 22A, upper panel; Fig. 22B, upper panel). Both MSX1 and MSX2 proteins were abundantly expressed in uterine epithelium and stroma on day 4 of pregnancy (Fig. 22A, lower panel a; Fig. 22B, lower panel a). The expression of MSX1 protein then declined on day 5 at the time of embryo implantation and was undetectable on days 5 to 7 overlapping the decidual phase of pregnancy (Fig. 22A, lower panels b-d). In contrast, we detected low but specific nuclear expression of MSX2 in the stromal cells as pregnancy progressed to days 5 and 6, the expression of MSX2 then intensified in the decidualizing stromal cells surrounding the implanted embryo on day 7 (Fig. 22B, lower panels b-d). These results showed that MSX2 is localized specifically in differentiating stromal cells during early pregnancy.

Ablation of *Msx1* and *Msx2* in the uterus leads to a defect in decidualization

To investigate the function of *Msx*1 and *Msx*2 in the uterus during decidualization, we employed the Cre-LoxP strategy to create conditional single knockout of *Msx1* or *Msx2* in the uteri of adult mice. Transgenic mice expressing Cre under the control of progesterone receptor (PR) promoter was previously used to ablate "floxed" genes selectively in cells expressing PR, including uterine cells. We, therefore, crossed the PR-Cre mice with mice harboring the "floxed" *Msx1* or *Msx2* to create $Msx1^{d/d}$ or $Msx2^{d/d}$ mice. We confirmed the deletion of *Msx1* or *Msx2* in the uteri of these mutant mice by real-time PCR (Fig. 23A). Interestingly, though, we found that deletion of *Msx2* in $Msx2^{d/d}$ and *Msx1* in $Msx1^{d/d}$ mice led to a marked elevation in the expression of *Msx1* and *Msx2* respectively, raising the possibility that function of one *Msx* gene would likely be compensated by the other in single mutants (Fig. 23B).

The effect of *Msx1* and *Msx2* in uterine decidualization was then investigated in a double knockout of *Msx1* and *Msx2* termed as $Msx1^{d/d}Msx2^{d/d}$ mice. Ovariectomized $Msx1^{f/f}Msx2^{f/f}$ and $Msx1^{d/d}Msx2^{d/d}$ mice were treated with a well-established regimen of steroid hormones and then decidualization reaction was initiated in one uterine horn by intra luminal injection of oil while the other horn was left unstimulated. We then examined the gross anatomy of the stimulated and unstimulated uterine horns of $Msx1^{f/f}Msx2^{f/f}$ and $Msx1^{d/d}Msx2^{d/d}$ mice. As expected, the uterine horn of $Msx1^{f/f}Msx2^{f/f}$ mice exhibited a robust decidual response at 72 h after receiving the artificial stimulation (Fig. 24, upper left panel). In contrast, the *Msx1Msx2*-deficient uteri under identical conditions failed to show any significant decidualization (Fig. 24, upper right panel). When the decidual response was assessed by measurement of uterine wet weight gain, the

Msx1Msx2-deficient uteri exhibited a markedly reduced weight gain relative to that seen in the *Msx1*^f/f^*Msx2*^f/f^ uteri (Fig. 24, lower panel).

Stromal proliferation is intact while differentiation is compromised in *Msx1Msx2*-deficient uteri

During the decidualization phase of pregnancy, the uterine stromal cells undergo proliferation for 24–48 h and then enter the differentiation program [243, 244]. The lack of decidual response in *Msx1Msx2*-null uteri raised the possibility that *Msx1* and *Msx2* are potential regulators of pathways directing stromal proliferation or differentiation or both.

To analyze the effect of *Msx1* and *Msx2* on stromal cell proliferation, we subjected *Msx1*^f/f^*Msx2*^f/f^ and *Msx1*^d/d^*Msx2*^d/d^ mice to experimentally induced decidualization as described in materials and methods and monitored the incorporation of BrdU in uterine stromal cells after decidual stimulation. We administered a 1h pulse of BrdU at 23h after the decidual stimulation and collected uteri at 24 h. As shown in Fig. 25A, the uterine sections of *Msx1*^f/f^*Msx2*^f/f^ and *Msx1*^d/d^*Msx2*^d/d^ exhibited similar pattern of BrdU immunostaining in the stromal cells indicating that *Msx1* and *Msx2* are not necessary for stromal cell proliferation during decidualization.

We further analyzed the decidualization response of *Msx1*^d/d^*Msx2*^d/d^ uteri by monitoring the expression of prolactin-related protein (PRP), Wnt4, and connexin 43 (Cx43), factors that are induced in stromal cells during decidualization and play important regulatory roles during this process [118,122,123]. As shown in Fig. 25B, when *Msx1*^f/f^*Msx2*^f/f^ and *Msx1Msx2*-deficient uteri were subjected to artificial decidual stimulation, we observed a marked downregulation of

mRNAs corresponding to PRP, Wnt4, and Cx43 in the uteri lacking *Msx1Msx2*, indicating that *Msx*1 and *Msx*2 are necessary for stromal cell differentiation.

Expression of *MSX1* and *MSX2* in human endometrial stromal cells during decidualization

To assess the phylogenetic conservation and possible clinical significance of these pathways, we next investigated the expression of *MSX1* and *MSX2* in human endometrial stromal cells during *in vitro* decidualization. Undifferentiated stromal cells isolated from human endometrial biopsies obtained from normal fertile women in the proliferative stage of the menstrual cycle were placed in culture and subjected to decidualization in response to a hormonal cocktail containing P, E, and 8-bromo-cAMP [121]. We observed the induction of classical decidualization biomarkers, prolactin (PRL) and insulin-like growth factor binding protein 1 (IGFBP1), during this *in vitro* decidualization process (data not shown). When we examined the expression of MSX1 and MSX2 mRNA during *in vitro* decidualization, we observed a marked induction of these genes in stromal cells in response to the hormone cocktail at 6 days of initiating the culture (Fig. 26A, upper panel, Fig. 26B, upper panel). Consistent with the RNA profile, distinct nuclear staining of MSX1 and MSX2 proteins was observed in human endometrial stromal cells with the onset of decidualization (Fig. 26A, lower panel, Fig. 26B, lower panel).

Our previous studies have shown that BMP2 is a key mediator of stromal decidualization in the human [121]. To further explore the relationship between BMP2 and MSX expression, and to test whether this important functional link is conserved among the species, we next investigated whether BMP2 regulates the expression of *MSX*1 and *MSX*2 in human endometrial stromal cells during *in vitro* decidualization. Human endometrial stromal cells were transduced with an

adenovirus expressing BMP2 or GFP (control) and then subjected to decidualization in the presence of progesterone, estrogen, and 8-bromo-cAMP. We observed the induction of classical decidualization biomarkers, prolactin (PRL) and insulin-like growth factor binding protein 1 (IGFBP1), and BMP2 downstream targets, WNT4 and SMAD6, in response to exogenous BMP2 during *in vitro* decidualization process (Fig. 27). We also observed a marked increase in the level of MSX1 and MSX2 mRNAs and proteins in response to BMP2 (Fig. 27) indicating that these homeobox genes are functioning downstream of BMP2 signaling in the human endometrial stromal cells during decidualization.

***MSX* genes regulate decidualization of human endometrial stromal cells**

We next investigated the role of *MSX*1 and *MSX*2 in human endometrial stromal cell differentiation by employing RNA interference strategy. Primary human endometrial stromal cells were transfected with siRNA targeted specifically to the *MSX*1 or *MSX*2 mRNA. In control experiments, cells were transfected with a scrambled siRNA. As shown in Fig. 28, endometrial stromal cells treated with a siRNA targeted to *MSX*1 mRNA efficiently suppressed the level of this mRNA. This specific downregulation of *MSX*1 expression was associated with a marked reduction in the expression of differentiation markers such as IGFBP1 and PRL compared to control scrambled siRNA-treated cells. Downregulation of *MSX*2 expression was also associated with a marked reduction in the level of IGFBP1. The expression of GAPDH remained unaltered under these conditions. Collectively, these results indicate that *MSX*1 and *MSX*2 are important mediators of BMP2-induced human stromal cell differentiation.

4.5 DISCUSSION

Decidualization is a critical process in which the fibroblastic stromal cells of the uterus proliferate and then differentiate into decidual cells. This steroid-dependent event is indispensable for embryo implantation and establishment of a functional maternal-fetal unit during early pregnancy. We previously reported the decidual stage-specific expression of BMP2 and its receptor in the uterine stroma during early pregnancy and provided a potential link between BMP2 signaling and the steroid-dependent changes underlying stromal differentiation during decidualization. The functional role of BMP2 during embryo implantation was demonstrated using transgenic mice carrying a conditional deletion of this gene in mouse uterus. BMP2-null mice are infertile due to the absence of a decidual response. Although the embryos attach to the uterine epithelium, the stromal cells fail to undergo decidualization. In parallel to the creation of the BMP2-null mice, the mouse and human primary stromal cultures were utilized to provide novel insights into the role of BMP2 and its downstream signaling pathways in uterine decidualization. These studies indicated that BMP2-mediated canonical Smad signaling in the uterus plays a critical role in stromal cell differentiation during early pregnancy.

Microarray analyses conducted with endometrial stromal cells treated with exogenous BMP2 revealed the involvement of *Msx1* and *Msx2* in BMP2 signaling. Like BMPs, the *Msx* family of homeobox proteins exerts pleiotropic effects including tissue morphogenesis and cell differentiation. The present study describes the expression of *Msx*1 and *Msx2* in uterus during decidualization and addresses, for the first time, their roles in stromal cell differentiation. Our studies revealed a marked induction of *Msx2* in mouse endometrial stromal cultures when BMP2 was added to induce differentiation. In contrast, the expression of *Msx1* was downregulated in

104

response to BMP2, suggesting that BMP2 differentially regulates *Msx* expression in mouse uterine stromal cells during decidualization. Interestingly BMP2 was able to promote the expression of both *Msx1* and *Msx2* in human endometrial stromal cells during decidualization. While the functional significance of this distinct pattern of *Msx1* and *Msx2* expression in mouse and human endometrium is not known, it is clear that BMP2-Msx pathway is a critical regulator of mouse and human decidualization.

BMPs and MSXs are often expressed at the same sites in many tissues including primitive streak, lateral mesoderm, limb bud, myocardium, hindbrain and tooth germ during embryonic development [141,144,184,185]. The expression of MSX1/2 is induced in response to BMP2/4 supplementation in tooth mesenchyme explant [186] and in facial primordia [187]. BMP2 mediates vascular calcification and osteoblastogenesis through the induction of *Msx2* [245-247]. In chick limb when BMP signaling was inhibited in response to a dominant-negative mutant of BMP-receptor, the level of *Msx2* transcript declined significantly [248]. The level of endogenous *Msx2* was markedly reduced in differentiating $Smad4^{-/-}$ ES cells compared to wild-type cells. Furthermore based on the reporter assays of the *Msx2* promoter in fibroblasts and ES cells, the absolute requirement of Smad4 for Msx2 activation was established indicating that *Msx2* is a direct target of BMP2 signaling [237,249]. While BMP2 has been shown to induce *Msx1* in the oral epithelium during tooth development [250] and in the explant culture of embryonic lateral telencephalic neuroectoderm [251], whether *Msx1* is a direct target of BMP2 signaling remains unknown.

Using mutant mouse models harboring conditional deletion of *Msx1* and *Msx2* in the uterus, we established that these factors play critical roles in stromal cell differentiation during decidualization. We observed that the expression of *Msx1* is markedly elevated in *Msx2*-null uterus during decidualization, supporting the concept that the loss of function of one *Msx* gene during early pregnancy is partially compensated by the other. Interestingly, mice lacking both *Msx1* and *Msx2* in their uteri show a severe defect in decidual response. Our studies further revealed that deletion of *Msx*1 and *Msx*2 did not affect stromal cell proliferation. However, stromal cell differentiation, as indicated by the expression of specific markers, was severely affected in $Msx1^{d/d}Msx2^{d/d}$ uteri. It indicates that *Msx*1 and *Msx*2 are not required for stromal cell proliferation but they are essential for terminal differentiation. Interestingly, uterine loss of BMP2 does not affect stromal cell proliferation but severely compromises differentiation, suggesting that *Bmp*2 mediates stromal cell differentiation through *Msx*1/2. Whether BMP2 directly regulates *Msx* expression in the uterus during decidualization requires further investigation.

Another important aspect of this study is its exploration of the role of MSX during decidualization of human endometrial stromal cells. Our studies revealed that MSX1 and MSX2 expression in the human endometrial stromal cells follow that of BMP2 during decidualization. Addition of exogenous *BMP*2 to human stromal cultures further enhanced their levels suggesting that *BMP*2 might mediate endometrial stromal differentiation through *MSX*1/2. Consistent with this notion, we demonstrated that downregulation of *MSX1* or *MSX2* by loss-of-function approaches markedly affected the differentiation program in the human endometrial stromal culture. These results indicated that a conserved molecular pathway involving BMP2 and MSX

operates during uterine stromal cell differentiation in mice and humans. It is of interest to note that unlike BMP2, *MSX*1/2 proteins are detectable even in the proliferating endometrial stromal cells. While the spatio-temporal expression pattern of *MSX*1/2 during different phases of the menstrual cycle in human has not been reported, microarray analysis performed on endometrial samples collected during different phases of menstrual cycle revealed that the expression of *MSX* genes were reduced during uterine receptivity. Hence it is tempting to speculate that *MSX* genes, as we have shown previously in mice, might also play a role during uterine receptivity in the human. The role of *MSX*1/2 in human endometrial receptivity needs further investigation.

4.6 FIGURES
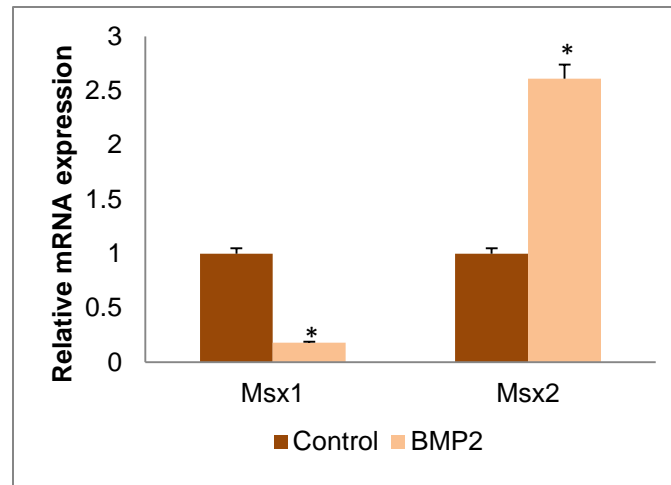
Figure 20 *Msx* homeobox genes are downstream targets of BMP2 during decidualization

Stromal cells isolated from day 4 pregnant uteri were cultured for 24h *in vitro* with or without Bmp2 as described in materials and methods. The cells were lysed and real-time PCR was performed to monitor the expression of mRNAs corresponding to *Msx1* and *Msx2*. The relative levels of gene expression were determined by setting the expression level of *Msx1* and *Msx2* mRNA in control at 1.0. *Rplp0,* encoding a ribosomal protein, was used to normalize the level of RNA (* $p < 0.05$).

Figure 21 Expression profile of *Msx1* and *Msx2* during *in vitro* stromal cell differentiation

A

24h

72h

B

24h

72h
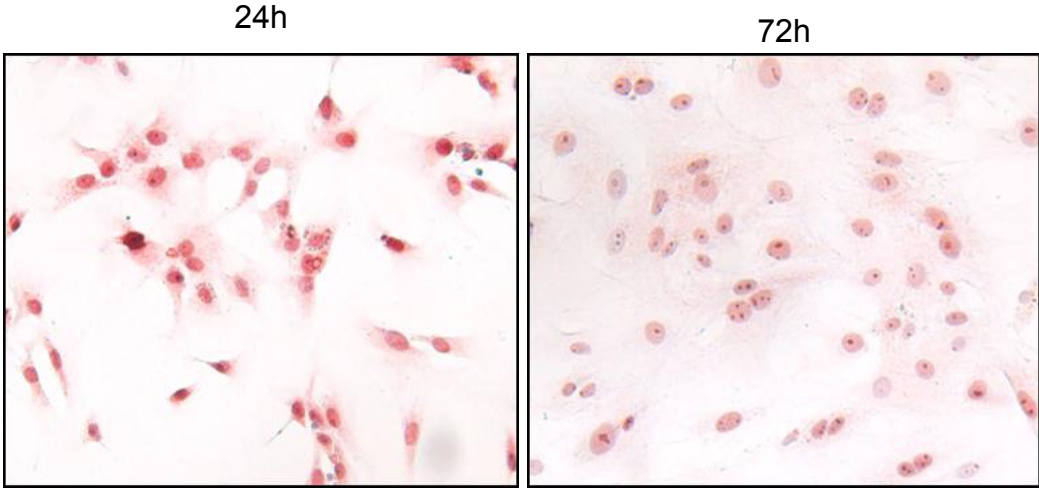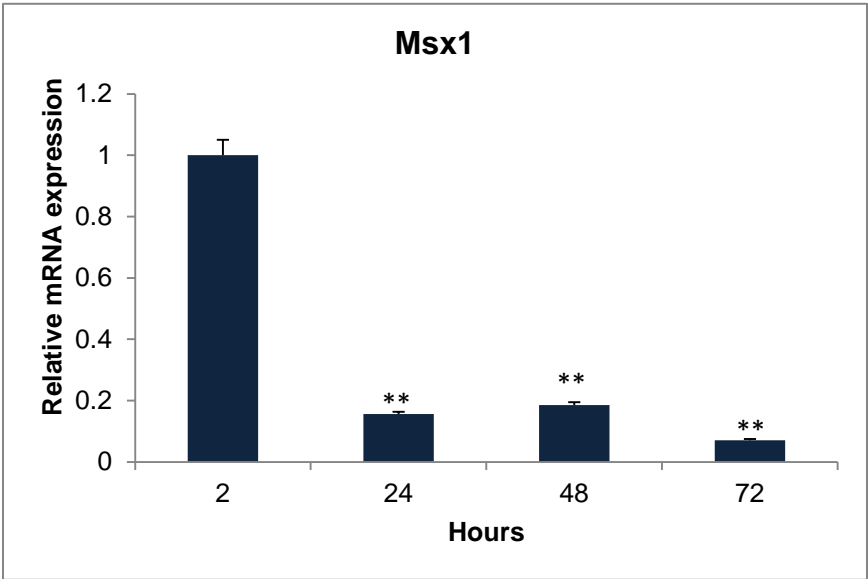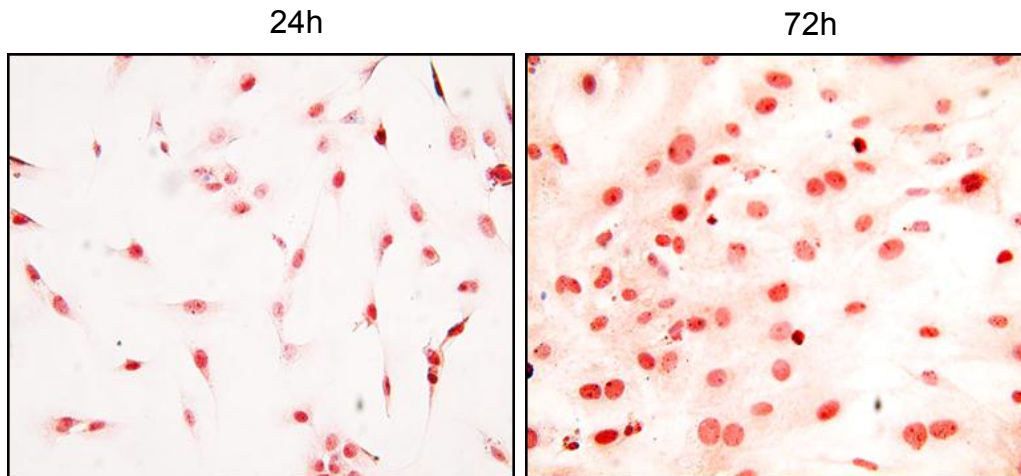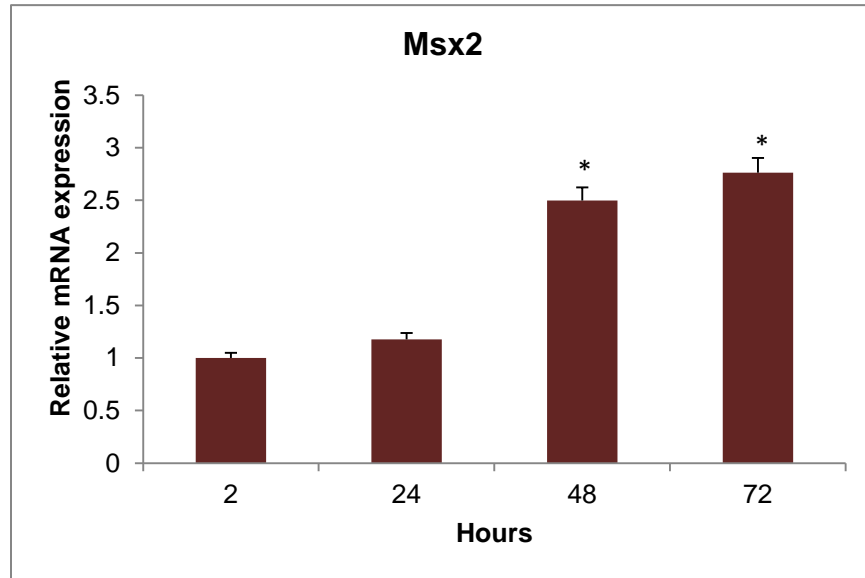
Figure 21 (Contd.) Expression profile of *Msx1* and *Msx2* during in vitro stromal cell differentiation

Stromal cells isolated from day 4 pregnant uteri were cultured in vitro as described in materials and methods. The cells were lysed at different time points and real-time PCR was performed to monitor the expression of mRNAs corresponding to Msx1 (A, Upper panel) and Msx2 (B, Upper panel) (* $p < 0.05$; ** $p < 0.005$). Stromal cells isolated from day 4 pregnant uteri were cultured in vitro as described in materials and methods. The cells were fixed at different time points and were subjected immunocytochemical staining using anti-Msx1 (A, Lower panel) and anti-Msx2 (B, Lower panel) antibodies.

Figure 22 Expression of *Msx1* and *Msx2* in the uterus during early pregnancy
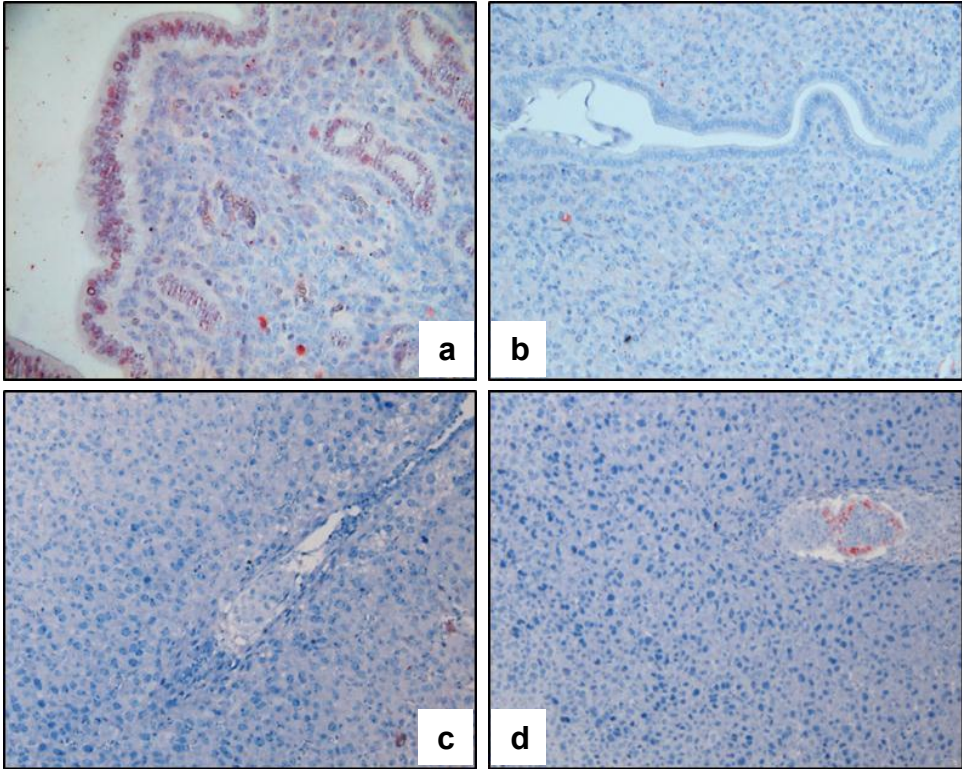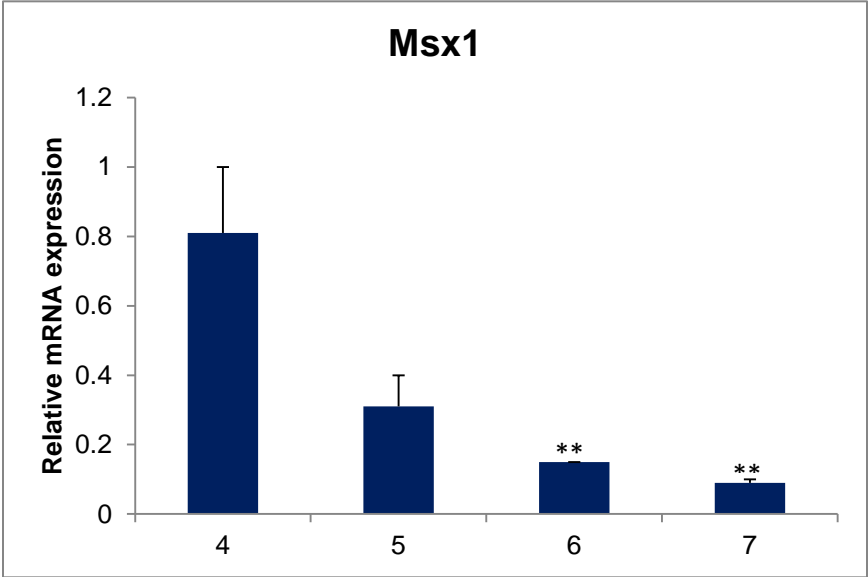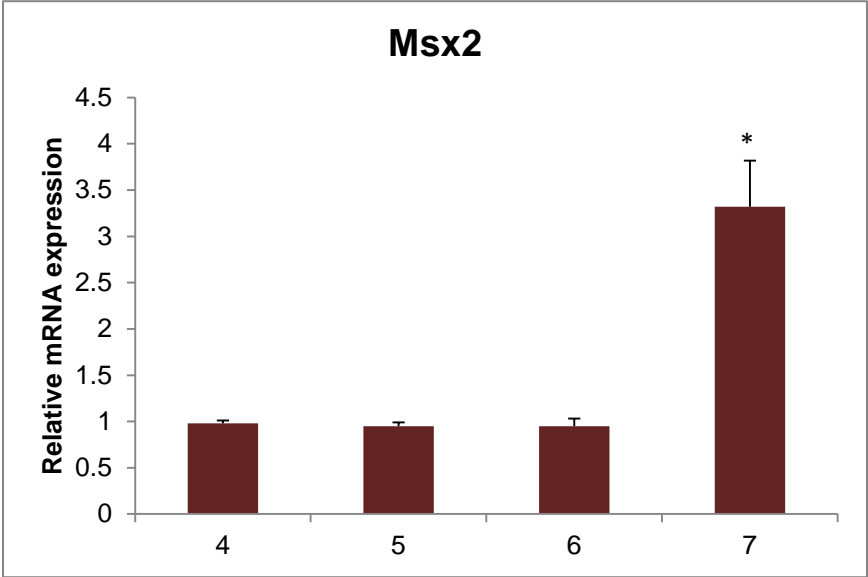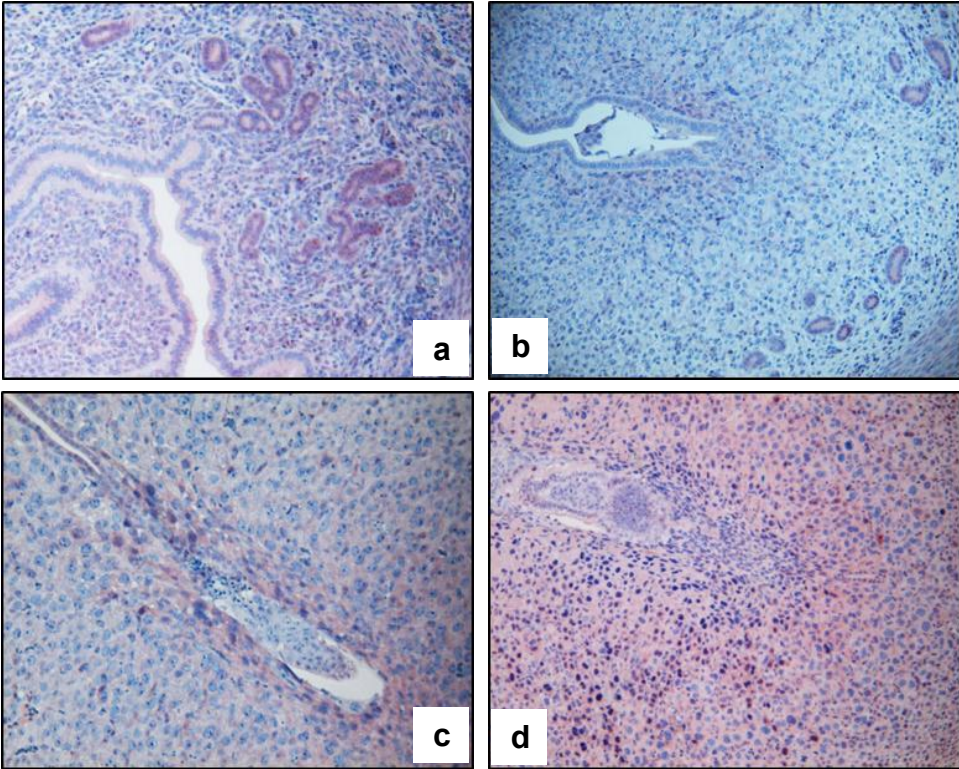
A

MSX1

Figure 22 (Contd.) Expression of *Msx1* and *Msx2* in the uterus during early pregnancy

B

MSX2

Figure 22 (Contd.) Expression of *Msx1* and *Msx2* in the uterus during early pregnancy

Real-time PCR was performed to monitor the expression of mRNAs corresponding to *Msx1* (A, Upper panel) and *Msx2* (B, Upper panel) in uterus on days 4 to 7 of gestation. The relative levels of gene expression on different days of pregnancy were determined by setting the expression level of mRNA on day 4 of pregnancy at 1.0. *Rplp0,* encoding a ribosomal protein, was used to normalize the level of RNA. Uterine sections from day 4 to day 7 (a-d) of pregnancy were subjected to immunohistochemical analysis using anti-MSX1 (A, Lower panel) and anti-MSX2 (B, Lower panel) antibodies. L, G, S and E indicate luminal epithelium, glandular epithelium, stroma and embryo, respectively (* $p < 0.05$; ** $p < 0.005$).

Figure 23 Functional redundancy of *Msx1* and *Msx2* during uterine decidualization

A
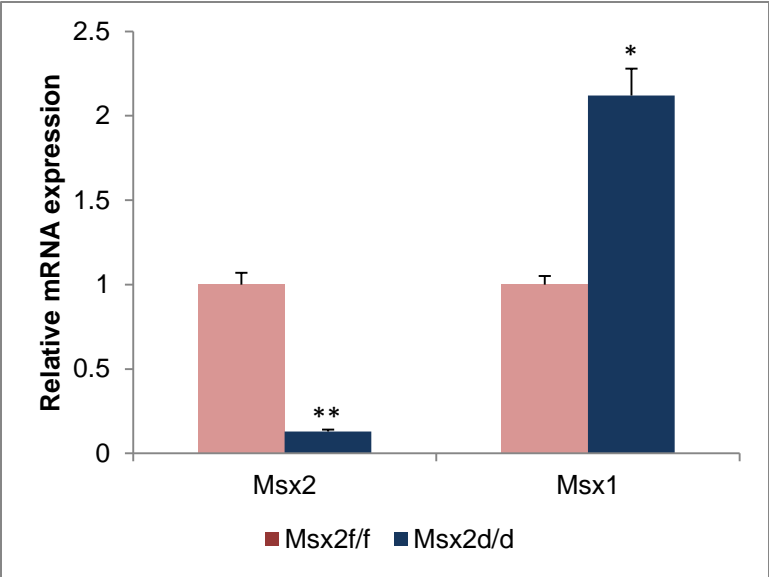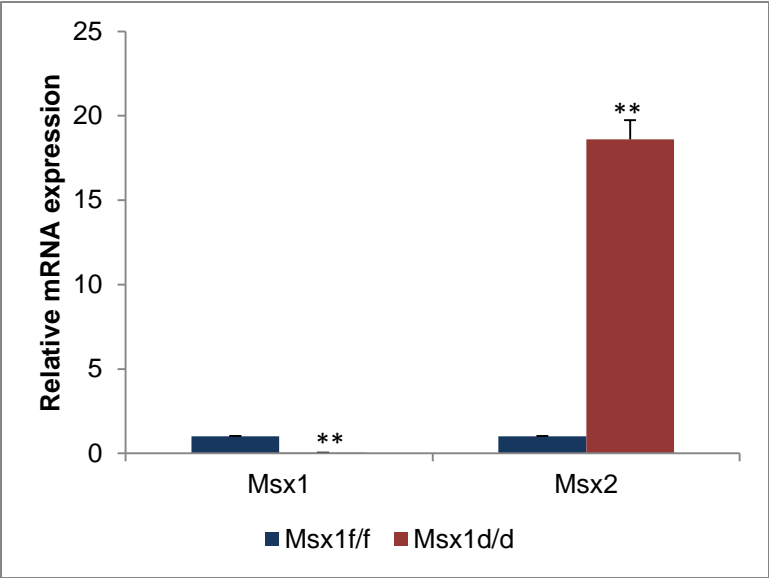
Figure 23 (Contd.) Functional redundancy of Msx1 and Msx2 during uterine decidualization

B

Figure 23 (Contd.) Functional redundancy of Msx1 and Msx2 during uterine decidualization

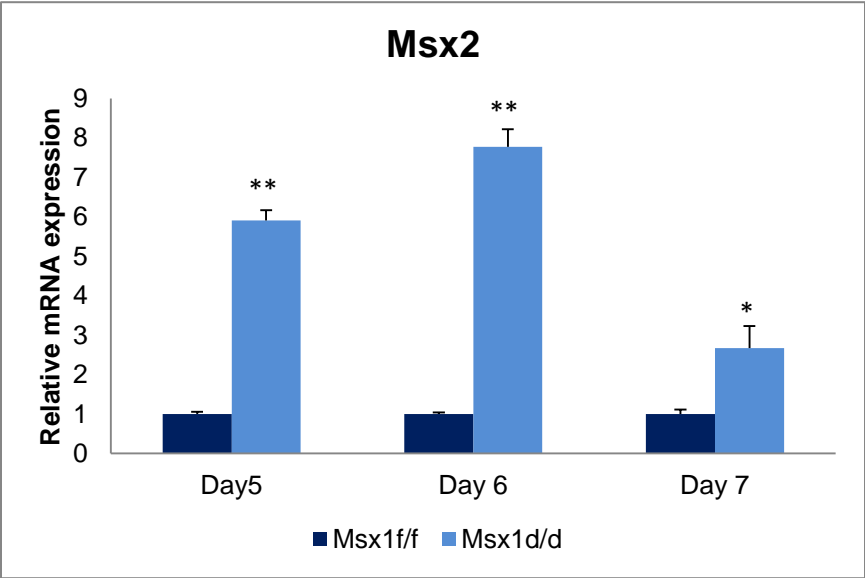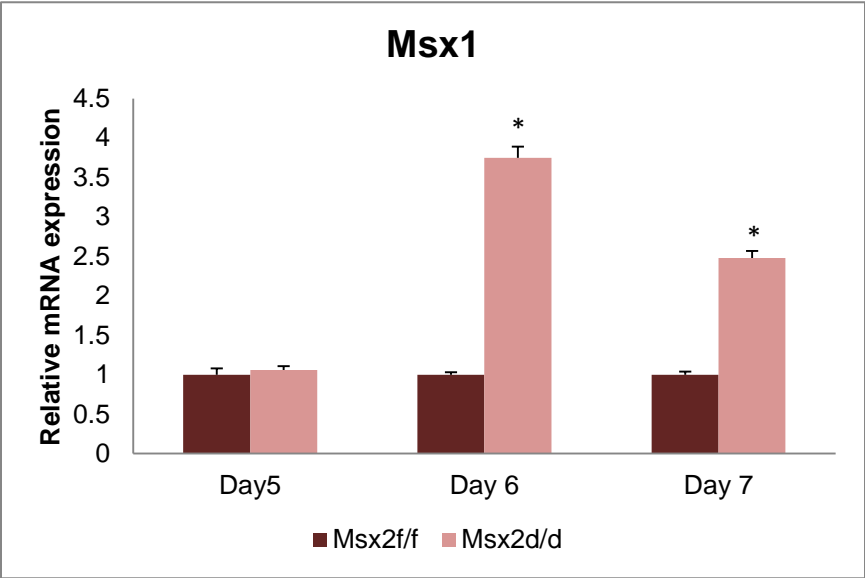A: Upper panel: Uterine RNA was purified from $Msx1^{f/f}$ and $Msx1^{d/d}$ mice on day 5 of pregnancy and analyzed by real-time PCR. Relative levels of Msx1 and Msx2 mRNA expression in uteri of $Msx1^{d/d}$ mice are compared to those in $Msx1^{f/f}$ control mice. The data are represented as the mean fold induction ± SEM (* $p < 0.05$; ** $p < 0.005$). Lower panel: Uterine RNA was purified from $Msx2^{f/f}$ and $Msx2^{d/d}$ mice on day 6 of pregnancy and analyzed by real-time PCR. Relative levels of $Msx2$ and $Msx1$ mRNA expression in uteri of $Msx2^{d/d}$ mice are compared to those in $Msx2^{f/f}$ control mice. The data are represented as the mean fold induction ± SEM (* $p < 0.05$; ** $p < 0.005$).

B: Upper panel: Uterine RNA was purified from $Msx2^{f/f}$ and $Msx2^{d/d}$ mice on day 5, 6 and 7 of pregnancy and analyzed by real-time PCR. Relative levels of $Msx1$ mRNA expression in uteri of $Msx2^{d/d}$ mice are compared to those in $Msx2^{f/f}$ control mice. The data are represented as the mean fold induction ± SEM (* $p < 0.05$; ** $p < 0.005$). Lower panel: Uterine RNA was purified from $Msx1^{f/f}$ and $Msx1^{d/d}$ mice on day 5, 6 and 7 of pregnancy and analyzed by real-time PCR. Relative levels of Msx2 mRNA expression in uteri of $Msx1^{d/d}$ mice are compared to those in $Msx1^{f/f}$ control mice. The data are represented as the mean fold induction ± SEM (* $p < 0.05$; ** $p < 0.005$).

Figure 24 Ablation of *Msx1* and *Msx2* in the uterus leads to a defect in decidualization

Upper panel: Ovariectomized $Msx1^{f/f}Msx2^{f/f}$ and $Msx1^{d/d}Msx2^{d/d}$ mice were subjected to experimentally induced decidualization as described in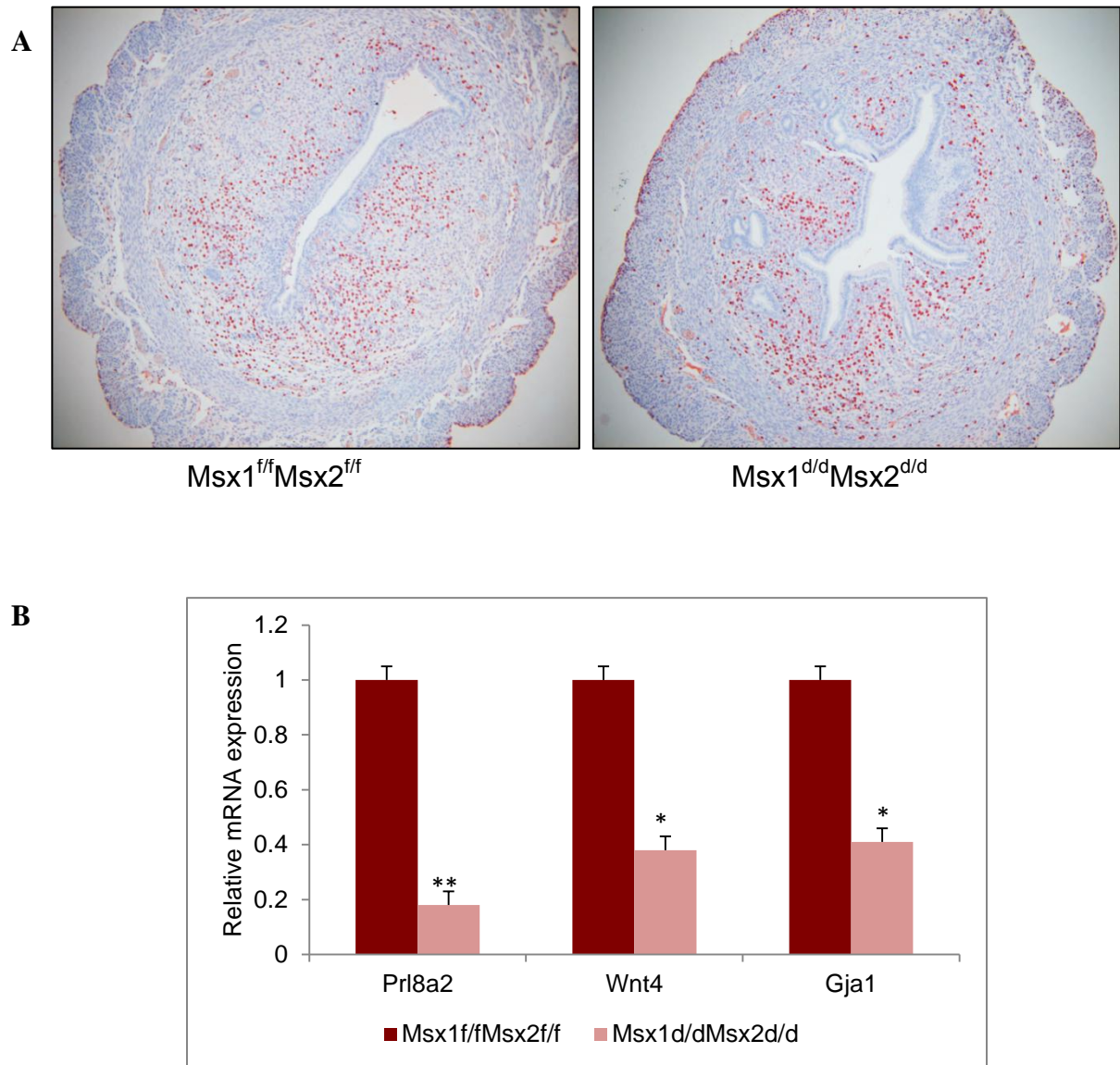 materials and methods. The stimulated horn is indicated as 'S' and the unstimulated horn as 'US'. Lower panel: The ratio of uterine wet weight gain between stimulated and unstimulated horns from $Msx1^{f/f}Msx2^{f/f}$ and $Msx1^{d/d}Msx2^{d/d}$ mice. The data are presented as mean ± SEM (*** $p < 0.0001$).

A

Msx1$^{f/f}$Msx2$^{f/f}$

Msx1$^{d/d}$Msx2$^{d/d}$

B

Figure 25 Stromal proliferation is intact while differentiation is compromised in _Msx1Msx2_-deficient uteri

A. Examination of uterine stromal cell proliferation of Msx1$^{d/d}$Msx2$^{d/d}$ mice using BrdU immunostaining. Ovariectomized Msx1$^{f/f}$Msx2$^{f/f}$ and Msx1$^{d/d}$Msx2$^{d/d}$ mice were subjected to experimentally induced decidualization as described in materials and methods. Mice were given BrdU injection at 23h after the infusion of oil and uterine tissues were collected at 24h. The uterine sections were subjected to immunohistochemistry using an antibody specific for BrdU. B. Realtime PCR was performed to assess the expression levels of Prl8a2, Wnt4 and Gja1 mRNA in the uteri of Msx1$^{f/f}$Msx2$^{f/f}$ and Msx1$^{d/d}$Msx2$^{d/d}$ mice uteri collected 72 h after the infusion of oil (* $p < 0.05$; ** $p < 0.005$).

Figure 26 Expression of MSX1 and MSX2 in human endometrial stromal cells during decidualization

A

MSX1

Day 0   Day 4

B

MSX2

Day 0   Day 4
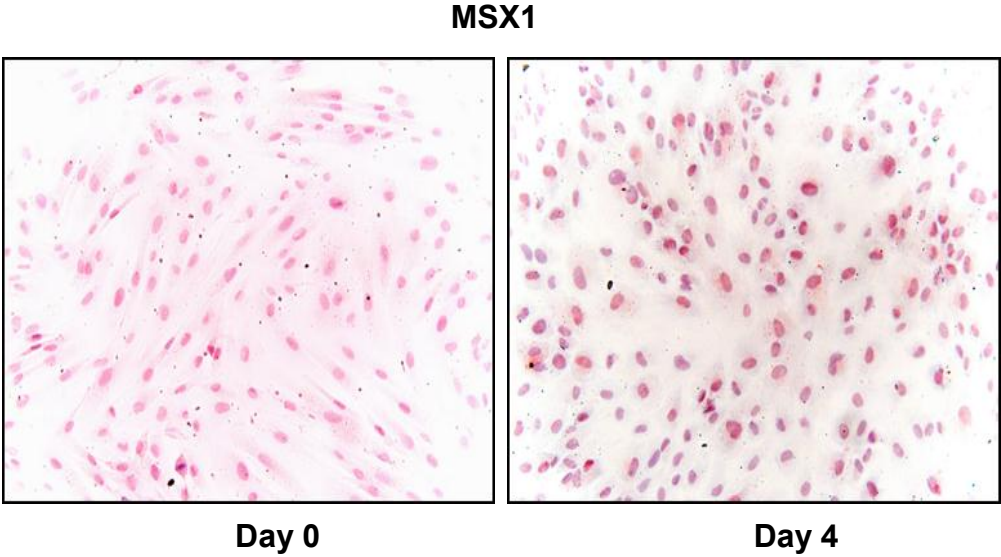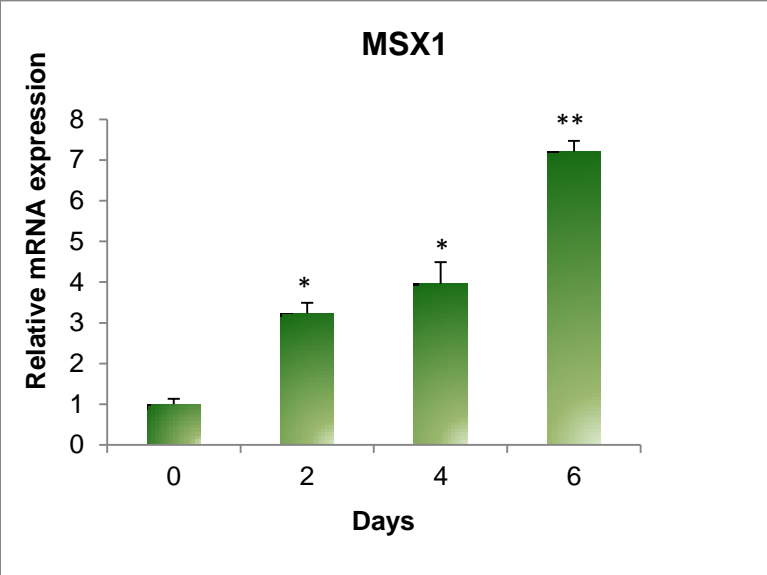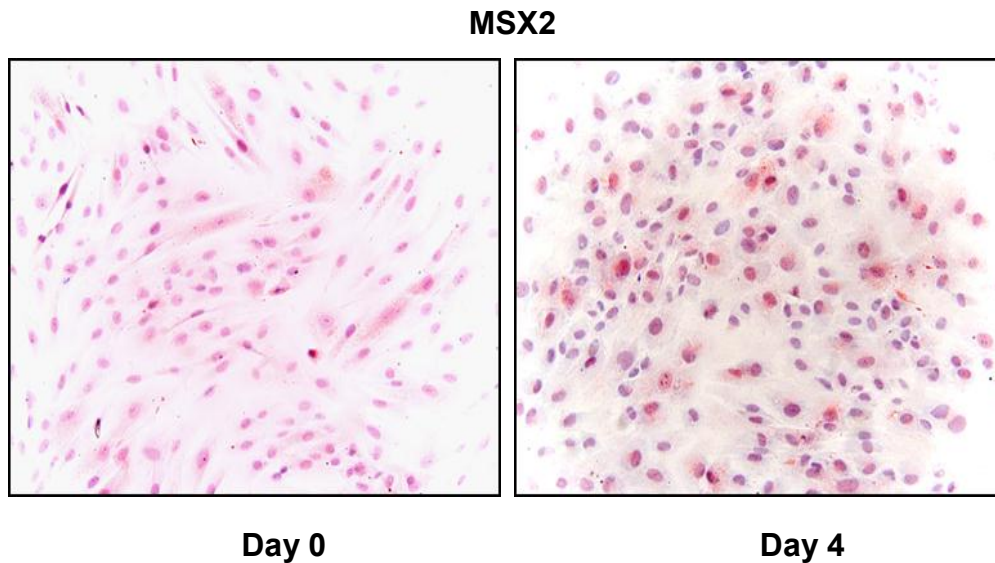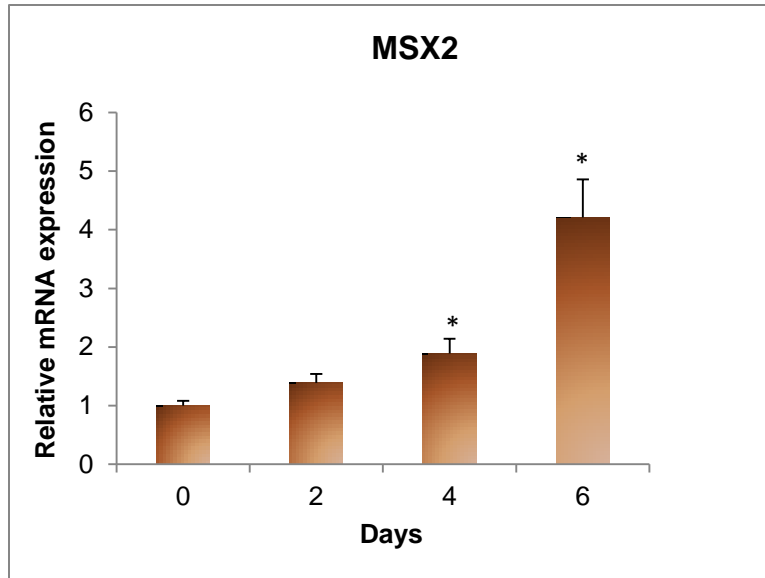
Figure 26 (Contd.) Expression of MSX1 and MSX2 in human endometrial stromal cells during decidualization

The primary cultures of human endometrial stromal cells were performed as described in materials and methods. The cells were lysed at different time points as indicated. Total RNA was isolated and real time PCR was performed to analyze the levels of MSX1 (A, Upper panel) and MSX2 (B, Upper panel). *RPLP0,* encoding a ribosomal protein, was used to normalize the level of RNA (* $p < 0.05$; ** $p < 0.005$). Immunocytochemical analysis of MSX1 (A, Lower panel) and MSX2 (B, Lower panel) on day 0 and day4 during in vitro stromal cell differentiation.

Figure 27 MSX1 and MSX2 mediate BMP2 induced human endometrial stromal cell decidualization
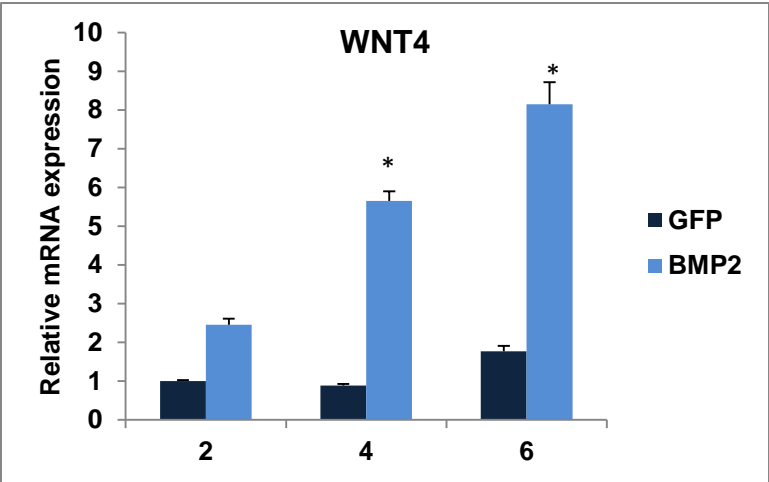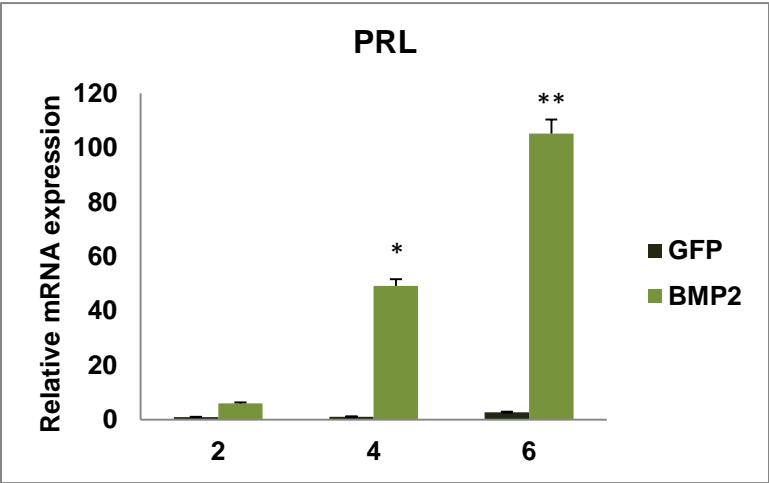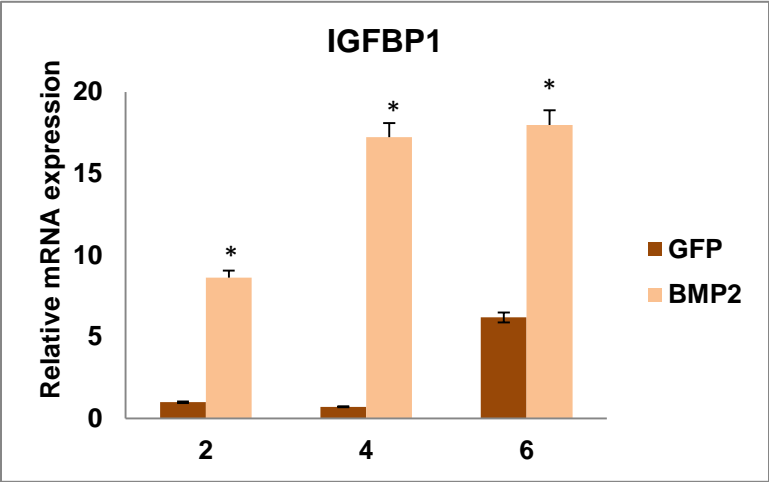
Figure 27 (Contd.) MSX1 and MSX2 mediate BMP2 induced human endometrial stromal cell decidualization
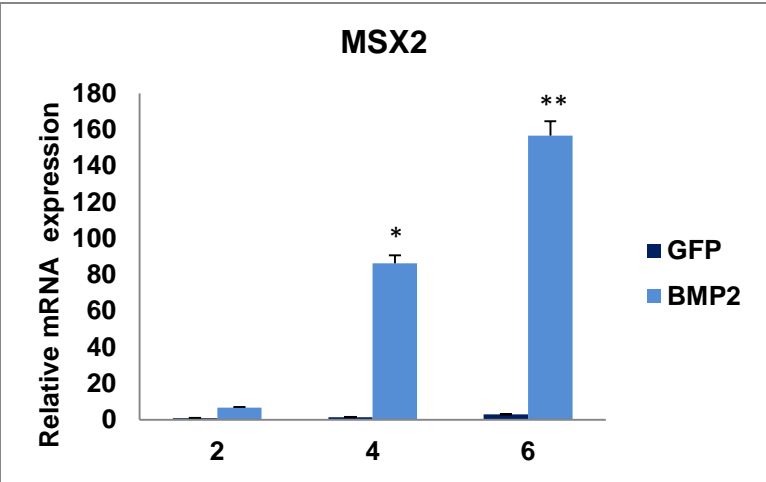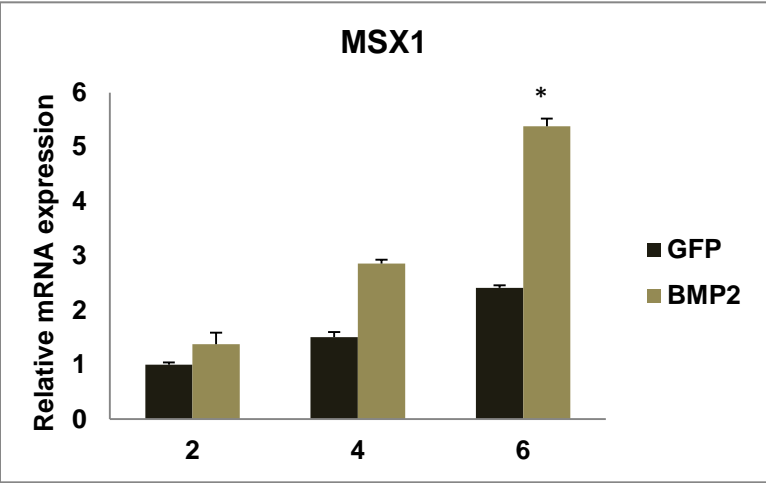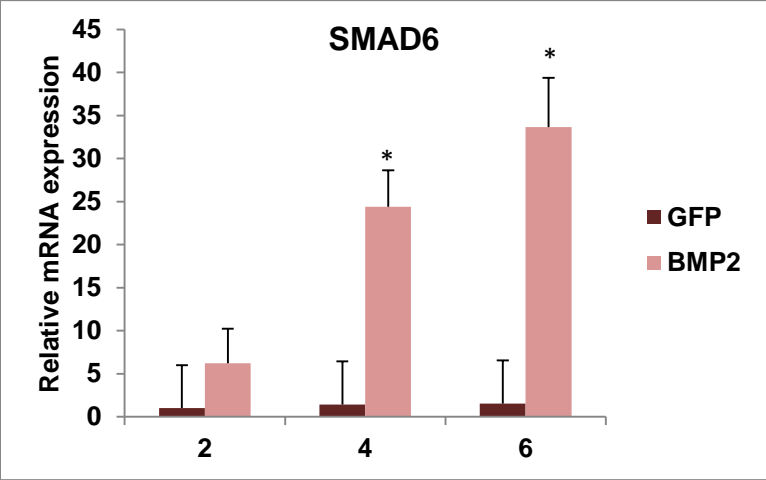
Figure 27 (Contd.) MSX1 and MSX2 mediate BMP2 induced human endometrial stromal cell decidualization

The primary cultures of human endometrial stromal cells were performed as described in materials and methods. The cells were transduced with adenovirus expressing BMP2 or GFP. The cells were lysed at different time points as indicated. Total RNA was isolated and real time PCR was performed to analyze the levels of IGFBP-1, PRL, WNT4, SMAD6, MSX1 and MSX2. The relative levels of gene expression were determined by setting the expression level on day 0 of GFP treated at 1.0. *RPLP0,* encoding a ribosomal protein, was used to normalize the level of RNA (* $p < 0.05$; ** $p < 0.005$).

Figure 28 *MSX* genes regulate decidualization of human endometrial stromal cells
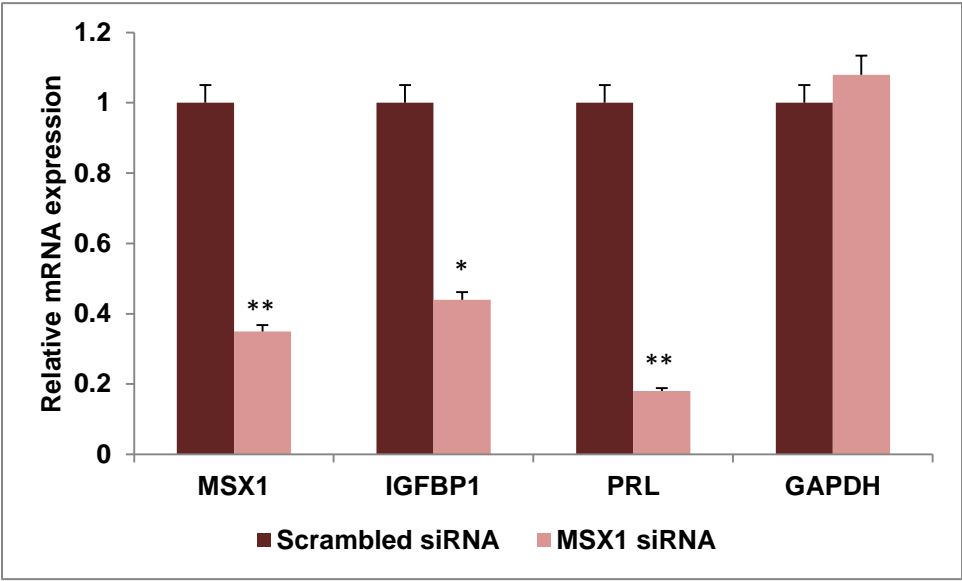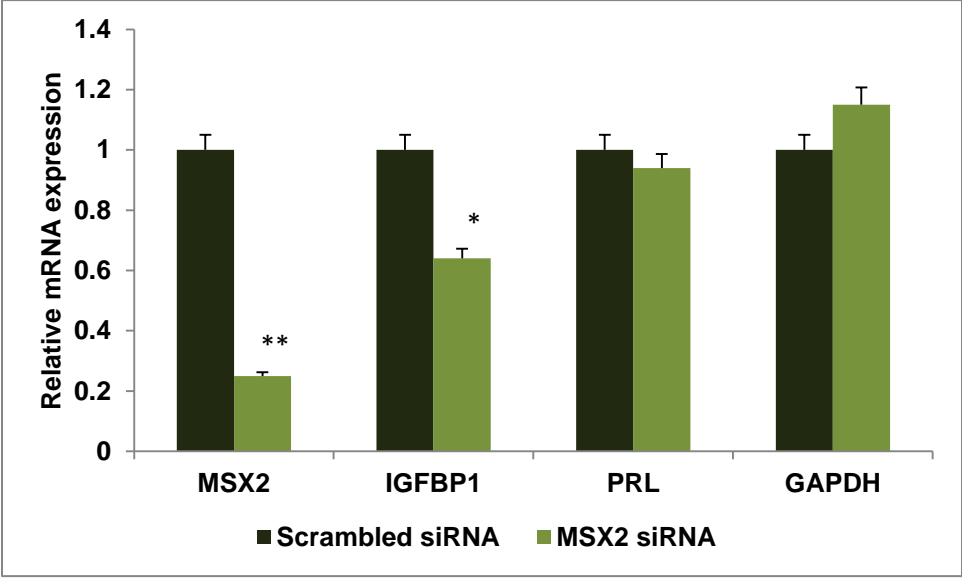
Figure 28 (Contd.) *MSX* **genes regulate decidualization of human endometrial stromal cells**

The human endometrial stromal cells were transfected with MSX1 siRNA (A) or MSX2 siRNA (B) after reaching approximately 70% confluency. The control group was transfected with scrambled siRNA. The siRNA was removed after 24 h and the culture was continued for additional 2 days after the addition of hormones and cAMP. The cells were lysed to isolate total RNA and real time PCR was performed to analyze the levels of MSX1, IGFBP-1 and PRL. The relative levels of gene expression were determined by setting the expression level of scrambled siRNA treated at 1.0. *RPLP0,* encoding a ribosomal protein, was used to normalize the level of RNA (* $p < 0.05$; ** $p < 0.005$).

CHAPTER V

CONCLUSIONS

The present study was designed to understand the role of homeobox transcription factors, *Msx*1 and *Msx*2, in the uterus during embryo implantation. To gain an insight into the function of *Msx* genes in uterus, we generated conditional knockout mice ($Msx1^{d/d}Msx2^{d/d}$) by crossing *Msx* floxed mice with progesterone receptor cre mice. Six months breeding studies revealed that the mice lacking both *Msx*1 and *Msx*2 in their uteri were infertile. Subsequent analysis revealed that $Msx1^{d/d}Msx2^{d/d}$ mice exhibited normal ovarian functions. While the preimplantation development of embryos and their transit into the uterus were normal, Chicago blue dye assay failed to exhibit blue bands in the uteri of $Msx1^{d/d}Msx2^{d/d}$ mice indicating implantation failure. Histological analysis of uterus revealed that the blastocysts failed to attach to the uterine epithelium. Ultrastructural analysis of uterine luminal epithelium using transmission electron microscopy demonstrated a failure of microvilli remodeling on day 4 of pregnancy. Further, estrogen signaling was highly elevated in the uterine luminal epithelium of $Msx1^{d/d}Msx2^{d/d}$ mice. The level of Muc1 (a marker of uterine receptivity) was greatly enhanced in the uterine luminal epithelium of $Msx1^{d/d}Msx2^{d/d}$ mice. The uterine epithelium lacking *Msx*1 and *Msx*2 exhibited persistent proliferative activity. The undifferentiated glandular epithelial cells fail to express critical glandular factors such as Lif and undifferentiated luminal epithelium fail to acquire the receptive state. These results indicate that uterine specific deletion of *Msx* homeobox genes renders mouse infertile due to a lack of uterine receptivity.

Gene expression profiling of uterine stromal and epithelial cells showed elevated expression of several members of the Wnt gene family. The enhanced Wnts activated β-catenin in uterine stromal cells and stimulated the production of a subset of fibroblast growth factors (FGFs). The FGFs secreted from the stromal cells acted through the FGF receptors present in the epithelium to promote epithelial proliferation. This persistent proliferation prevented the uterus to achieve the receptive phase during embryo implantation. Collectively, these results uncovered a unique signaling network, involving Msx, Wnts, and FGFs, which regulate stromal-epithelial communication critical for acquisition of uterine receptivity.

Finally, we investigated the role of *Msx* homeobox genes during stromal decidualization. Mice lacking *Msx*1 and *Msx*2 in their uteri failed to exhibit decidual response during experimentally induced decidualization. Further experiments revealed that these genes regulate stromal cell differentiation but not proliferation during decidualization. Our studies also revealed that *MSX*1 and *MSX*2 critically regulate human endometrial stromal cell differentiation. In both mice and humans, the *Msx* genes act downstream of BMP2 in mediating stromal cell decidualization.

Collectively, this study provides an insight into the molecular mechanisms underlying endometrial receptivity and stromal decidualization for embryo implantation. It may help to design the treatment protocol for reproductive disorders and to improve the success rate of assisted reproductive technologies in treating infertility in women.

REFERENCES

1. Carson DD, Bagchi I, Dey SK, Enders AC, Fazleabas AT, et al. (2000) Embryo Implantation. Developmental Biology 223: 217-237.

2. Lee KY, Jeong J-W, Tsai SY, Lydon JP, DeMayo FJ (2007) Mouse models of implantation. Trends in Endocrinology & Metabolism 18: 234-239.

3. Wang H, Dey SK (2006) Roadmap to embryo implantation: clues from mouse models. Nat Rev Genet 7: 185-199.

4. Dey SK, Lim H, Das SK, Reese J, Paria BC, et al. (2004) Molecular Cues to Implantation. Endocr Rev 25: 341-373.

5. Tabibzadeh S, Babaknia A (1995) Molecular aspects of implantation: The signals and molecular pathways involved in implantation, a symbiotic interaction between blastocyst and endometrium involving adhesion and tissue invasion. Human Reproduction 10: 1579-1602.

6. Edwards RG (1988) Human Uterine Endocrinology and the Implantation Window. Annals of the New York Academy of Sciences 541: 445-454.

7. Tabibzadeh S (1998) Molecular control of the implantation window. Human Reproduction Update 4: 465-471.

8. Psychoyos A (1986) Uterine Receptivity for Nidation. Annals of the New York Academy of Sciences 476: 36-42.

9. Beir-Hellwig K, Sterzik K, Bonn B, Beir H (1989) Contribution to the physiology and pathology of endometrial receptivity: the determination of protein patterns in human uterine secretions. Hum Reprod 4: 115 - 120.

10. Yoshinaga K (1988) Uterine Receptivity for Blastocyst Implantation. Annals of the New York Academy of Sciences 541: 424-431.

11. Paria BC, Huet-Hudson YM, Dey SK (1993) Blastocyst's state of activity determines the "window" of implantation in the receptive mouse uterus. Proceedings of the National Academy of Sciences of the United States of America 90: 10159-10162.

12. Achache H, Revel A (2006) Endometrial receptivity markers, the journey to successful embryo implantation. Human Reproduction Update 12: 731-746.

13. Lessey BA (2000) The role of the endometrium during embryo implantation. Human Reproduction 15: 39-50.

14. Diedrich K, Fauser BCJM, Devroey P, Griesinger G (2007) The role of the endometrium and embryo in human implantation. Human Reproduction Update 13: 365-377.

15. The European IVF-monitoring programme ftESoHR, Embryology (2005) Assisted reproductive technology in Europe, 2001. Results generated from European registers by ESHRE. Human Reproduction 20: 1158-1176.

16. de los Santos MJ, Mercader A, Galán A, Albert C, Romero JL, et al. (2003) Implantation Rates after Two, Three, or Five Days of Embryo Culture. Placenta 24, Supplement 2: S13-S19.

17. Rinehart J (2007) Recurrent implantation failure: definition. Journal of Assisted Reproduction and Genetics 24: 284-287.

18. Margalioth EJ, Ben-Chetrit A, Gal M, Eldar-Geva T (2006) Investigation and treatment of repeated implantation failure following IVF-ET. Human Reproduction 21: 3036-3043.

19. Ola B LT (2006) Implantation failure following in-vitro fertilization. Current opinion in obstetrics & gynecology 18: 440-445.

20. Tan BK, Vandekerckhove P, Kennedy R, Keay SD (2005) Investigation and current management of recurrent IVF treatment failure in the UK. Bjog-an International Journal of Obstetrics and Gynaecology 112: 773-780.

21. Sharkey AM, Smith SK (2003) The endometrium as a cause of implantation failure. Best Practice & Research Clinical Obstetrics & Gynaecology 17: 289-307.

22. Simon C, Moreno C, Remohi J, Pellicer A (1998) Cytokines and embryo implantation. Journal of Reproductive Immunology 39: 117-131.

23. Bourgain C, Devroey P (2003) The endometrium in stimulated cycles for IVF. Human Reproduction Update 9: 515-522.

24. Senturk LM, Erel CT (2008) Thin endometrium in assisted reproductive technology. Current Opinion in Obstetrics and Gynecology 20: 221-228 210.1097/GCO.1090b1013e328302143c.

25. Mahutte NG, Arici A (2001) Endometriosis and assisted reproductive technologies: are outcomes affected? Current Opinion in Obstetrics and Gynecology 13: 275-279.

26. Lessey BA (2002) Implantation Defects in Infertile Women with Endometriosis. Annals of the New York Academy of Sciences 955: 265-280.

27. Linda C G (2006) Endometrium in PCOS: Implantation and predisposition to endocrine CA. Best Practice & Research Clinical Endocrinology & Metabolism 20: 235-244.

28. Zeyneloglu HB (2001) Hydrosalpinx and assisted reproduction: options and rationale for treatment. Current Opinion in Obstetrics and Gynecology 13: 281-286.

29. Savaris RF, Giudice LC (2007) The Influence of Hydrosalpinx on Markers of Endometrial Receptivity. Semin Reprod Med 25: 476,482.

30. Donaghay M, Lessey BA (2007) Uterine Receptivity: Alterations Associated with Benign Gynecological Disease. Semin Reprod Med 25: 461,475.

31. Acosta AA, Elberger L, Borghi M, Calamera JC, Chemes H, et al. (2000) Endometrial dating and determination of the window of implantation in healthy fertile women. Fertility and Sterility 73: 788-798.

32. Lessey BA, Castelbaum AJ, Wolf L, Greene W, Paulson M, et al. (2000) Use of integrins to date the endometrium. Fertility and Sterility 73: 779-787.

33. Lee KY, DeMayo FJ (2004) Animal models of implantation. Reproduction 128: 679-695.

34. Enders AC, Schlafke S (1967) A morphological analysis of the early implantation stages in the rat. American Journal of Anatomy 120: 185-225.

35. Enders AC, Schlafke S (1969) Cytological aspects of trophoblast-uterine interaction in early implantation. American Journal of Anatomy 125: 1-29.

36. Psychoyos A (1973) Endocrine control of egg implantation. In: Greep RO, Astwood EG, Geiger SR, editors. Handbook of physiology, Washington, DC: American Physiological Society. pp. 187-215.

37. Murphy CR (2004) Uterine receptivity and the plasma membrane transformation. Cell Res 14: 259-267.

38. Tachi S, Tachi C, Lindner HR (1970) Ultrastructural features of blastocyst attachment and trophoblastic invasion in rat. Journal of Reproduction and Fertility 21: 37-&.

39. Smith AF, Wilson IB (1974) Cell-interaction at maternal-embryonic interface during implantation in mouse. Cell and Tissue Research 152: 525-542.

40. Hartsock A, Nelson WJ (2008) Adherens and tight junctions: Structure, function and connections to the actin cytoskeleton. Biochimica et Biophysica Acta (BBA) - Biomembranes 1778: 660-669.

41. Paria BC, Zhao X, Das SK, Dey SK, Yoshinaga K (1999) Zonula Occludens-1 and E-cadherin are coordinately expressed in the mouse uterus with the initiation of implantation and decidualization. Developmental Biology 208: 488-501.

42. Li Q, Wang J, Armant DR, Bagchi MK, Bagchi IC (2002) Calcitonin Down-regulates E-cadherin Expression in Rodent Uterine Epithelium during Implantation. Journal of Biological Chemistry 277: 46447-46455.

43. Large MJ, DeMayo FJ (2011) The regulation of embryo implantation and endometrial decidualization by progesterone receptor signaling. Molecular and Cellular Endocrinology.

44. Stewart CL, Kaspar P, Brunet LJ, Bhatt H, Gadi I, et al. (1992) Blastocyst implantation depends on maternal expression of leukaemia inhibitory factor. Nature 359: 76-79.

45. Lubahn DB, Moyer JS, Golding TS, Couse JF, Korach KS, et al. (1993) Alteration of reproductive function but not prenatal sexual development after insertional disruption of the mouse estrogen receptor gene. Proceedings of the National Academy of Sciences of the United States of America 90: 11162-11166.

46. Dupont S, Krust A, Gansmuller A, Dierich A, Chambon P, et al. (2000) Effect of single and compound knockouts of estrogen receptors alpha (ERalpha) and beta (ERbeta) on mouse reproductive phenotypes. Development 127: 4277-4291.

47. Lydon JP, DeMayo FJ, Funk CR, Mani SK, Hughes AR, et al. (1995) Mice lacking progesterone receptor exhibit pleiotropic reproductive abnormalities. Genes & Development 9: 2266-2278.

48. Franco HL, Rubel CA, Large MJ, Wetendorf M, Fernandez-Valdivia R, et al. (2011) Epithelial progesterone receptor exhibits pleiotropic roles in uterine development and function. The FASEB Journal.

49. Conneely OM, Lydon JP (2000) Progesterone receptors in reproduction: functional impact of the A and B isoforms. Steroids 65: 571-577.

50. Mantena SR, Kannan A, Cheon Y-P, Li Q, Johnson PF, et al. (2006) C/EBPβ is a critical mediator of steroid hormone-regulated cell proliferation and differentiation in the uterine epithelium and stroma. Proceedings of the National Academy of Sciences of the United States of America 103: 1870-1875.

51. Tranguch S, Cheung-Flynn J, Daikoku T, Prapapanich V, Cox MB, et al. (2005) Cochaperone immunophilin FKBP52 is critical to uterine receptivity for embryo implantation. Proceedings of the National Academy of Sciences of the United States of America 102: 14326-14331.

52. Lee K, Jeong J, Kwak I, Yu C-T, Lanske B, et al. (2006) Indian hedgehog is a major mediator of progesterone signaling in the mouse uterus. Nat Genet 38: 1204-1209.

53. Kurihara I, Lee D-K, Petit FG, Jeong J, Lee K, et al. (2007) COUP-TFII Mediates Progesterone Regulation of Uterine Implantation by Controlling ER Activity. PLoS Genet 3: e102.

54. Li Q, Kannan A, DeMayo FJ, Lydon JP, Cooke PS, et al. (2011) The Antiproliferative Action of Progesterone in Uterine Epithelium Is Mediated by Hand2. Science 331: 912-916.

55. Kimber SJ (2005) Leukaemia inhibitory factor in implantation and uterine biology. Reproduction 130: 131-145.

56. Bhatt H, Brunet LJ, Stewart CL (1991) Uterine expression of leukemia inhibitory factor coincides with the onset of blastocyst implantation. Proceedings of the National Academy of Sciences 88: 11408-11412.

57. Couse JF, Korach KS (1999) Estrogen Receptor Null Mice: What Have We Learned and Where Will They Lead Us? Endocrine Reviews 20: 358-417.

58. Tan J, Paria BC, Dey SK, Das SK (1999) Differential Uterine Expression of Estrogen and Progesterone Receptors Correlates with Uterine Preparation for Implantation and Decidualization in the Mouse. Endocrinology 140: 5310-5321.

59. Tibbetts TA, Mendoza-Meneses M, O'Malley BW, Conneely OM (1998) Mutual and Intercompartmental Regulation of Estrogen Receptor and Progesterone Receptor Expression in the Mouse Uterus. Biology of Reproduction 59: 1143-1152.

60. Krege JH, Hodgin JB, Couse JF, Enmark E, Warner M, et al. (1998) Generation and reproductive phenotypes of mice lacking estrogen receptor β. Proceedings of the National Academy of Sciences 95: 15677-15682.

61. Bagchi IC, Cheon YP, Li Q, Bagchi MK (2003) Progesterone receptor-regulated gene networks in implantation. Front Biosci 8: s852-861.

62. Cheon Y-P, Li Q, Xu X, DeMayo FJ, Bagchi IC, et al. (2002) A Genomic Approach to Identify Novel Progesterone Receptor Regulated Pathways in the Uterus during Implantation. Mol Endocrinol 16: 2853-2871.

63. Conneely OM, Mulac-Jericevic B, Lydon JP, De Mayo FJ (2001) Reproductive functions of the progesterone receptor isoforms: lessons from knock-out mice. Molecular and Cellular Endocrinology 179: 97-103.

64. Quarmby VE, Korach KS (1984) The influence of 17 beta-estradiol on patterns of cell division in the uterus. Endocrinology 114(3):694-702.

65. Lee K, Jeong J, Tsai MJ, Tsai S, Lydon JP, et al. (2006) Molecular mechanisms involved in progesterone receptor regulation of uterine function. The Journal of Steroid Biochemistry and Molecular Biology 102: 41-50.

66. Teilmann SC, Clement CA, Thorup J, Byskov AG, Christensen ST (2006) Expression and localization of the progesterone receptor in mouse and human reproductive organs. Journal of Endocrinology 191: 525-535.

67. Wetendorf M, DeMayo FJ (2011) The progesterone receptor regulates implantation, decidualization, and glandular development via a complex paracrine signaling network. Molecular and Cellular Endocrinology.

68. Mulac-Jericevic B, Mullinax RA, DeMayo FJ, Lydon JP, Conneely OM (2000) Subgroup of reproductive functions of progesterone mediated by progesterone receptor-B-isoform. Science 289: 1751-1754.

69. Ramathal C, Bagchi IC, Bagchi MK (2010) Lack of CCAAT Enhancer Binding Protein Beta (C/EBP{beta}) in Uterine Epithelial Cells Impairs Estrogen-Induced DNA Replication,

Induces DNA Damage Response Pathways, and Promotes Apoptosis. Mol Cell Biol 30: 1607-1619.

70. Wang W, Li Q, Bagchi IC, Bagchi MK (2010) The CCAAT/Enhancer Binding Protein {beta} Is a Critical Regulator of Steroid-Induced Mitotic Expansion of Uterine Stromal Cells during Decidualization. Endocrinology 151: 3929-3940.

71. Takamoto N, Zhao B, Tsai SY, DeMayo FJ (2002) Identification of Indian Hedgehog as a Progesterone-Responsive Gene in the Murine Uterus. Mol Endocrinol 16: 2338-2348.

72. Franco HL, Lee KY, Broaddus RR, White LD, Lanske B, et al. (2010) Ablation of Indian Hedgehog in the Murine Uterus Results in Decreased Cell Cycle Progression, Aberrant Epidermal Growth Factor Signaling, and Increased Estrogen Signaling. Biology of Reproduction 82: 783-790.

73. Lee D-K, Kurihara I, Jeong J-W, Lydon JP, DeMayo FJ, et al. (2010) Suppression of ERα Activity by COUP-TFII Is Essential for Successful Implantation and Decidualization. Molecular Endocrinology 24: 930-940.

74. Burton GJ, Watson AL, Hempstock J, Skepper JN, Jauniaux E (2002) Uterine Glands Provide Histiotrophic Nutrition for the Human Fetus during the First Trimester of Pregnancy. J Clin Endocrinol Metab 87: 2954-2959.

75. Given RL EA (1981) Mouse uterine glands during the peri-implantation period. II. Autoradiographic studies. The Anatomical record 199: 109-127.

76. Gray CA, Bartol FF, Tarleton BJ, Wiley AA, Johnson GA, et al. (2001) Developmental Biology of Uterine Glands. Biology of Reproduction 65: 1311-1323.

77. Gray CA, Taylor KM, Ramsey WS, Hill JR, Bazer FW, et al. (2001) Endometrial Glands Are Required for Preimplantation Conceptus Elongation and Survival. Biology of Reproduction 64: 1608-1613.

78. Hempstock J, Cindrova-Davies T, Jauniaux E, Burton G (2004) Endometrial glands as a source of nutrients, growth factors and cytokines during the first trimester of human pregnancy: A morphological and immunohistochemical study. Reproductive Biology and Endocrinology 2: 58.

79. Hayashi K, Yoshioka S, Reardon SN, Rucker EB, Spencer TE, et al. (2011) WNTs in the Neonatal Mouse Uterus: Potential Regulation of Endometrial Gland Development. Biology of Reproduction 84: 308-319.

80. Jeong J-W, Kwak I, Lee KY, Kim TH, Large MJ, et al. (2010) Foxa2 Is Essential for Mouse Endometrial Gland Development and Fertility. Biology of Reproduction 83: 396-403.

81. Chen W, Han B-C, Wang R-C, Xiong G-F, Peng J-P (2010) Role of secretory protease inhibitor SPINK3 in mouse uterus during early pregnancy. Cell and Tissue Research 341: 441-451.

82. Bartol FF, Wiley AA, Coleman DA, Wolfe DF, Riddell MG (1988) Ovine Uterine Morphogenesis: Effects of Age and Progestin Administration and Withdrawal on Neonatal Endometrial Development and DNA Synthesis. Journal of Animal Science 66: 3000-3009.

83. Spencer TE, Stagg AG, Joyce MM, Jenster G, Wood CG, et al. (1999) Discovery and Characterization of Endometrial Epithelial Messenger Ribonucleic Acids Using the Ovine Uterine Gland Knockout Model. Endocrinology 140: 4070-4080.

84. Cooke PS, Ekman GC, Kaur J, Davila J, Bagchi IC, et al. (2011) Brief Exposure to Progesterone During a Critical Neonatal Window Prevents Uterine Gland Formation in Mice. Biology of Reproduction.

85. Mericskay M, Kitajewski J, Sassoon D (2004) Wnt5a is required for proper epithelial-mesenchymal interactions in the uterus. Development 131: 2061-2072.

86. Miller C, Sassoon DA (1998) Wnt-7a maintains appropriate uterine patterning during the development of the mouse female reproductive tract. Development 125: 3201-3211.

87. Dunlap KA, Filant J, Hayashi K, Rucker EB, Song G, et al. (2011) Postnatal Deletion of Wnt7a Inhibits Uterine Gland Morphogenesis and Compromises Adult Fertility in Mice. Biology of Reproduction 85: 386-396.

88. Parr BA, McMahon AP (1998) Sexually dimorphic development of the mammalian reproductive tract requires Wnt-7a. Nature 395: 707-710.

89. Jeong JW, Lee HS, Franco HL, Broaddus RR, Taketo MM, et al. (2008) [beta]-catenin mediates glandular formation and dysregulation of [beta]-catenin induces hyperplasia formation in the murine uterus. Oncogene 28: 31-40.

90. Rubel CA, Jeong J-W, Tsai SY, Lydon JP, DeMayo FJ (2010) Epithelial-Stromal Interaction and Progesterone Receptors in the Mouse Uterus. Semin Reprod Med 28: 027,035.

91. Cunha GR, Cooke PS, Kurita T (2004) Role of stromal-epithelial interactions in hormonal responses. Arch Histol Cytol 67: 417 - 434.

92. Bigsby RM (2002) Control of Growth and Differentiation of the Endometrium: The Role of Tissue Interactions. Annals of the New York Academy of Sciences 955: 110-117.

93. Chung D, Das SK (2011) Mouse Primary Uterine Cell Coculture System Revisited: Ovarian Hormones Mimic the Aspects of in Vivo Uterine Cell Proliferation. Endocrinology 152: 3246-3258.

94. Cooke PS, Buchanan DL, Young P, Setiawan T, Brody J, et al. (1997) Stromal estrogen receptors mediate mitogenic effects of estradiol on uterine epithelium. Proceedings of the National Academy of Sciences of the United States of America 94: 6535-6540.

95. Winuthayanon W, Hewitt SC, Orvis GD, Behringer RR, Korach KS (2010) Uterine epithelial estrogen receptor α is dispensable for proliferation but essential for complete biological and biochemical responses. Proceedings of the National Academy of Sciences 107: 19272-19277.

96. Ma W-g, Song H, Das SK, Paria BC, Dey SK (2003) Estrogen is a critical determinant that specifies the duration of the window of uterine receptivity for implantation. Proceedings of the National Academy of Sciences of the United States of America 100: 2963-2968.

97. Martin L, Finn CA, Trinder G (1973) Hypertrophy and hyperplasia in the mouse uterus after oestrogen treatment: an autoradiographic study. Journal of Endocrinology 56: 133-NP.

98. McCormack JT, Greenwald GS (1974) Evidence for a preimplantation rise in oestradiol-17β levels on day 4 of pregnancy in the mouse. Journal of Reproduction and Fertility 41: 297-301.

99. Das RM, Martin L (1973) Progesterone inhibition of mouse uterine epithelial proliferation. Journal of Endocrinology 59: 205-206.

100. Martin L, Das RM, Finn CA (1973) The inhibition by progesterone of uterine epithelial proliferation in the mouse. Journal of Endocrinology 57: 549-554.

101. Nelson KG, Takahashi T, Bossert NL, Walmer DK, McLachlan JA (1991) Epidermal growth factor replaces estrogen in the stimulation of female genital-tract growth and differentiation. Proceedings of the National Academy of Sciences 88: 21-25.

102. Diaugustine RP, Petrusz P, Bell GI, Brown CF, Korach KS, et al. (1988) Influence of Estrogens on Mouse Uterine Epidermal Growth Factor Precursor Protein and Messenger Ribonucleic Acid. Endocrinology 122: 2355-2363.

103. Murphy LJ, Ghahary A (1990) Uterine Insulin-Like Growth Factor-1: Regulation of Expression and Its Role in Estrogen-Induced Uterine Proliferation. Endocrine Reviews 11: 443-453.

104. Nelson KG, Takahashi T, Lee DC, Luetteke NC, Bossert NL, et al. (1992) Transforming growth factor-alpha is a potential mediator of estrogen action in the mouse uterus. Endocrinology 131: 1657-1664.

105. Zhu L, Pollard JW (2007) Estradiol-17β regulates mouse uterine epithelial cell proliferation through insulin-like growth factor 1 signaling. Proceedings of the National Academy of Sciences 104: 15847-15851.

106. Kurita T, Young P, Brody JR, Lydon JP, O'Malley BW, et al. (1998) Stromal Progesterone Receptors Mediate the Inhibitory Effects of Progesterone on Estrogen-Induced Uterine Epithelial Cell Deoxyribonucleic Acid Synthesis. Endocrinology 139: 4708-4713.

107. Matsumoto H, Zhao X, Das SK, Hogan BL, Dey SK (2002) Indian hedgehog as a progesterone-responsive factor mediating epithelial-mesenchymal interactions in the mouse uterus. Dev Biol 245: 280-290.

108. Cavagna M, Mantese JC (2003) Biomarkers of Endometrial Receptivity—A Review. Placenta 24, Supplement 2: S39-S47.

109. Bruce A L (2011) Assessment of endometrial receptivity. Fertility and Sterility 96: 522-529.

110. Quinn CE, Casper RF (2009) Pinopodes: a questionable role in endometrial receptivity. Human Reproduction Update 15: 229-236.

111. Meseguer M, Pellicer A, Simón C (1998) MUC1 and endometrial receptivity. Molecular Human Reproduction 4: 1089-1098.

112. Brayman M, Thathiah A, Carson D (2004) MUC1: A multifunctional cell surface component of reproductive tissue epithelia. Reproductive Biology and Endocrinology 2: 4.

113. Aplin J (1997) Adhesion molecules in implantation. Rev Reprod 2: 84-93.

114. Surveyor GA, Gendler SJ, Pemberton L, Das SK, Chakraborty I, et al. (1995) Expression and steroid hormonal control of Muc-1 in the mouse uterus. Endocrinology 136: 3639-3647.

115. Braga VM, Gendler SJ (1993) Modulation of Muc-1 mucin expression in the mouse uterus during the estrus cycle, early pregnancy and placentation. Journal of Cell Science 105: 397-405.

116. Genbacev OD (2003) Trophoblast L-selectin-mediated adhesion at the maternal-fetal interface. Science 299: 405-408.

117. Abrahamsohn PA, Zorn TMT (1993) Implantation and decidualization in rodents. Journal of Experimental Zoology 266: 603-628.

118. Ramathal CY, Bagchi IC, Taylor RN, Bagchi MK (2010) Endometrial Decidualization: Of Mice and Men. Semin Reprod Med 28: 17-26.

119. Paria BC, Ma W-g, Tan J, Raja S, Das SK, et al. (2001) Cellular and molecular responses of the uterus to embryo implantation can be elicited by locally applied growth factors.

Proceedings of the National Academy of Sciences of the United States of America 98: 1047-1052.

120. Lee KY, Jeong J-W, Wang J, Ma L, Martin JF, et al. (2007) Bmp2 Is Critical for the Murine Uterine Decidual Response. Mol Cell Biol 27: 5468-5478.

121. Li Q, Kannan A, Wang W, DeMayo FJ, Taylor RN, et al. (2007) Bone Morphogenetic Protein 2 Functions via a Conserved Signaling Pathway Involving Wnt4 to Regulate Uterine Decidualization in the Mouse and the Human. Journal of Biological Chemistry 282: 31725-31732.

122. Franco HL, Dai D, Lee KY, Rubel CA, Roop D, et al. (2011) WNT4 is a key regulator of normal postnatal uterine development and progesterone signaling during embryo implantation and decidualization in the mouse. The FASEB Journal 25: 1176-1187.

123. Laws MJ, Taylor RN, Sidell N, DeMayo FJ, Lydon JP, et al. (2008) Gap junction communication between uterine stromal cells plays a critical role in pregnancy-associated neovascularization and embryo survival. Development 135: 2659-2668.

124. McGinnis W, Levine MS, Hafen E, Kuroiwa A, Gehring WJ (1984) A conserved DNA sequence in homoeotic genes of the Drosophila Antennapedia and bithorax complexes. Nature 308: 428-433.

125. Favier B, Dollé P (1997) Developmental functions of mammalian Hox genes. Molecular Human Reproduction 3: 115-131.

126. Robb K (1994) Hox genes in vertebrate development. Cell 78: 191-201.

127. Gehring WJ, Affolter M, Burglin T (1994) Homeodomain proteins. Annual Review of Biochemistry 63: 487-526.

128. Gehring W (1987) Homeo boxes in the study of development. Science 236: 1245-1252.

129. Chen H, Sukumar S (2003) Role of Homeobox Genes in Normal Mammary Gland Development and Breast Tumorigenesis. Journal of Mammary Gland Biology and Neoplasia 8: 159-175.

130. Stein S, Fritsch R, Lemaire L, Kessel M (1996) Checklist: Vertebrate homeobox genes. Mechanisms of Development 55: 91-108.

131. Taylor HS (2000) The Role of HOX Genes in the Development and Function of the Female Reproductive Tract. Semin Reprod Med 18: 081,090.

132. Taylor HS, Vanden Heuvel GB, Igarashi P (1997) A conserved Hox axis in the mouse and human female reproductive system: late establishment and persistent adult expression of the Hoxa cluster genes. Biology of Reproduction 57: 1338-1345.

133. Daftary GS, Taylor HS (2006) Endocrine Regulation of HOX Genes. Endocrine Reviews 27: 331-355.

134. Vitiello D, Kodaman PH, Taylor HS (2007) HOX Genes in Implantation. Semin Reprod Med 25: 431,436.

135. Eun Kwon HYE, Taylor HS (2004) The Role of HOX Genes in Human Implantation. Annals of the New York Academy of Sciences 1034: 1-18.

136. Taylor H (2000) The role of HOX genes in human implantation. Hum Reprod Update 6: 75 - 79.

137. Satokata I, Benson G, Maas R (1995) Sexually dimorphic sterility phenotypes in Hoxa10-deficient mice. Nature 374: 460-463.

138. Benson GV, Lim H, Paria BC, Satokata I, Dey SK, et al. (1996) Mechanisms of reduced fertility in Hoxa-10 mutant mice: uterine homeosis and loss of maternal Hoxa-10 expression. Development 122: 2687-2696.

139. Hsieh-Li HM, Witte DP, Weinstein M, Branford W, Li H, et al. (1995) Hoxa 11 structure, extensive antisense transcription, and function in male and female fertility. Development 121: 1373-1385.

140. Hill RE, Jones PF, Rees AR (1989) A new family of mouse homeo box-containing genes: molecular structure, chromosomal location, and developmental expression of Hox-7.1. Genes Dev 3: 26-37.

141. Davidson D (1995) The function and evolution of Msx genes: pointers and paradoxes. Trends in Genetics 11: 405-411.

142. Banerjee-Basu S, Baxevanis AD (2001) Molecular evolution of the homeodomain family of transcription factors. Nucleic Acids Research 29: 3258-3269.

143. Alappat S, Zhang ZY, Chen YP (2003) Msx homeobox gene family and craniofacial development. Cell Res 13: 429-442.

144. Davidson DR, Hill RE (1991) Msh-like genes: a family of homeo-box genes with wide-ranging expression during vertebrate development. Sem in Dev Biol 2: 405-412.

145. Bendall AJ, Abate-Shen C (2000) Roles for Msx and Dlx homeo-proteins in vertebrate development. Gene 247: 17-31.

146. Ramos C, Robert B (2005) msh/Msx gene family in neural development. Trends in Genetics 21: 624-632.

147. Maas R, Chen YP, Bei M, Woo I, Satokata I (1996) The Role of Msx Genes in Mammalian Development. Annals of the New York Academy of Sciences 785: 171-181.

148. Goupille O, Saint Cloment C, Lopes M, Montarras D, Robert B (2008) Msx1 and Msx2 are expressed in sub-populations of vascular smooth muscle cells. Developmental Dynamics 237: 2187-2194.

149. Shimeld SM, McKay IJ, Sharpe PT (1996) The murine homeobox gene Msx-3 shows highly restricted expression in the developing neural tube. Mech Dev 55: 201-210.

150. Wang W, Chen X, Xu H, Lufkin T (1996) Msx3: a novel murine homologue of the Drosophila msh homeobox gene restricted to the dorsal embryonic central nervous system. Mechanisms of Development 58: 203-215.

151. Berdal A, Molla M, Hotton D, AÃ¯oub M, LÃ©zot F, et al. (2009) Differential Impact of Msx1 and Msx2 Homeogenes on Mouse Maxillofacial Skeleton. Cells Tissues Organs 189: 126-132.

152. Catron KM, Iler N, Abate C (1993) Nucleotides flanking a conserved TAAT core dictate the DNA binding specificity of three murine homeodomain proteins. Mol Cell Biol 13: 2354-2365.

153. Catron KM, Zhang H, Marshall SC, Inostroza JA, Wilson JM, et al. (1995) Transcriptional repression by Msx-1 does not require homeodomain DNA-binding sites. Mol Cell Biol 15: 861-871.

154. Zhang H, Hu G, Wang H (1997) Heterodimerization of Msx and Dlx homeoproteins results in functional antagonism. Mol Cell Biol 17: 2920-2932.

155. Bendall AJ, Rincon-Limas DE, Botas J, Abate-Shen C (1998) Protein complex formation between Msx1 and Lhx2 homeoproteins is incompatible with DNA binding activity. Differentiation 63: 151-157.

156. Bendall AJ, Ding J, Hu G, Shen MM, Abate-Shen C (1999) Msx1 antagonizes the myogenic activity of Pax3 in migrating limb muscle precursors. Development 126: 4965-4976.

157. Jumlongras D, Bei M, Stimson JM (2001) A nonsense mutation in Msx1 causes Witkop syndrome. Am J Hum Genet 69: 67-74.

158. Hu G, Vastardis H, Bendall AJ (1998) Haploinsufficiency of MSX1: a mechanism for selective tooth agenesis. Mol Cell Biol 18: 6044-6051.

159. Lurie IW, Lazjuk GI, Ussova EB, Presman EB, Gurevich DB (1989) The Wolf-Hirschhorne syndrome. Clin Genet 17: 375-384.

160. Ma L, Golden S, Wu L, Maxson R (1996) The molecular basis of Boston-type craniosynostosis: the Pro148 [rarr] His mutation in the N-terminal arm of the MSX2 homeodomain stabilizes DNA binding without altering nucleotide sequence preferences. Hum Mol Genet 5: 1915-1920.

161. Wilkie AO, Tang Z, Elanko N (2000) Functional haploinsufficiency of the human homeobox gene Msx2 causesdefects in skull ossification. Nat Genet 24: 387-390.

162. Catron KM, Wang H, Hu G, Shen MM, Abate-Shen C (1996) Comparison of MSX-1 and MSX-2 suggests a molecular basis for functional redundancy. Mechanisms of Development 55: 185-199.

163. Satokata I, Maas R (1994) Msx1 deficient mice exhibit cleft palate and abnormalities of craniofacial and tooth development. Nat Genet 6: 348-356.

164. Satokata I, Ma L, Ohshima H (2000) Msx2 deficiency in mice causes pleiotropic defects in bone growth and ectodermal organ formation. Nat Genet 24: 391-395.

165. Ishii M, Han J, Yen H-Y, Sucov HM, Chai Y, et al. (2005) Combined deficiencies of Msx1 and Msx2 cause impaired patterning and survival of the cranial neural crest. Development 132: 4937-4950.

166. Han J, Ishii M, Bringas Jr P, Maas RL, Maxson Jr RE, et al. (2007) Concerted action of Msx1 and Msx2 in regulating cranial neural crest cell differentiation during frontal bone development. Mechanisms of Development 124: 729-745.

167. Satoh K, Ginsburg E, Vonderhaar BK (2004) Msx-1 and Msx-2 in Mammary Gland Development. Journal of Mammary Gland Biology and Neoplasia 9: 195-205.

168. Pavlova A, Boutin E, Cunha G, Sassoon D (1994) Msx1 (Hox-7.1) in the adult mouse uterus: cellular interactions underlying regulation of expression. Development 120: 335-345.

169. Stelnicki EJ, Harrison MR, Holmes D, Adzick NS, Kömüves LG, et al. (1997) The human homeobox genes MSX-1, MSX-2, and MOX-1 are differentially expressed in the dermis and epidermis in fetal and adult skin. Differentiation 62: 33-41.

170. Quinn LM, Latham SE, Kalionis B (2000) The Homeobox Genes MSX2 and MOX2 are Candidates for Regulating Epithelial–Mesenchymal Cell Interactions in the Human Placenta. Placenta 21, Supplement A: S50-S54.

171. Bach A, Lallemand Y, Nicola M-A, Ramos C, Mathis L, et al. (2003) Msx1 is required for dorsal diencephalon patterning. Development 130: 4025-4036.

172. Iler N, Abate-Shen C (1996) Rapid Identification of Homeodomain Binding Sites in theWnt-5aGene Using an Immunoprecipitation Strategy. Biochemical and Biophysical Research Communications 227: 257-265.

173. Huang W-W, Yin Y, Bi Q, Chiang T-C, Garner N, et al. (2005) Developmental Diethylstilbestrol Exposure Alters Genetic Pathways of Uterine Cytodifferentiation. Molecular Endocrinology 19: 669-682.

174. Shao J-S, Cheng S-L, Pingsterhaus JM, Charlton-Kachigian N, Loewy AP, et al. (2005) Msx2 promotes cardiovascular calcification by activating paracrine Wnt signals. The Journal of Clinical Investigation 115: 1210-1220.

175. Cheng S-L, Shao J-S, Cai J, Sierra OL, Towler DA (2008) Msx2 Exerts Bone Anabolism via Canonical Wnt Signaling. Journal of Biological Chemistry 283: 20505-20522.

176. Monsoro-Burq A-H, Wang E, Harland R (2005) Msx1 and Pax3 Cooperate to Mediate FGF8 and WNT Signals during Xenopus Neural Crest Induction. Developmental Cell 8: 167-178.

177. Song L, Li Y, Wang K, Wang Y-Z, Molotkov A, et al. (2009) Lrp6-mediated canonical Wnt signaling is required for lip formation and fusion. Development 136: 3161-3171.

178. Kim HJ, Rice DP, Kettunen PJ, Thesleff I (1998) FGF-, BMP- and Shh-mediated signalling pathways in the regulation of cranial suture morphogenesis and calvarial bone development. Development 125: 1241-1251.

179. Zhang Z, Song Y, Zhao X, Zhang X, Fermin C, et al. (2002) Rescue of cleft palate in Msx1 -deficient mice by transgenic Bmp4 reveals a network of BMP and Shh signaling in the regulation of mammalian palatogenesis. Development 129:: 4135-4146.

180. Lallemand Y, Bensoussan V, Cloment CS, Robert B (2009) Msx genes are important apoptosis effectors downstream of the Shh/Gli3 pathway in the limb. Developmental Biology 331: 189-198.

181. Thomas T, Kurihara H, Yamagishi H (1998) A signaling cascade involving endothelin-1, dHAND and Msx1 regulates development gene HOX7 maps to chromosome 4p16.1 and may be implicated of neural-crest-derived branchial arch mesenchyme. Development 125: 3005-3014.

182. Kettunen P, Thesleff I (1998) Expression and function of FGFs-4, -8, and -9 suggest functional redundancy and repetitive use as epithelial signals during tooth morphogenesis. Dev Dyn 211: 256-268.

183. Bei M, Maas R (1998) FGFs and BMP4 induce both Msx1-independent and Msx1-dependent signaling pathways in early tooth development. Development 125: 4325-4333.

184. Chen Y, Bei M, Woo I, Satokata I, Maas R (1996) Msx1 controls inductive signaling in mammalian tooth morphogenesis. Development 122: 3035-3044.

185. Tureckova J, Sahlberg C, Aberg T, Ruch JV, Thesleff I, et al. (1995) Comparison of expression of the msx-1, msx-2, BMP-2 and BMP-4 genes in the mouse upper diastemal and molar tooth primordia. Int J Dev Biol 39:: 459-468.

186. Vainio S, Karavanova I, Jowett A, Thesleff I (1993) Identification of BMP-4 as a signal mediating secondary induction between epithelial and mesenchymal tissues during early tooth development. Cell 75: 45-58.

187. Barlow AJ, Francis-West PH (1997) Ectopic application of recombinant BMP-2 and BMP-4 can change patterning of developing chick facial primordia. Development 124: 391-398.

188. Tirosh-Finkel L, Zeisel A, Brodt-Ivenshitz M, Shamai A, Yao Z, et al. (2010) BMP-mediated inhibition of FGF signaling promotes cardiomyocyte differentiation of anterior heart field progenitors. Development 137: 2989-3000.

189. Moon RT, Brown JD, Torres M (1997) WNTs modulate cell fate and behavior during vertebrate development. Trends in Genetics 13: 157-162.

190. Kratochwil K, Galceran J, Tontsch S, Roth W, Grosschedl R (2002) FGF4, a direct target of LEF1 and Wnt signaling, can rescue the arrest of tooth organogenesis in Lef1-/- mice. Genes & Development 16: 3173-3185.

191. Wang Y, Song L, Zhou CJ (2011) The canonical Wnt/ß-catenin signaling pathway regulates Fgf signaling for early facial development. Developmental Biology 349: 250-260.

192. Cohen ED, Wang Z, Lepore JJ, Lu MM, Taketo MM, et al. (2007) Wnt/β-catenin signaling promotes expansion of Isl-1–positive cardiac progenitor cells through regulation of FGF signaling. The Journal of Clinical Investigation 117: 1794-1804.

193. Kawakami Y, Capdevila J, Büscher D, Itoh T, Esteban CRg, et al. (2001) WNT Signals Control FGF-Dependent Limb Initiation and AER Induction in the Chick Embryo. Cell 104: 891-900.

194. Katoh M, Katoh M (2006) Cross-talk of WNT and FGF signaling pathways at GSK3ß to regulate ß-catenin and SNAIL signaling cascades. Cancer Biology & Therapy 5: 1059-1064.

195. Shimokawa T, Furukawa Y, Sakai M, Li M, Miwa N, et al. (2003) Involvement of the FGF18 Gene in Colorectal Carcinogenesis, as a Novel Downstream Target of the β-Catenin/T-Cell Factor Complex. Cancer Research 63: 6116-6120.

196. Chen Y-H, Ishii M, Sucov H, Maxson R (2008) Msx1 and Msx2 are required for endothelial-mesenchymal transformation of the atrioventricular cushions and patterning of the atrioventricular myocardium. BMC Developmental Biology 8: 75.

197. Friedmann Y, Daniel CW (1996) Regulated Expression of Homeobox GenesMsx-1andMsx-2in Mouse Mammary Gland Development Suggests a Role in Hormone Action and Epithelial–Stromal Interactions. Developmental Biology 177: 347-355.

198. Jowett AK, Vainio S, Ferguson MW, Sharpe PT, Thesleff I (1993) Epithelial-mesenchymal interactions are required for msx 1 and msx 2 gene expression in the developing murine molar tooth. Development 117: 461-470.

199. Mericskay M, Carta L, Sassoon D (2005) Diethylstilbestrol exposure in utero: A paradigm for mechanisms leading to adult disease. Birth Defects Research Part A: Clinical and Molecular Teratology 73: 133-135.

200. Yin Y, Lin C, Ma L (2006) Msx2 Promotes Vaginal Epithelial Differentiation and Wolffian Duct Regression and Dampens the Vaginal Response to Diethylstilbestrol. Molecular Endocrinology 20: 1535-1546.

201. Parr MB, Parr, E.L. (1989) The implantation reaction; Jollie RMWaWP, editor: Plenum press, New York.

202. Ernst M (2001) Defective gp130-mediated signal transducer and activator of transcription (STAT) signaling results in degenerative joint disease, gastrointestinal ulceration, and failure of uterine implantation. J Exp Med 194: 189-203.

203. Robb L, Li R, Hartley L, Nandurkar HH, Koentgen F, et al. (1998) Infertility in female mice lacking the receptor for interleukin 11 is due to a defective uterine response to implantation. Nat Med 4: 303-308.

204. Wang W, Van De Water T, Lufkin T (1998) Inner ear and maternal reproductive defects in mice lacking the Hmx3 homeobox gene. Development 125: 621-634.

205. Ye X (2005) LPA3-mediated lysophosphatidic acid signalling in embryo implantation and spacing. Nature 435: 104-108.

206. Afshar Y, Jeong J-W, Roqueiro D, DeMayo F, Lydon J, et al. (2012) Notch1 mediates uterine stromal differentiation and is critical for complete decidualization in the mouse. The FASEB Journal 26: 282-294.

207. Bilinski P, Roopenian D, Gossler A (1998) Maternal IL-11R[alpha] function is required for normal decidua and fetoplacental development in mice. Genes Dev 12: 2234-2243.

208. Maas R, Bei M (1997) The genetic control of early tooth development. Crit Rev Oral Biol Med. 1997; 8(1):4-39.

209. Daikoku T, Song H, Guo Y, Riesewijk A, Mosselman S, et al. (2004) Uterine Msx-1 and Wnt4 Signaling Becomes Aberrant in Mice with the Loss of Leukemia Inhibitory Factor or Hoxa-10: Evidence for a Novel Cytokine-Homeobox-Wnt Signaling in Implantation. Molecular Endocrinology 18: 1238-1250.

210. Fu H, Ishii M, Gu Y, Maxson R (2007) Conditional alleles of Msx1 and Msx2. genesis 45: 477-481.

211. Soyal SM, Mukherjee A, Lee KYS, Li J, Li H, et al. (2005) Cre-mediated recombination in cell lineages that express the progesterone receptor. genesis 41: 58-66.

212. Li Q, Cheon YP, Kannan A, Shanker S, Bagchi IC, et al. (2004) A novel pathway involving progesterone receptor, 12/15-lipoxygenase-derived eicosanoids, and peroxisome proliferator-activated receptor gamma regulates implantation in mice. J Biol Chem 279: 11570-11581.

213. Kato S, Endoh H, Masuhiro Y, Kitamoto T, Uchiyama S, et al. (1995) Activation of the Estrogen Receptor Through Phosphorylation by Mitogen-Activated Protein Kinase. Science 270: 1491-1494.

214. Bagchi IC, Li Q, Cheon YP (2001) Role of steroid hormone-regulated genes in implantation. Ann N Y Acad Sci 943: 68-76.

215. Pan H, Deng Y, Pollard JW (2006) Progesterone blocks estrogen-induced DNA synthesis through the inhibition of replication licensing. Proceedings of the National Academy of Sciences 103: 14021-14026.

216. McMaster MT, Teng CT, Dey SK, Andrews GK (1992) Lactoferrin in the mouse uterus: analyses of the preimplantation period and regulation by ovarian steroids. Molecular Endocrinology 6: 101-111.

217. Jeong J-W, Lee KY, Lydon JP, DeMayo FJ (2006) Steroid hormone regulation of Clca3 expression in the murine uterus. Journal of Endocrinology 189: 473-484.

218. Huang H, Chu S, Chen Y (1999) Ovarian steroids regulate 24p3 expression in mouse uterus during the natural estrous cycle and the preimplantation period. Journal of Endocrinology 162: 11-19.

219. Bigsby RM, Cooke PS, Cunha GR (1986) A simple efficient method for separating murine uterine epithelial and mesenchymal cells. American Journal of Physiology - Endocrinology And Metabolism 251: E630-E636.

220. Finn CA, Martin L (1974) The control of implantation. Journal of Reproduction and Fertility 39: 195-206.

221. Gordon MD, Nusse R (2006) Wnt Signaling: Multiple Pathways, Multiple Receptors, and Multiple Transcription Factors. Journal of Biological Chemistry 281: 22429-22433.

222. Angers S, Moon RT (2009) Proximal events in Wnt signal transduction. Nat Rev Mol Cell Biol advanced online publication.

223. Logan CY, Nusse R (2004) The WNT signaling pathway in development and disease. Annual Review of Cell and Developmental Biology 20: 781-810.

224. Reinhold MI, Naski MC (2007) Direct Interactions of Runx2 and Canonical Wnt Signaling Induce FGF18. Journal of Biological Chemistry 282: 3653-3663.

225. Eswarakumar VP, Lax I, Schlessinger J (2005) Cellular signaling by fibroblast growth factor receptors. Cytokine & Growth Factor Reviews 16: 139-149.

226. Beenken A, Mohammadi M (2009) The FGF family: biology, pathophysiology and therapy. Nat Rev Drug Discov 8: 235-253.

227. Turner N, Grose R (2010) Fibroblast growth factor signalling: from development to cancer. Nat Rev Cancer 10: 116-129.

228. Koziczak M, Holbro T, Hynes NE (2004) Blocking of FGFR signaling inhibits breast cancer cell proliferation through downregulation of D-type cyclins. Oncogene 23: 3501-3508.

229. Chamorro MN, Schwartz DR, Vonica A, Brivanlou AH, Cho KR, et al. (2005) FGF-20 and DKK1 are transcriptional targets of [beta]-catenin and FGF-20 is implicated in cancer and development. EMBO J 24: 73-84.

230. Chen C, Spencer TE, Bazer FW (2000) Fibroblast Growth Factor-10: A Stromal Mediator of Epithelial Functionin the Ovine Uterus. Biology of Reproduction 63: 959-966.

231. Satterfield MC, Hayashi K, Song G, Black SG, Bazer FW, et al. (2008) Progesterone Regulates FGF10, MET, IGFBP1, and IGFBP3 in the Endometrium of the Ovine Uterus. Biology of Reproduction 79: 1226-1236.

232. Hogan BL (1996) Bone morphogenetic proteins: multifunctional regulators of vertebrate development. Genes Dev 10: 1580-1594.

233. Chen D, Zhao M, Mundy GR (2004) Bone Morphogenetic Proteins. Growth Factors 22: 233-241.

234. Shimasaki S, Moore RK, Otsuka F, Erickson GF (2004) The Bone Morphogenetic Protein System In Mammalian Reproduction. Endocrine Reviews 25: 72-101.

235. Canalis E, Economides AN, Gazzerro E (2003) Bone Morphogenetic Proteins, Their Antagonists, and the Skeleton. Endocrine Reviews 24: 218-235.

236. Phippard DJ, Weber-Hall SJ, Sharpe PT, Naylor MS, Jayatalake H, et al. (1996) Regulation of Msx-1, Msx-2, Bmp-2 and Bmp-4 during foetal and postnatal mammary gland development. Development 122: 2729-2737.

237. Cheng S-L, Shao J-S, Charlton-Kachigian N, Loewy AP, Towler DA (2003) Msx2 Promotes Osteogenesis and Suppresses Adipogenic Differentiation of Multipotent Mesenchymal Progenitors. Journal of Biological Chemistry 278: 45969-45977.

238. Kim Y-J, Lee M-H, Wozney JM, Cho J-Y, Ryoo H-M (2004) Bone Morphogenetic Protein-2-induced Alkaline Phosphatase Expression Is Stimulated by Dlx5 and Repressed by Msx2. Journal of Biological Chemistry 279: 50773-50780.

239. Matsubara T, Kida K, Yamaguchi A, Hata K, Ichida F, et al. (2008) BMP2 Regulates Osterix through Msx2 and Runx2 during Osteoblast Differentiation. Journal of Biological Chemistry 283: 29119-29125.

240. Dollar JR, Graham CE, Reyes FI (1982) Postovulatory predecidual development in the baboon, chimpanzee, and human. American Journal of Primatology 3: 307-313.

241. Strauss Iii JF, Lessey BA (2009) CHAPTER 9 - The Structure, Function, and Evaluation of the Female Reproductive Tract. Yen & Jaffe's Reproductive Endocrinology (Sixth Edition). Philadelphia: W.B. Saunders. pp. 191-233.

242. Gellersen B, Brosens IA, Brosens JJ (2007) Decidualization of the Human Endometrium: Mechanisms, Functions, and Clinical Perspectives. Semin Reprod Med 25: 445,453.

243. Das RM, Martin L (1978) Uterine DNA synthesis and cell proliferation during early decidualization induced by oil in mice. Journal of Reproduction and Fertility 53: 125-NP.

244. Finn CA, Martin L (1967) Patterns of cell division in the mouse uterus during early pregnancy. Journal of Endocrinology 39: 593-597.

245. Shao J-S, Aly ZA, Lai C-F, Cheng S-L, Cai JUN, et al. (2007) Vascular Bmp–Msx2–Wnt Signaling and Oxidative Stress in Arterial Calcification. Annals of the New York Academy of Sciences 1117: 40-50.

246. Hruska KA, Mathew S, Saab G (2005) Bone Morphogenetic Proteins in Vascular Calcification. Circulation Research 97: 105-114.

247. Lian J, Stein G, Javed A, van Wijnen A, Stein J, et al. (2006) Networks and hubs for the transcriptional control of osteoblastogenesis. Reviews in Endocrine & Metabolic Disorders 7: 1-16.

248. Zou H, Niswander L (1996) Requirement for BMP Signaling in Interdigital Apoptosis and Scale Formation. Science 272: 738-741.

249. Sirard C, Kim S, Mirtsos C, Tadich P, Hoodless PA, et al. (2000) Targeted Disruption in Murine Cells Reveals Variable Requirement for Smad4 in Transforming Growth Factor β-related Signaling. Journal of Biological Chemistry 275: 2063-2070.

250. Dassule HR, McMahon AP (1998) Analysis of Epithelial–Mesenchymal Interactions in the Initial Morphogenesis of the Mammalian Tooth. Developmental Biology 202: 215-227.

251. Furuta Y, Piston DW, Hogan BL (1997) Bone morphogenetic proteins (BMPs) as regulators of dorsal forebrain development. Development 124: 2203-2212.